FINAL REPORT

Demonstration of Crawler-Towed Sensor Technologies in Challenging Nearshore Sites

ESTCP Project MR-201422

DECEMBER 2018

Gregory Schultz
White River Technologies

Distribution Statement A
This document has been cleared for public release

ESTCP

Page Intentionally Left Blank

Page Intentionally Left Blank

REPORT DOCUMENTATION PAGE

Form Approved
OMB No. 0704-0188

1. REPORT DATE *(DD-MM-YYYY)*	2. REPORT TYPE	3. DATES COVERED *(From - To)*
12/31/2019	ESTCP Final Report	8/25/2014 - 2/28/2019

4. TITLE AND SUBTITLE
Demonstration of Crawler-Towed Sensor Technologies in Challenging Nearshore Sites

5a. CONTRACT NUMBER
14-C-0057

5b. GRANT NUMBER

5c. PROGRAM ELEMENT NUMBER

6. AUTHOR(S)
Gregory Schultz

5d. PROJECT NUMBER
MR-201422

5e. TASK NUMBER

5f. WORK UNIT NUMBER

7. PERFORMING ORGANIZATION NAME(S) AND ADDRESS(ES)
White River Technologies
1242 Chestnut Street
Newton, MA 02464

8. PERFORMING ORGANIZATION REPORT NUMBER
MR-201422

9. SPONSORING/MONITORING AGENCY NAME(S) AND ADDRESS(ES)
Environmental Security Technology Certification Program
4800 Mark Center Drive, Suite 17D03
Alexandria, VA 22350-3605

10. SPONSOR/MONITOR'S ACRONYM(S)
ESTCP

11. SPONSOR/MONITOR'S REPORT NUMBER(S)
MR-201422

12. DISTRIBUTION/AVAILABILITY STATEMENT
DISTRIBUTION STATEMENT A. Approved for public release: distribution unlimited.

13. SUPPLEMENTARY NOTES

14. ABSTRACT
Environmental remediation of UXO in nearshore environments is significantly complicated by the dynamics of the environment. The overarching goal of this demonstration project was to assess a combination of platform and sensing systems in order to deliver a UXO mapping survey and characterization technology in surf zones, salt marshes, shallow bays and tidal estuaries where robust mobility and stability of sensing platforms is needed in order to acquire high quality geophysical data.

15. SUBJECT TERMS
Crawler-Towed Sensor Technologies, Nearshore, Battery Management System, Explosive Ordnance Disposal Electromagnetic

16. SECURITY CLASSIFICATION OF:			17. LIMITATION OF ABSTRACT	18. NUMBER OF PAGES	19a. NAME OF RESPONSIBLE PERSON
a. REPORT	b. ABSTRACT	c. THIS PAGE			Gregory Schultz
UNCLASS	UNCLASS	UNCLASS	UNCLASS	140	19b. TELEPHONE NUMBER *(Include area code)* 603-678-8385

Page Intentionally Left Blank

FINAL REPORT
Project: MR-201422

TABLE OF CONTENTS

Page

TABLE OF CONTENTS (Continued)

Page

TABLE OF CONTENTS (Continued)

Page

Page Intentionally Left Blank

LIST OF FIGURES

Page

LIST OF FIGURES

Page

LIST OF FIGURES

Page

LIST OF FIGURES

Page

LIST OF FIGURES

Page

LIST OF TABLES

Page

ACRONYMS AND ABBREVIATIONS

˚C	Degrees Celsius
ADC	Analog to Digital Conversion
AFB	Air Force Base
BLDC	BrushLess Direct Current
BMS	Battery Management System
CERCLA	Comprehensive Environmental Response, Compensation and Liability Act
CH	Channel
cm	Centimeter
COTS	Commercial Off The Shelf
CPA	Closest Point of Approach
CRAB	Coastal Research Amphibious Buggy
CST	Conductivity, Salinity, Temperature
CTD	Conductivity, Temperature, Depth
dB	Decibels
DC	Direct Current
DD	Dynamic Discriminator
DERP	Defense Environmental Restoration Program
DGPS	Differential Global Positioning System
DOD	Department of Defense
DVL	Doppler Velocity Log
E	Easting
EE/CA	Engineering Evaluation and Cost Analysis
EOD	Explosive Ordnance Disposal
EM	Electromagnetic
EMI	Electromagnetic Induction
EMF	Electromotive Force
EMPACT	Packable Electromagnetic Technology
ERDC	Environmental Research and Development Center
ESTCP	Environmental Security Technology Certification Program
FA	False Alarms
FRF	Field Research Facility
FREQ	Frequency
FUDS	Formerly Used Defense Sites
GNSS	Global Navigation Satellite System
GPS	Global Positioning System
GUI	Graphical User Interface

HDT	Heading Made True
HDOP	Horizontal Dilution of Precision
HPU	Hydraulic Power Drive Unit
Hz	Hertz
INS	Inertial Navigation System
IVS	Instrument Verification Strip
ISO	Industry Standard Objects
Kbps	Kilobits Per Second
kg	Kilogram
kgf	Kilogram Force
kHz	Kilohertz
kph	Kilometers Per Hour
kW	Kilowatt
kWh	Kilowatt-hour
LAR	Launch and Recovery
LARC	Light Amphibious Resupply Cargo
LED	Light Emitting Diode
LBL	Long Baseline
Li-Ion	Lithium Ion
m	Meter
MEC	Munitions and Explosives of Concern
MMRP	Military Munitions Response Program
MPPEH	Material Potentially Presenting an Explosive Hazard
MR	Munitions Response
N	Northing
NAVD88	North American Vertical Datum of 1988
NCS	Navigation and Control System
NMEA	National Marine Electronics Association
NOAA	National Oceanic and Atmospheric Administration
OCS	Operator Control Station
OEM	Original Equipment Manufacturer
PCB	Printed Circuit Board
Pclass	Probability of Classification
Pd	Probability of Detection
Pfa	Probability of False Alarm
ppt	parts per thousand
PSI	Pounds Per Square Inch
RA	Removal Action

RGB	Red Green Blue
RMS	Root Mean Square
ROC	Receiver Operating Characteristic
ROI	Region of Interest
ROV	Remotely-Operated Vehicle
RPM	Revolutions Per Minute
RTCM	Radio Technical Commission for Maritime Services
RTK	Real-time Kinematic
Rx	Receiver
S	Siemens
SBIR	Small Business Innovative Research
SI	Site Investigation
SNR	Signal to Noise Ratio
SWAP	Size, Weight, and Power
TCRA	Time Critical Removal Action
TDOP	Time Dilution of Precision
TOI	Target of Interest
UDP	User Datagram Protocol
UI	User Interface
USACE	US Army Corps of Engineers
USBL	Ultra-Short Baseline
UTC	Coordinated Universal Time
UTM	Universal Transverse Mercator
UTV	All-Terrain Utility Vehicle
UUV	Unmanned Undersea Vehicle
UXO	Unexploded Ordnance
WIS	Wave Information System
WRT	White River Technologies, Inc.
WWII	World War II

Page Intentionally Left Blank

ACKNOWLEDGEMENTS

This work was conducted as part of Environmental Security Technology Certification Program (ESTCP) Project MR-201422 led by White River Technologies. Dr. Gregory Schultz was the Principal Investigator. Joe Keranen of White River Technologies provided significant effort in data collection and analysis. Chet Bassani, Randall Reynolds, and Erik Russell of White River Technologies supported system engineering, mobilization, and documentation of the integrated Crawler-EM system. Drs. Jesse McNinch and Heidi Wadman of the USACE Field Research Facility in Duck, North Carolina provided technical guidance, site access/preparation and test support for the demonstration. Matthew Cook, Geoffery Cook, Ed Celkis, and Dr. Tim Crandle of Seaview Systems provided engineering and operational expertise on the SurfROVer crawler system as well as on-site test support.

Funding for this project was provided by the ESTCP. We wish to express our sincere appreciation to Dr. Herb Nelson and Drs. Michael Richardson and Michael Tuley for providing support and guidance for this project.

Page Intentionally Left Blank

INTRODUCTION AND OBJECTIVES

Environmental remediation of UXO in nearshore environments is significantly complicated by the dynamics of the environment. The overarching goal of this demonstration project was to assess a combination of platform and sensing systems in order to deliver a UXO mapping survey and characterization technology in surf zones, salt marshes, shallow bays and tidal estuaries where robust mobility and stability of sensing platforms is needed in order to acquire high quality geophysical data.

TECHNOLOGY DESCRIPTION

For this demonstration, we integrated and implemented a robotic amphibious crawler platform with a towed electromagnetic induction (EMI) sensor array designed to provide a stable and mobile geophysical sensing platform for seafloor investigations. The crawler system is an amphibious robot with radio telemetry or integrated fiber optic tether system, track controller, lights and cameras, and GPS/INS positioning system. The towed EMI sensor payload technology is the WRT FlexEM 3D system suitable for underwater UXO mapping, detection and dynamic target classification. The crawler platform and integrated tow sled system were successfully deployed multiple times and proved to be a stable operating platform with adequate tractive control on all substrates on which it was tested (dry grass and gravel, soft sand, mud and silt, shelly sands, dry and saturated fine to coarse sand).

PERFORMANCE AND COST ASSESSMENT

The demonstrations performed during this project among the first of their kind in terms of quantification of UXO detection survey performance metrics for a system that can traverse back and forth between fully submerged and dry land environments. Results from experiments conducted in both surf zone and marsh environments on the North Carolina coast illustrate the potential for detecting and characterizing UXO over a range of hydrodynamic conditions. All targets were detected at SNR > 20 dB for a 100% probability of detection. This far exceeded our detection metric of 100% detection using a 9 dB threshold. We found the crawler-towed system to be stable in the face of crashing waves up to 1.8 meters tall and forceful currents in the swash and surf zones during ebb and flood cycles between wave breaking events. We assessed potential cost savings using this technology for a UXO site study where 500 survey contacts required reacquisition and further investigation. In this case, the crawler-EM system reveals as much as a 50% cost savings relative to conventional diver-based methods.

IMPLEMENTATION ISSUES

While it was somewhat challenging for smaller test targets to remain covered and in-place over more than a tidal cycle, we were able to perform a 100% coverage surveys over the entirety of our test area. These surveys resulted in data covering approximately 3500m^2 of coverage area at an approximate full coverage rate of 0.5 acres per hour. Overall, the demonstrations reported on here illustrated the degree to which the crawler-towed EM system can fill gaps in current nearshore geophysical mapping, detection, and UXO classification.

PUBLICATIONS

Schultz, G., Keranen, J., McNinch, J., and Miller, J., 2017, Detection and classification of UXO using unmanned undersea electromagnetic sensing platforms, AGU Annual Meeting, OS53E-06.

Cook, M., Crandle, T., Celkis, E., 2017, Vehicle design for the littoral zone, Sea Technology, May 2017 Issue, pp. 37-40.

Schultz, G., Bassani, C., Keranen, J., Foley, J., 2017, Deployment of New Magnetic and Electromagnetic Arrays from Unmanned Undersea Platforms, MARELEC Conference Proceedings, MARELEC 2017, Liverpool.

Schultz, G., Keranen, J., Bassani, C., Cook, M., Crandle, T., 2017, Littoral applications of advanced 3D marine electromagnetics from remotely and autonomously operated platforms: Infrastructure and hazard detection and characterization, OCEANS 2017 – Aberdeen, Conference Proceedings, DOI: 10.1109/OCEANSE.2017.8084818.

Page Intentionally Left Blank

EXECUTIVE SUMMARY

OBJECTIVES OF THE DEMONSTRATION

Environmental remediation in nearshore environments is significantly complicated by the dynamics of the environment. Applications related directly to detection and characterization of UXO in nearshore environments as well as those required to support UXO surveys are challenging due to the nature of the environment. There are a wide variety of problems presented:

- Limited mobility, traction and control,
- Poor visibility and overall situational awareness,
- Various physics-based challenges for sensing, such as acoustic backscatter and multi-path propagation, lack of radio frequency transmission, and moving free surface, and
- Accurate positioning and navigation.

Despite these challenges, there is a need for geophysical surveying in very nearshore areas. Underwater munitions are becoming increasingly problematic as ports & harbors, seashores, and other underwater environments are commercially developed or utilized for work or recreational activities. These environments vary significantly with respect to depth, morphology, geology, munitions density and human exposure scenarios.

Our focus was on relatively shallow-water areas such as surf zones, marshes, mudflats, swamps, intertidal/littoral zones, and other water bodies less than 5 m deep. Concentrated human activities and potential intrusive interactions occur in these areas due to fishing, shellfish gathering, swimming, surfing, bathing, jet-skiing, etc. Additionally, construction activity (i.e., dredging, infrastructure repair, pipeline installations) occur in these settings. These areas are also settings for munitions constituent pathways through direct consumption or via consumption of fish or shellfish.

The main goal of this demonstration project was to assess a combination of platform and sensing systems in order to deliver a UXO mapping survey and characterization technology in very challenging nearshore environments. Nearshore environments such as swash zones, surf zones with breaking waves, and shallow tidal areas provide hydrodynamic and bottom conditions that are particularly challenging from the standpoint of mobility and stability of sensing platforms in order to acquire high quality geophysical data. To overcome the limitations of current diver/man-portable or ship-towed configurations in these nearshore regimes, we evaluated both platform and sensor performance to demonstrate and characterize a tailored and integrated robotic bottom crawler-towed sensor solution in representative shoreline UXO sites. The tests and demonstrations reported on here are among the first of their kind in terms of quantification of UXO detection survey performance metrics for a system that can traverse back and forth between fully submerged and dry land environments.

We report here on the final demonstration in a series of graduated and systematic tests that progressed from basic system evaluations on land, to crawler mobility assessments in varying hydrodynamic conditions and on different bottom types, to engineering tests of initial integrated prototype systems, to full-scale demonstrations. Prior evaluations, system testing, and initial engineering trials and demonstrations are provided in interim project reports completed in 2015 and 2016. Validation is conducted through analysis of integrated EMI array, position, and attitude data collected during execution of several dry (beach) and submerged survey profiles. We tracked the cost and time of using the demonstrated system to complete the various missions for comparison against the cost and time efficiency of currently used methods. The final objective of this demonstration was to identify shortcomings and areas of improvement in the hardware, software, and operation of the integrated system.

TECHNOLOGY DESCRIPTION

For this demonstration, we integrated and implemented a robotic amphibious crawler platform with a towed electromagnetic induction (EMI) sensor array designed to provide a stable and mobile geophysical sensing platform for seafloor investigations. Figure ES-1 shows the primary elements of the system. The crawler system is the SeaView SurfROVer, an amphibious robot with radio telemetry or integrated fiber optic tether system, track controller, lights and cameras, and GPS/INS positioning system. The crawler is transported in the self-powered / self-contained operator control station (OCS) trailer system. The OCS contains the subunits for radio communication and data interface with the robotic crawler, GPS base station, helmsman navigation and control units and displays and sensor analyst computing facilities. The towed EMI sensor payload technology is the WRT FlexEM 3D system suitable for underwater UXO mapping, detection and dynamic target classification. It comprises two transmitters and six triaxial "cube" receivers across its 2-meter swath width. The integrated system contains subsea power supplies in the form of two 7.5 kWh smart battery pods in addition to an isolated and independent battery power supply for the EMI array, which enables 6-8 hours of continuous operations. Command and control of the crawler-EM unit is provided through a wireless radio link from the crawler antenna mast to the operator control station (located either on shore or on a vessel). Positioning of crawler and tow sled is provided through a mast-mounted realtime kinematic (RTK) GPS rover antenna on the crawler and a set of inertial measurements units combined with a tow-point optical encoder for translating yaw as well as roll and pitch motions from the GPS locations.

Figure ES-1. Photographs of the Integrated Crawler-towed EM System (LEFT) and Display Units (RIGHT) in the Operator Control Station.

The crawler-EM platform contains 3 basic elements: i) the mobility platform with track motors for driving the tracks, camera and sonar sensors, and data interface backbone; ii) antenna mast system with RTK-GPS rover and wireless ethernet radios; and iii) the towed FlexEM 3D EMI sensor array sled. The operator control station is housed in a self-powered trailer unit and contains the helmsman navigation and control systems, communications, displays, and sensor analyst computing facilities.

The crawler platform and integrated tow sled system were successfully deployed multiple times and proved to be a stable operating platform with adequate tractive control on all substrates on which it was tested (dry grass and gravel, soft sand, mud and silt, shelly sands, dry and saturated fine to coarse sand). Initial deployment testing exposed the need for improvements to the fiber optic tether system, the tow-point encoder and positioning system, and to the EM array sled. Analyses of EM data acquired during these preliminary tests were used to optimize system configuration and data acquisition parameters. Specifically, we made iterative modifications to the mechanical tow sled assemblies and EM system electronics to reduce the overall noise floor of the system by a factor of 6. Additionally, these tests yielded significant improvements for the mission operations and methods used to survey with the system. This included waypoint following and user interface navigation guidance software as well as assessments and planning tools for turn radius and traction/trafficability potential of the system.

DEMONSTRATION RESULTS

To support the preparation of the system, we began in 2015 with a series of instrumented sensor array sled tests and evaluations of amphibious vehicles to pull the sled. This progressed in 2016 to integration and shakedown testing with the SurfROVer crawler system including initial engineering trials in Lake Erie. These efforts culminated in a demonstration of the first prototype version of the integrated crawler-EM system at the USACE Field Research Facility (FRF) in Duck, North Carolina in November of 2016. These early demonstrations exercised the system in a variety of hydrodynamic conditions (from waves and surf to marsh and lake) and bottom types (from sandy beach to muddy marsh). The results of accumulated work in 2015 and 2016 were summarized in an interim report submitted to ESTCP.

We utilized many observations and lessons learned from those prior demonstrations to formulate a series of modifications and improvements toward the demonstrations reported on in this report. The primary modifications to the system included replacement of the fiber-optic tether system with a wireless radio link from the crawler to the topside control station in addition to topside user interface improvements and various additions or improvements to optimize the subsea platform and integration with EM sled. On the crawler, we implemented a greatly improved battery management system, a new tow point encoder unit, and completely self-sufficient and isolated power supply for the EM array. These improvements all benefited the overall operations of the system during our demonstrations.

In our 2017 demonstration, we also attempted to learn from and improve upon the installation of a target grid in the shallow nearshore areas at the USACE FRF surf zone site. An array of 20 targets were installed in a grid pattern over an area extending from the beach approximately 70 meters into the surf zone just south of the FRF pier in water up to approximately 2 meters deep. Figure ES-2 shows some photographs of the test set up. While it was somewhat challenging for particular targets to remain covered and in-place over more than a tidal cycle, we were able to perform a 100% coverage surveys over the entirety of the target grid area. These surveys resulted in data covering approximately 3500m^2 of coverage area at an approximate full coverage rate of 0.5 acres per hour.

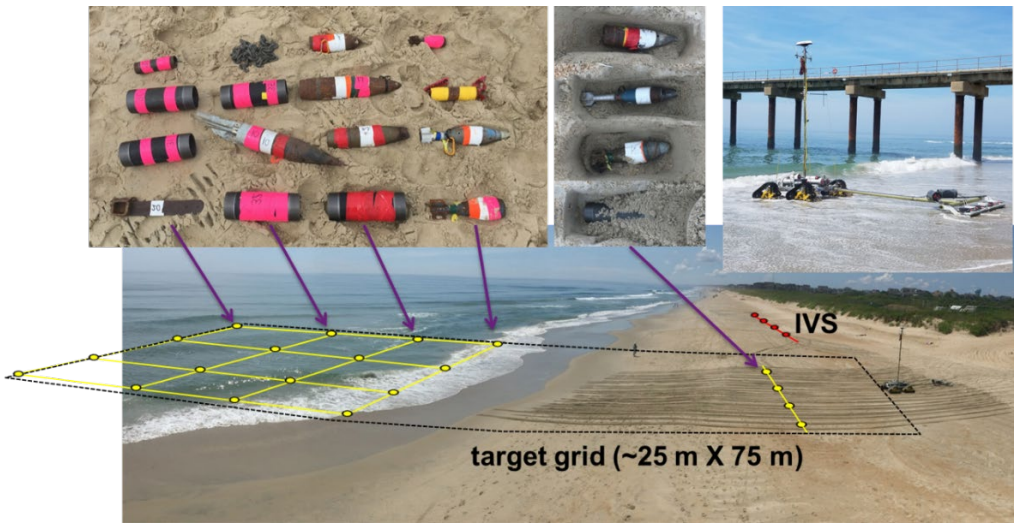

Figure ES-2. Photographs of the Targets Used in Our Demonstration.

Targets ranged from small ISO simulants and 60mm mortars to 105mm projectiles. Targets were buried approximately 25cm below the seafloor surface along shore-parallel lines in similar water depth. The deepest targets were submerged under 1.5-2.2 meters of water

To assess system stability, we analyzed and compared inertial data from the crawler and tow sled IMUs. Typical target area transects began on the beach and progressed directly into the surf perpendicular to the shoreline. Once in the surf, the crawler-EM system rate of forward advance would slow due to hydrodynamic resistance and possibly also due to softer sediments on the seafloor. Among the most dynamic and challenging regimes was deep swash and surf inside of the wave break where strong wave induced currents ebb and flow. This phenomena is illustrated in the data and photographs shown in Figure ES-3.

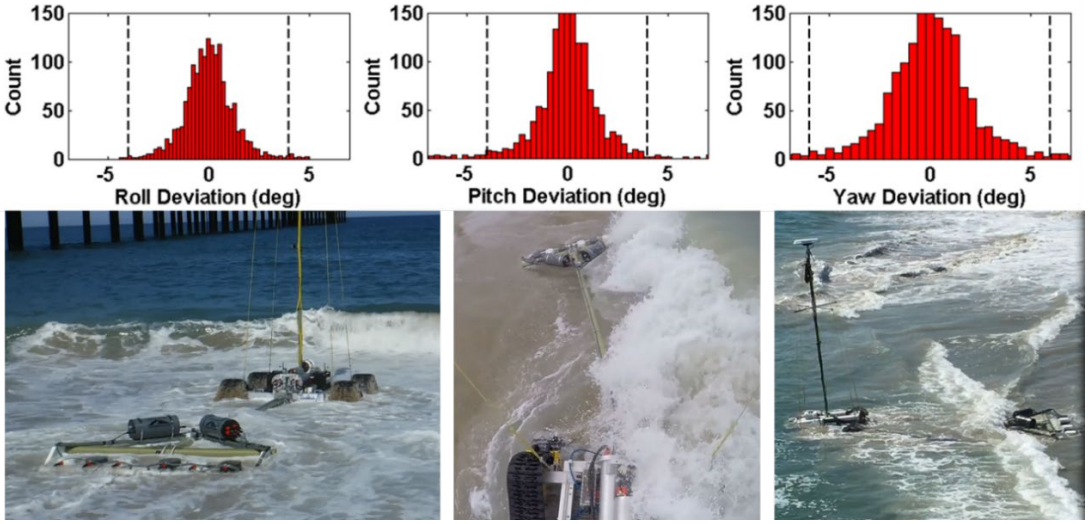

Figure ES-3. TOP: Histograms of the Roll, Pitch, and Yaw Deviations During Shore Perpendicular Transect Surveys into the Surf Zone. BOTTOM: Photographs Showing Various Viewpoints of the Crawler and Towed EM Sled During Operations in the Surf and Swash Zones.

Data from our full coverage surf zone surveys were analyzed using post-processing software to measure area coverage, target detection and localization, and classification performance. All targets were detected at SNR > 20 dB for a 100% probability of detection. This far exceeded our detection metric of 100% detection using a 9 dB threshold. A map of the coverage data and detection localization results are shown Figure ES-4. The target localization accuracy was better than 30cm CEP for all target encounters exceeding our performance metric of 100cm CEP. However, the variance in target positions were approximately 50cm, which was higher than our target metric of 35cm. This was found to be mainly due to wobble and sway of the GPS mast and motion of the GPS rover antenna atop of the mast. We also observed and analyzed data to assess the overall stability of the system in the relatively dynamic surf zone conditions during our operations. We found the crawler-towed system to be very stable in the face of crashing waves up to 1.8 meters tall and forceful currents in the swash and surf zones during ebb and flood cycles between wave breaking events. In some cases, the EM sled appeared to lift from the bottom (perhaps related to heavy cavitation) and sway before the motion of the crawler was enough to pull it back in track. This added to the uncertainty of the array position, although we were able to mitigate this through analysis of tow point encoder and relative differences between crawler- and sled-mounted IMU data.

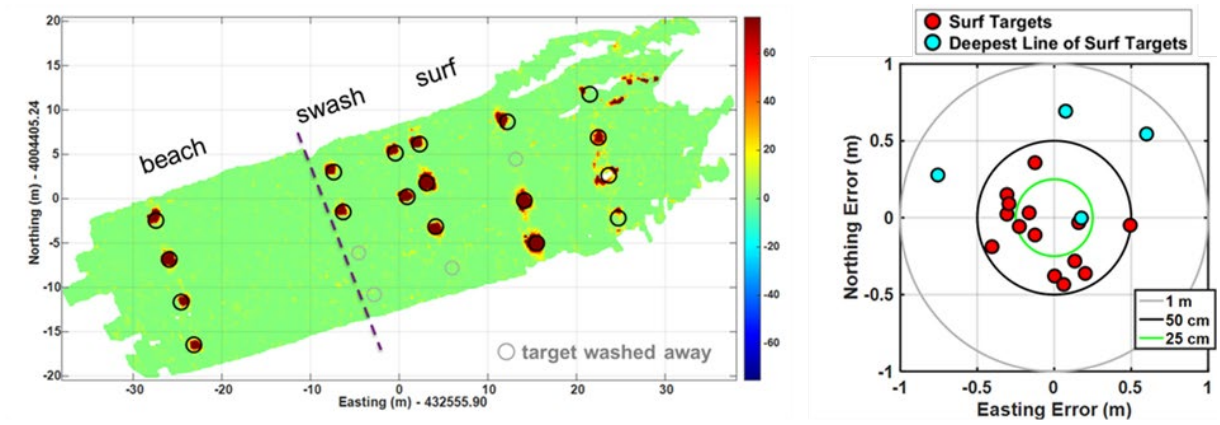

Figure ES-4. LEFT: EM Signal Map from 100% Coverage Surveys Over the Target Grid. The Black Circles Indicate Ground Truth Locations. High Signal-to-noise Anomalies Are Shown Near Each Target Location with Only a Few Anomalies Not Associated with Emplaced Items Shown. Three of the Originally Installed Targets Washed Away Overnight Prior to Our Surveys. RIGHT: Summary Plot of Target Localization Deviations from Ground Truth. All Targets Were Localized to Within 1.0 m, and All But 3 (86%) Were Located within 50 cm. Offset of the Aggregate Detection Localization Data Were Less Than 5 cm in Either Northing or Easting, Although the Standard Deviations Were Nearly 35 cm. This Was Likely Due to Motion of the GPS Antenna Mast, Which Was Especially Evident in Deeper Areas (As Designated as the Deepest Line of Surf Targets).

We also showed that the demonstrated configuration of the EM array was capable of target classification when multiple transects were aggregated together and inverted for magnetic polarizability curves. Inverted polarizability curves were matched to library curves for a subset of targets and analyzed. A few examples are shown in Figure ES-5. Although we were only able to compile a limited number of target encounters and even fewer clutter encounters, the consistency of the inverted polarizabilities yield promise for reducing the number of clutter by as much as 50-75%.

Additional experiments with methods to switch the two side-by-side transmitter coils on the array indicate potential paths to improved classification that are less dependent on (or completely independent of) on relative positioning between adjacent transect overpasses. This holds great promise for dynamic classification implementations in the marine environment.

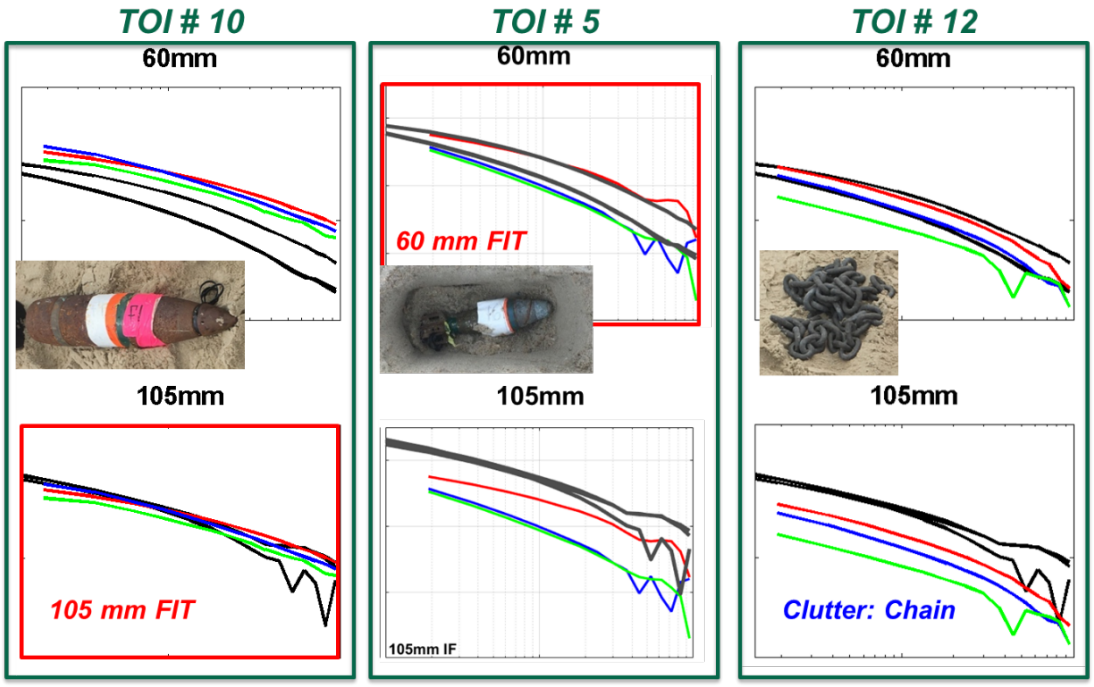

Figure ES-5. Examples of Magnetic Polarizability Curve Matches to Library Curves for Target Encounters.

The inverted polarizability curves (red, blue, and green curves) match most closely to the library curves for most targets (gray curves). Good fits to the largest (105mm, as shown on LEFT) and the smallest (60mm, as shown in CENTER) were observed. Clutter objects did not exhibit the size and symmetry characteristics generally associated with UXO target classification.

In addition, we conducted assessments of the cost and logistical complexities for potential deployment and operation of the technology. Projected daily rates of approximately $8,500 for the integrated demonstration system (including a crawler helmsman operator) lead to considerable savings relative to deployment of an EOD-trained dive team searching the seafloor for UXO. Estimation of incurred labor and equipment costs estimated during survey mode operations yields a 100% real coverage costs of approximately $2,500/acre or $1,250/hour. We assessed potential cost savings using this technology for a particular UXO site study where 500 survey contacts required reacquisition and further investigation. In this case, the crawler-EM system reveals as much as a 50% cost savings relative to conventional diver-based methods. Previous assessments have identified as many as 420 underwater ranges at over 120 different military sites comprising approximately 10 million acres of marine or lacustrine environment potentially contaminated with UXO. Of these 420 sites, it projected that 100 or more contain water depths that prohibit the use of towed geophysical survey systems or EOD divers. In many highly dynamic or otherwise challenging nearshore sites, it is likely not cost effective or just plain impossible to use dive teams for geophysical surveying.

IMPLEMENTATION ISSUES

In general, we experienced relatively smooth operations from the set-up stage through to completing surveys to demobilization at the end of the day. Very little calibration of the system is required. A functional test of power and communications of all systems was conducted without any issues. The crawler platform was mobilized and positioned initially through a small handheld controller that attaches directly to the crawler platform. The demonstration surveys were conducted without any particular issues; however, we noted some observations toward future implementation and optimization for potential cost-effective production operations. These include: (i) added perception and control for obstacle avoidance and navigational awareness; (ii) automation of the grid surveys to reduce operator demands and potential fatigue; and (iii) stability of the antenna mast and sensor sled to maximize positioning accuracy and tracking.

After completion of our full grid coverage surveys, we performed a couple of additional surveys to test the system in water deeper than that in our grid surveys. During one of these "deep water" surveys, the system halted its forward advance and stopped moving. Subsequent investigations revealed that one of the crawler track axles had become entangled in a 2.5-inch treated manila docking line rope (the type usually used for deck, docking, and anchoring lines on a vessel). The system was pulled back to shore and it was obvious that the rope entanglement was the unfortunate cause of the survey stoppage. This resulted in a bent axle and some minor damage to the crawler track assembly. Repairs have been made so that the system is fully functional again and ready for follow-on surveys. It was determined that this type of entanglement is unlikely to be a common occurrence during operations and was an unfortunate event rather than more likely event that requires mitigation. A possible mitigation strategy for such an entanglement event may be to add flooded cowling covers around the sprocket and axle.

While the demonstrations of this crawler-based EM technology showed effective surveying over moderately sized (1-2 acres) areas, larger areas may prove more challenging. Implementation effectiveness will depend highly on the hydrodynamic and bottom conditions at a site as well as the overall shape and size of the survey area. In general, we might anticipate a need to clear areas from a beach or shoreline to a prescribed closure depth. This is generally the depth of water along a shoreline profile at which sediment transport is very small or essentially non-existent and coincides with the foreshore region including swash, surf, and longshore current dominated nearshore. In this case, it would likely be more effective to plan surveys along shore-parallel transects and, thus, stability to shore-normal hydrodynamics such as currents from impinging waves and ebb/flow in swash areas is critical to maintaining high quality towed EM data.

Overall, the demonstrations reported on here illustrated the degree to which the crawler-towed EM system can fill gaps in current nearshore geophysical mapping, detection, and UXO classification. Specifically, we proved that the system could: (i) be mobilized and deployed in a cost-effective manner for shore-based operations; (ii) effectively cover surf zone target areas with 100% coverage transects; (iii) detect and localize UXO targets from 60mm to 105mm in size buried beneath the seafloor to within 50cm radius; and (iv) reduce clutter through analyses of inverted polarizabilities with moderate levels of confidence and effectiveness.

Page Intentionally Left Blank

1.0 INTRODUCTION

The boundary between land and sea has historically been a key strategic military environment and thus numerous training ranges have been established in these areas (e.g., Vieques Island, Camp Lejeune, Cherry Point, Raritan Arsenal, Duck, New River Estuary, Vandenberg AFB). Not only are many of these sites highly contaminated with UXO due to their pervasive use in live fire training, they also pose special risks due to their geographic and/or ecological importance. Nearshore environments such as salt marshes, coastal wetlands, surf zones, shallow bays and tidal estuaries present a number of unique and challenging technical problems for detection and classification of UXO:

- These environments can be fully or partially submerged, or a mix of the two depending on wave and/or tidal conditions.
- UXO can be shallow or deeply buried in cohesive substrates beneath coastal vegetation, typically found in marsh or lagoon environments, or under unconsolidated sand and gravel of the surf zone.
- The geologic and hydrodynamic spatio-temporal conditions tend to vary much more than in pure offshore or terrestrial environments (e.g., highly variable shallow lithology; strong and highly dynamic wave energy and tidal currents).

Currently, only helicopter-based magnetometer or electromagnetic arrays are able to efficiently survey these areas, but they do not provide the detail necessary to both detect all hazardous munitions (due to range limitations) and provide only limited clutter rejection or classification potential. Conventional offshore and terrestrial methods are not appropriate for these environments due to the deployment methods and vehicles used to transport sensor arrays, the sensor modalities used, and the logistics required. Marine methods that rely on EOD-trained divers or thruster-driven remotely operated vehicles for sonar and/or visual inspection will be severely limited in these environments. Previously demonstrated towed sensor systems, limited to water depths greater than 1 meter, were not amphibious and were therefore unable to perform surveys offshore to onshore (e.g., ESTCP MR-200935). Our goal was to demonstrate a UXO detection system that addresses these challenges and presents a new integrated amphibious sensor technology for challenging nearshore UXO sites.

1.1 BACKGROUND

Environmental remediation in nearshore environments is significantly complicated by the dynamics of the environment. Applications related directly to detection and characterization of UXO in nearshore environments as well as those required to support UXO surveys are challenging due to the nature of the environment. There are a wide variety of problems presented:

- Limited mobility, traction and control,
- Poor visibility and overall situational awareness,
- Various physics-based challenges for sensing, such as acoustic backscatter and multi-path propagation, lack of radio frequency transmission, and moving free surface,
- Accurate positioning and navigation,

Despite these challenges, there is a need for geophysical surveying in very nearshore areas. Underwater munitions are becoming increasingly problematic as ports & harbors, seashores, and other underwater environments are commercially developed or utilized for work or recreational activities. These environments vary significantly with respect to depth, morphology, geology, munitions density and human exposure scenarios.

Our focus is on relatively shallow-water conditions – where elevated DoD liability exists due to increased probability of human encounter. These areas include surf zones, marshes, mudflats, swamps, intertidal/littoral zones, and other water bodies of less than 10 m deep such as ponds, streams and shallow lakes. Concentrated human activities and potential intrusive interactions occur in these areas due to fishing, shellfish gathering, swimming, surfing, bathing, jet-skiing, etc. Additionally, construction activity (i.e., dredging, infrastructure repair, pipeline installations) occur in these settings. These areas are also settings for munitions constituent pathways through direct consumption or via consumption of fish or shellfish.

While critical for DoD liability, these areas fall outside present paradigms for terrestrial and underwater detection and characterization. Ground-based methods are ineffectual due to platform inadequacies related to limitations of standoff, cost, mobility/capability, and destruction of the environment. Underwater methods based on acoustic sensors and/or towed arrays are challenged by limited or absent water conditions. Through this executed project, we present ESTCP an efficient and innovative underwater mapping technology that advances current capabilities and provides significant added benefits to DoD.

1.2 OBJECTIVE OF THE DEMONSTRATION

The primary objective of this demonstration was to validate the integration of the EMI array sensor tow, navigation and control system, and the robotic crawler mobility platform in a realistic underwater environment. Validation was conducted through analysis of integrated EMI array, position, and attitude data collected during execution of several dry (beach) and submerged survey profiles. We tracked the cost and time of using the demonstrated system to complete the various missions for comparison against the cost and time efficiency of currently used methods. The final objective of this demonstration was to identify shortcomings and areas of improvement in the hardware, software, and operation of the integrated system.

1.3 REGULATORY DRIVERS

The Department of Defense (DoD) is responsible for assessment and remediation of numerous munitions sites, many containing in-water areas, in the United States. When the transfer of responsibility to other government agencies or to the civilian sector takes place, the DoD lands fall under the compliance requirements of the Superfund statutes. Section 2908 of the 1993 Public Law 103-160 requires adherence to Comprehensive Environmental Response, Compensation, and Liability Act (CERCLA) provisions. The basic drivers are related to assumption of liability for ordnance contamination on the previously DoD-controlled sites.

Site cleanup is performed using the Superfund CERCLA process, which provides the liability of persons responsible for waste at these sites and provides details on the steps required for site cleanup from initial assessment to redevelopment. EMI and magnetic detection sensors are standard technology used in various stages of the CERCLA process in cleanup of ground sites.

The technology demonstrated is towards implementation of a similar technology set for the cleanup of in-water sites.

There are no explicit regulatory drivers or considerations associated directly with this demonstration. All demonstration activities were conducted in waters regulated by federal and state (North Carolina) laws.

Page Intentionally Left Blank

2.0 TECHNOLOGY

We demonstrated an amphibious robotic crawler system integrated with an EMI sensor tow sled that, together, can detect UXO in challenging nearshore environments. The crawler system is the SeaView SurfROVer amphibious robot with radio telemetry or integrated fiber optic tether system, track controller, lights and cameras, and GPS/INS positioning system. The primary EMI sensor payload technology is the FlexEM system suitable for underwater UXO detection and some level of clutter rejection and target classification.

2.1 TECHNOLOGY DESCRIPTION

The primary topside components comprise; (i) a GPS base station, (ii) hand controller, (iii) communications breakout and multi-plexer, and (iv) operator displays (3-6 separate display monitors). Subsea components include those required to power and propel the system as well as transmit payload data to the topside unit. Subsea components include the battery-based power supply, driver and control electronics, brushless direct-current (BLDC) motors, hydraulic pumps, and track systems as well as the pressure compensated junction box housing on-board electronics for data handling and communications. Additional components specific to the UXO survey payload kit demonstrated are described further below.

2.1.1 Amphibious Robotic Crawler Platform

The SeaView Systems SurfROVer crawler is a battery-operated platform designed to traverse from shore to the surf-zone targeting applications such as route surveys, UXO surveys, cable/pipeline tracking, and active bathymetric surveying. The basic platform sits on a set of crawler tracks, each driven by a 3 kW hydraulic power drive unit (HPU). The tracks are comprised of 4 individual "Mattracks" made of mild steel, composite and rubberized plastic guide wheels, and 330mm wide (13-inch wide) rubber tracks. The contact area of each track is approximately 1200mm x 220mm, which is estimated to exhibit a modest ground pressure of around 10KPa (1 psi). This prevents the system from sinking into all seabed materials but soft mud. The vehicle has been designed to accept more ballast should operations prove to warrant an increase. Each track is driven by a hydraulic propulsion unit that combines BLDC motors and gerotor drives for hydraulic control of forward and backward motion. The ge-roller is a "generated roller rotor" consisting of concentric inner and outer rotors that act as a positive displacement pump (Ivantysynova, 2000). Figure 1 shows a photograph of the SurfROVer crawler system.

The SurfROVer utilizes a “ROV Backbone” system which has been designed by SeaView Systems to aid in the rapid development of custom underwater vehicles such as tunnel crawlers, customized ROVs, and articulated underwater robots. The ROV backbone provides power, fiber optic telemetry and peripheral device control options. System control is performed using an ethernet and RS-485 control protocol referred to as the “ROVbus”. This protocol is used to control devices such as the drive motor speed and direction, camera pan and tilt units, LED lights and dimmers, drive actuators (antenna poles, UXO sensor arm etc.). The fiber optic tether system is a proven and rapidly customizable technology used in multiple SeaView Systems ROVs and crawler units. Figure 2 illustrates the overall layout of the system including location of subunits and auxiliary sensors.

Figure 1. The SeaView SurfROVer Crawler System.

The platform sits on 4 rubber tracks with an axle baseline of 142 cm and total track base width (i.e., width of the platform) of 203 cm. The system is driven by 2 x 3 kW hydraulic geroller drives powered by two 7.5 kWh subsea lithium ion battery array (the two center cylinders on the platform). The frame and mechanical fixtures are comprised of anodized aluminum.

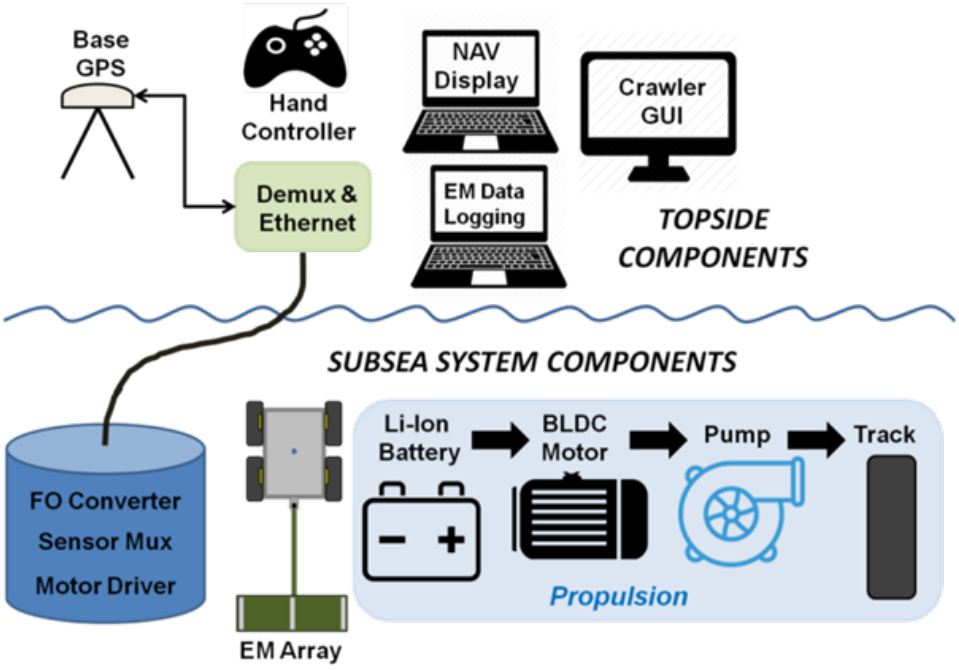

Figure 2. Block Diagram of the Overall System Configuration Split Between Topside and Subsea Components.

Subsea systems that travel with the crawler include the bottomside motor drive and multiplexer unit, the FlexEM array, and the power and mobility subsystem. Topside comprises the demultiplexer, handheld operator controller, GPS base station, and data processing and visualization computers and monitors.

Power is provided subsea (on the crawler - see Figure 3) through two 7.5 kWh battery pods that yield a nominal 12-16 hours of endurance. A non-tethered option is also available using a set of ethernet radios (Ubiquiti Bullet M radios) mounted on the GPS mast that telemeter data to linked radios at the operator control station. This wireless crawler telemetry system works for link distances of up to 1.5 km line-of-site (50+ km specification depending on antennas selected).

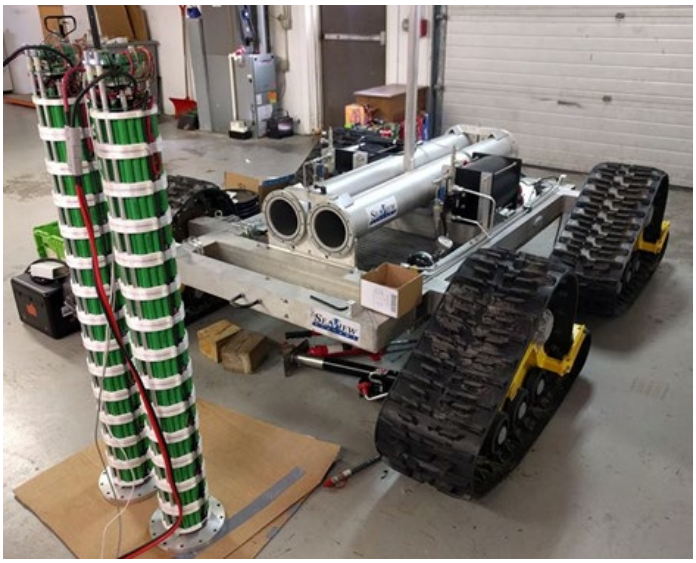

Figure 3. Cylindrical Battery Pod Pressure Vessels and Battery Cell Stacks.

Each stack contains 600 Li-ion cells to produce a total of 7.5 kWh power supply.

System control is performed using the ethernet-based ROVbus protocol. This protocol is used to control devices such as the drive motor speed and direction, camera pan and tilt units, LED lights and dimmers, drive actuators (antenna poles, manipulator arm, etc.). The fiber optic tether system is a proven and rapidly customizable technology proven in prior robotic marine units. Figure 4 illustrates the overall layout of the system including location of subunits and auxiliary sensors.

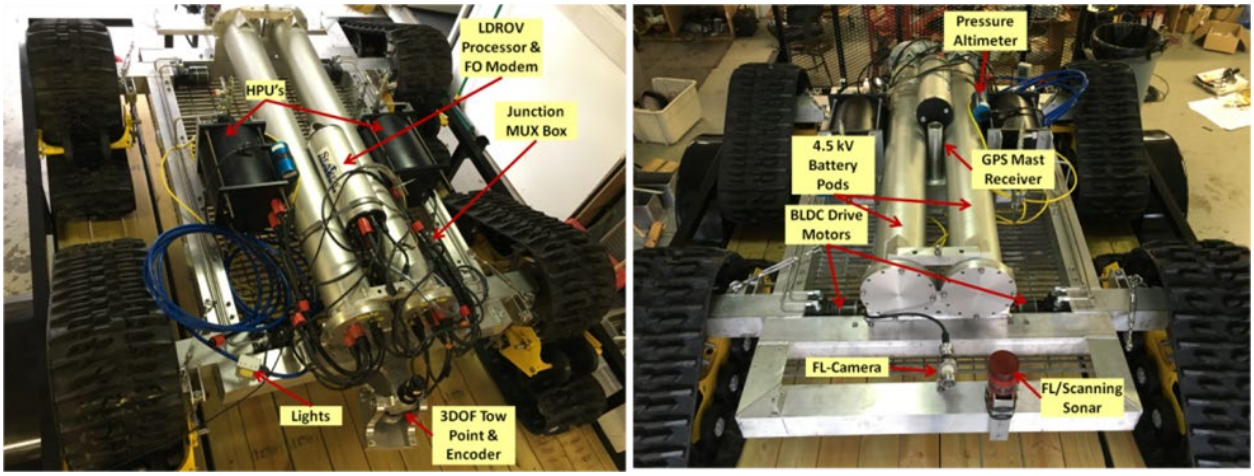

Figure 4. SeaView SurfROVer Crawler System with Annotations Describing the System Features and Subunits.

The crawler system is stable in sea states up to SS3 and sustained current conditions of 3 knots. One hundred liters of payload volume is available for carrying up to 150 kg of equipment or sensors. A range of payload power and data communication formats are available to accommodate most types of towed or rigidly attached sensors such as pipe/cable trackers, electromagnetic or magnetic sensor systems, sonar systems, optical systems, and sampling instrumentation. The maximum ground speed is approximately 5 kph with over 350 kgf of drawbar pulling force available for towing. Standard auxiliary sensing includes three RGB fixed view cameras, two sets of LED lamps, forward scanning sonar, obstacle avoidance camera, inertial measurement unit, pressure depth sensor, and compass. The position of the crawler is determined from a GNSS-enabled RTK-DGPS dual heading system mounted on a 6-meter mast for shallow water operations. Inertial guided underwater positioning can be readily augmented with USBL or LBL positioning systems.

2.1.2 Electromagnetic Induction Sensor Array

In conjunction with previous efforts (e.g., ESTCP MR-201225 and Army SBIR Topic A12-040) WRT has developed the Flex-EM marine array as a configurable high-resolution digital geophysical mapping system. The Flex-EM was developed as a marine version of the EMPACT Dynamic Discriminator (DD) time-domain EMI array (Laudato et al., 2016; Schultz et al., 2014). This system has been tested as an alternate to the EM61 for both terrestrial and marine surveys. It was specifically designed for detection and classification of UXO in challenging environments where ruggedization and mobility are key requirements.

The sensor tow package is comprised of two marinized transmitters and six small high-resolution marinized 3D EMI receivers mounted on a non-metallic sled riding on three ultra-high molecular weight (UHMW) skids. The sensor head features a form factor that is comparable to that of the EM61 coil and comprises base units with 1.0 m x 0.5 m transmitter coils that encompass 6 small (8x8x8 cm) 3-axis receiver cubes (see Figure 5). In the configuration for these demonstrations, the two transmitters are excited in series to form an effective single 2m by 0.5m loop. They are protected by a fiberglass and epoxy housing with wet-mateable marine connector and coil interconnects. Each receiver is also housed in custom PVC or delrin housing machined from monolithic blocks and fitted with O-ring seals and wet-mateable connectors. The enclosures were designed for and rated to seawater depths of up to 100 m. These receiver enclosures were previously tested in SERDP project MR-1714.

The system driver and data acquisition electronics are housed in a 9-inch outer-diameter cylindrical pressure vessel. The pressure vessel has been verified to accommodate other electronics modules such as an EM-61 console or MetalMapper 2x2 electronics. For the EM-61S marine coil, the sensor array mounting is very similar to the Flex-EM and readily accommodated through simple bracketry and fixturing. The electronics requires only internal jumper cables to the marine connectors on the pressure vessel (RS232 signals are readily handled by our existing wet-mateable connectors) and incorporation of a data consolidation and power supply circuit boards. Both PCBs have been developed, tested, and used with other systems. The data consolidation PCB has been validated to receive and converts EM-61 serial data to Ethernet format that transmits up the tow cable and/or written to local data storage devices.

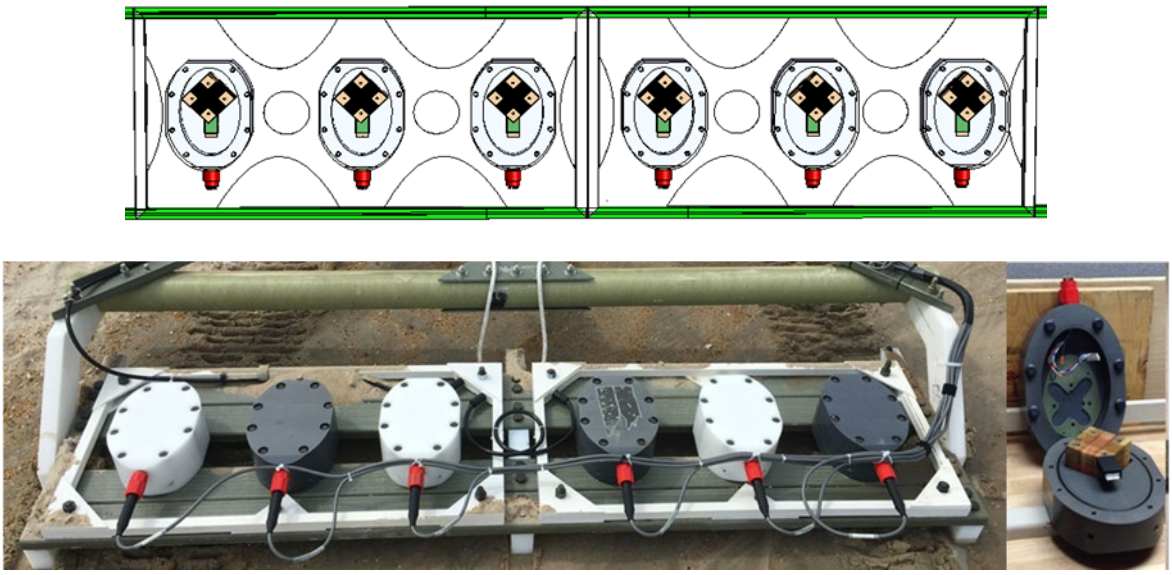

Figure 5. Top: Plan View Drawing of the Flex-EM Array Layout with 6 Triaxial Receivers Mounted in Pressure Vessels and Surrounded by 2 Transmitter Coils that Operate in Series. Bottom: Photograph of Half of the FlexEM Array Including the Transmitter and Receivers.

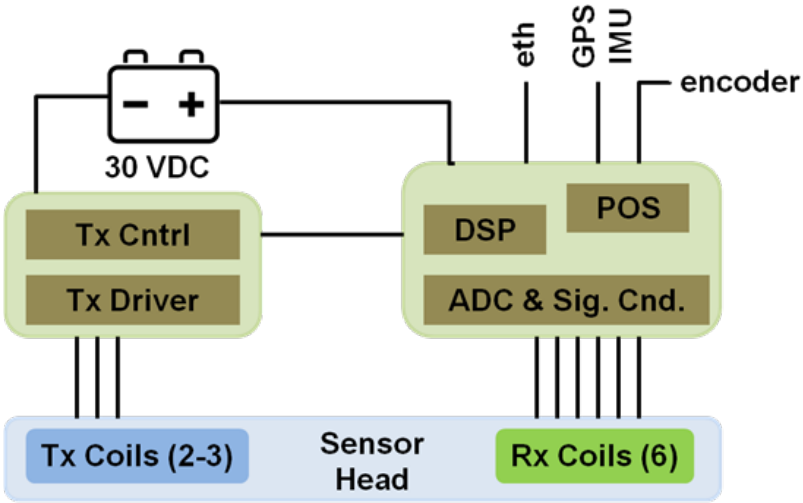

Figure 6. Schematic Diagram of the FlexEM System Elements.

The tow system with Flex-EM array weighs approximately 280 lbs in air and runs on 3 skids that exert a maximum static bearing pressure of 2 PSI on land and as low as 0.06 PSI in seawater. The tow sled also has a pair of low-profile foam-filled non-metal wheels that attach directly to the skids. These are primarily used for transit to and from the site location and surveys on dry beach or solid ground. Figure 7 shows the tow sled with the Flex-EM sensor mounted.

Figure 7. The FlexEM Array Including the Transmitter and Receiver Electronics Pressure Vessels, the Sled Attachment, and Transmitter and Receiver Components Mounted to the FRP Sled System.

The overall system components, developed in conjunction with previous DOD-funded efforts (i.e., Army SBIR A12-040), were completed in 2014 and implemented for terrestrial UXO surveys. This version of the system (known as the EMPACT Dynamic Discriminator) underwent terrestrial verification testing and evaluations at DOD UXO test sites between 2014 and 2016. Independent scoring of the Flex-EM array during these tests yielded unmatched performance relative to all previous man-portable systems in blind UXO grid trials achieving approximately 50% clutter rejection and approximately 88% background false alarm rejection while retaining a 99% detection probability. Localization accuracy was within 3 cm in lateral and 2.5 cm in depth (Figure 8). Subsequent dynamic classification testing at the Army's UXO site yielded 100% detection probability against small submunitions with 89% clutter rejection.

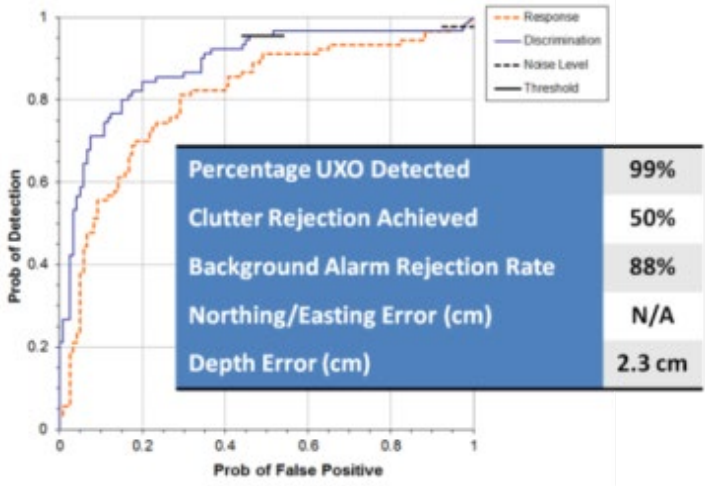

Figure 8. In April 2014, the Prototype EMPACT System Conducted Data Collections at the Aberdeen Proving Ground (APG) Standardized UXO Test Sites. Excellent Signal-to-noise Was Attained Over Small Targets and Deeply Buried Larger Munitions. ROC and Associated Analyses Were Performed by Independent DOD Analysts that Support the Army's Standardized UXO Test Site.

As the transmitter passes over the target, any offset of the sensor from directly over the target produces a different angle of incidence between the impinging transmitter field and the target. Alternatively, a multi-axis switching transmitter can be used to produce multiple angles of illumination from a single position. Raw decay transients received during transmitter off times are stacked (averaged) with appropriate sign changes for positive and negative half cycles. The resultant data are saved as a single scan consisting of multiple gate values between 50 us and 15 ms for each of the 3 triaxial components on all receivers. This nominally yields 288 individual data channels on each scan, which is repeated at a rate of 10 Hz. This data has been shown to produce adequate angular illumination and data quality so that dipole inversion methods can be applied for generating axial magnetic polarizability response curves.

2.1.3 Positioning and Vehicle Control

Positioning and navigation options for the crawler-towed system include both GPS-based and underwater positioning technologies such inertial navigation and ultra-short baseline (USBL) or long baseline (LBL) systems. Positional accuracy varies depending on the method used and can be dependent on site and deployment conditions. Practical experience with USBL positioning of ROV systems in a number of environments has yielded accuracies of approximately 1 m in less than 25 m water depths but larger positioning errors are typical. Although USBL is relatively simple to operate, bearing accuracies exceeding ~3 degrees lead to unsuitable positional errors for UXO detection operations that increase with range from the USBL transducer.

Our positioning problem is exacerbated by the fact that we have a two-body system comprised of the crawler itself and the tow platform. Although the tow platform is coupled to the crawler through a rigid tow bar, the tow point has 3 rotational degrees of freedom to allow motion over roll, pitch, and yaw angles. This means that the tow platform is not necessarily following directly in-line with the crawler trajectory. Therefore, we need to provide instantaneous relative position and orientation estimates of the tow platform relative to the crawler. This is accomplished through an absolute angle encoder at the tow point to measure the yaw (azimuth) and an inertial measurement unit on the tow bar that provides roll and pitch angles. These measurements can be combined with those measured on the crawler platform itself to generate relative orientation between the two bodies.

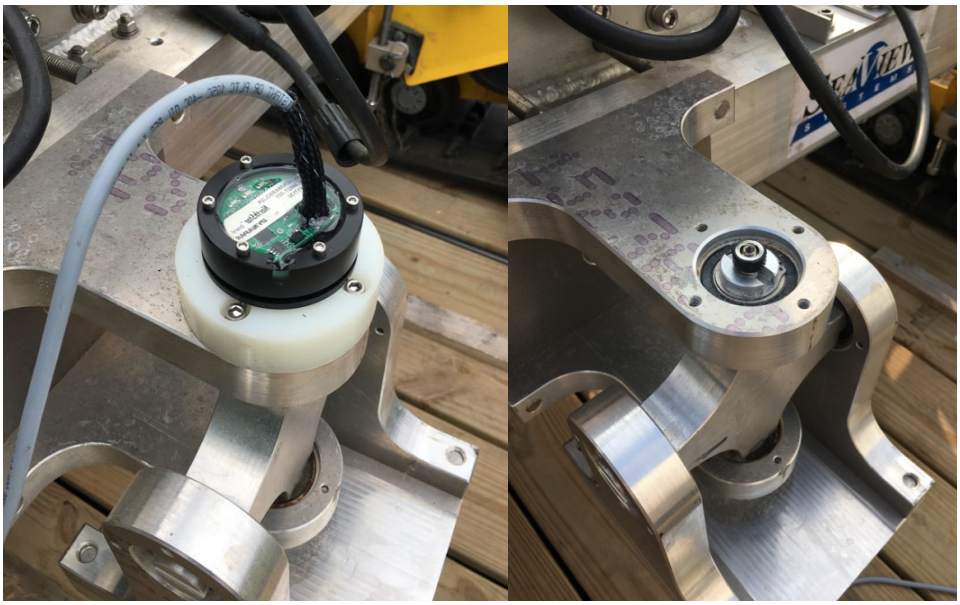

Figure 9. Photograph of the 3 DOF Tow Point Hitch and Absolute Angle Encoder on the Aft Portion of the Crawler.

The marine-grade encoder supplies serial data to the multiplexer and fiber optic tether modem or wireless radio network for topside data logging and integration with other navigation and positioning information.

Mounted on the crawler platform itself are sensors for positioning and orientation when the crawler is in sufficiently shallow water (<4m) and when it is in relatively deep water (>4m). In shore-based and shallow water operations, a rigid GPS mast provides a mounting point for an RTK-DGPS antenna at 6 meters above the base of the tracks (i.e., the seafloor in non sinkage/scour conditions). The mast extends down to a base point in the center of the crawler body. Mounted to the mast is a Hemisphere V320 dual heading marine-grade RTK DGPS system. This system allows acquisition of GNSS-enabled RTK-DGPS data. The Hemisphere V320 is based on the Eclipse Vector GNSS technology utilizing the all-in-one GNSS Eclipse vector-based receiver and two integrally separated rover antennas with a baseline of 50 cm. The V320 specifications indicate a heading accuracy of up to 0.17 degrees RMS and positioning accuracy down to 2 cm RMS depending on survey conditions. Precise RTK positioning is achieved through the Athena L1/L2 technology which is capable of integrated SBAS, beacon, and Atlas L-band. It also supports GLONASS, BeiDou, and GNSS augmentation automatically.

The rover antenna is 629mm long and 208mm wide, make it a bit larger than conventional single antennal RTK DPGS rovers. Once installed, the system has three serial ports for receiving differential corrections via full-duplex RS232 or RS422 connections. This is handled through a serial-to-NMEA 2000 port that contains both signal and power conductors through a single waterproof connector. A photograph and drawing of the V320 rover antenna are shown in Figure 10.

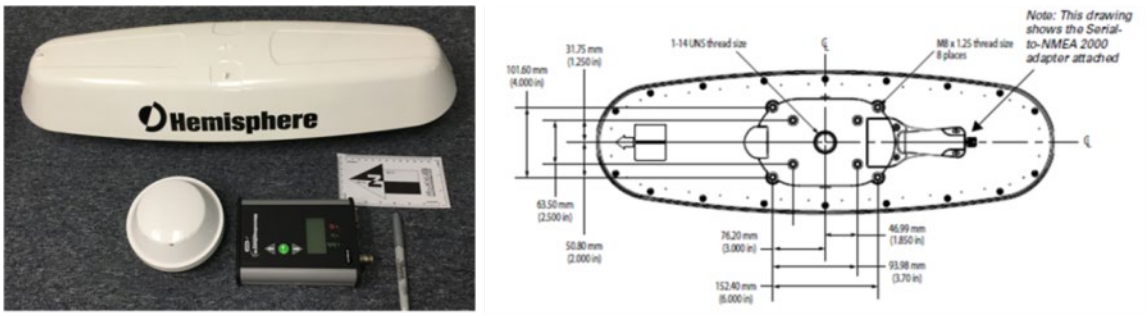

Figure 10. Photograph of the Hemisphere V320 GNSS Smart Antenna RTK DPGS System (Left) and Drawing of the Plan View Aspect of the Rover Antenna (Right).

The rover antenna is mounted to the GPS mast through a flush mounting template to ensure alignment relative to the tow point encoder and vehicle. The mast is comprised of multiple sections of schedule-40 fiber-reinforced plastic (FRP) and aluminum jointing fixtures. Two 10-foot long sections can be coupled to create a total mast height of 655 cm above the receiver base on the crawler, which is approximately 35cm above the track base. For the extended 6.5-meter-high mast, a series of spreader booms and dyneema rope stays are used to stabilize the mast under water. Photographs of the V320 GPS rover mounted on the mast are shown in Figure 11.

Figure 11. The Crawler System with Dual Heading RTK DGPS Rover Attached to Its mast (Left). The Extended GPS Mast and Tensioned Stays Are Shown With Antenna 6.5 Meters Above the Ground (Right).

2.1.4 Topside Operator Interface

The topside interface for the crawler-EM system is focused around the operator workspace and user interface. This contains a graphical user interface (GUI) and a joystick control box. The GUI is based on a software environment that provides correlation of navigation, control, and EM sensor data on multiple screens. Data are distributed and shared over an ethernet-based network via the topside de-multiplexer and ethernet switch. This provides a common network such that all subsea and topside networked devices can communicate, synchronize, share resources, and access common data.

An overview of the operator workspace is shown in Figure 12. The operator uses the joystick controller to guide the crawler based on the navigation display and 3-4 camera views placed on and around the crawler. We utilized: 1) mast camera, 2) forward-looking camera, 3) backward looking camera, and 4) downward looking camera views for the operator. The operator may also view real-time updated sonar image views from the sector scanning sonar display as well as real-time feedback from the battery management system.

Figure 12. The Topside Operator Control Station With Multiple Operator Displays.

These include (from left to right) the navigation and mission control user interface, 3 crawler-based cameras, the FlexEM array data acquisition and real-time display, the power management system interface and scanning sonar display.

The workspace environment enables real-time data acquisition and logging and mission pre-planning. The workspace also supports navigation with left/right indicators to keep the operator tracking the current profile line plan and waypoints. The navigation display also marks areas to avoid or site boundaries and alarms the user when the system is coming close to these areas. Global position and inertial data are updated on the display including RTK northing and easting updates, roll, pitch, and heading updates, as well as GPS UTC time and data quality indicator. Photographs of select camera views, the navigation software display, and the sonar and battery management GUI are shown in Figure 13.

Figure 13. Close-up Views of Some of the Operator Displays.

The top two monitors show camera views from the crawler, while the bottom tow monitors display the navigation and control interface software and the battery management and scanning sonar information to the operator.

For our demonstration, we added the Flex-EM data logging and real-time display on a separate laptop computer. The data logger GUI displays both GPS data information as well as waterfall trace profiles from each channel component of the array (6 tri-axial receiver channels). The GPS information displayed includes UTC time, latitude, longitude, northing, easting, number of satellites, signal quality type indicator, and the UTM zone used for UTM northing and easting values. The logger portion of the display includes the elapsed sortie time, EM time gates to display, axial component selection, display gain, and logging toggle buttons and filename entry as shown in Figure 14.

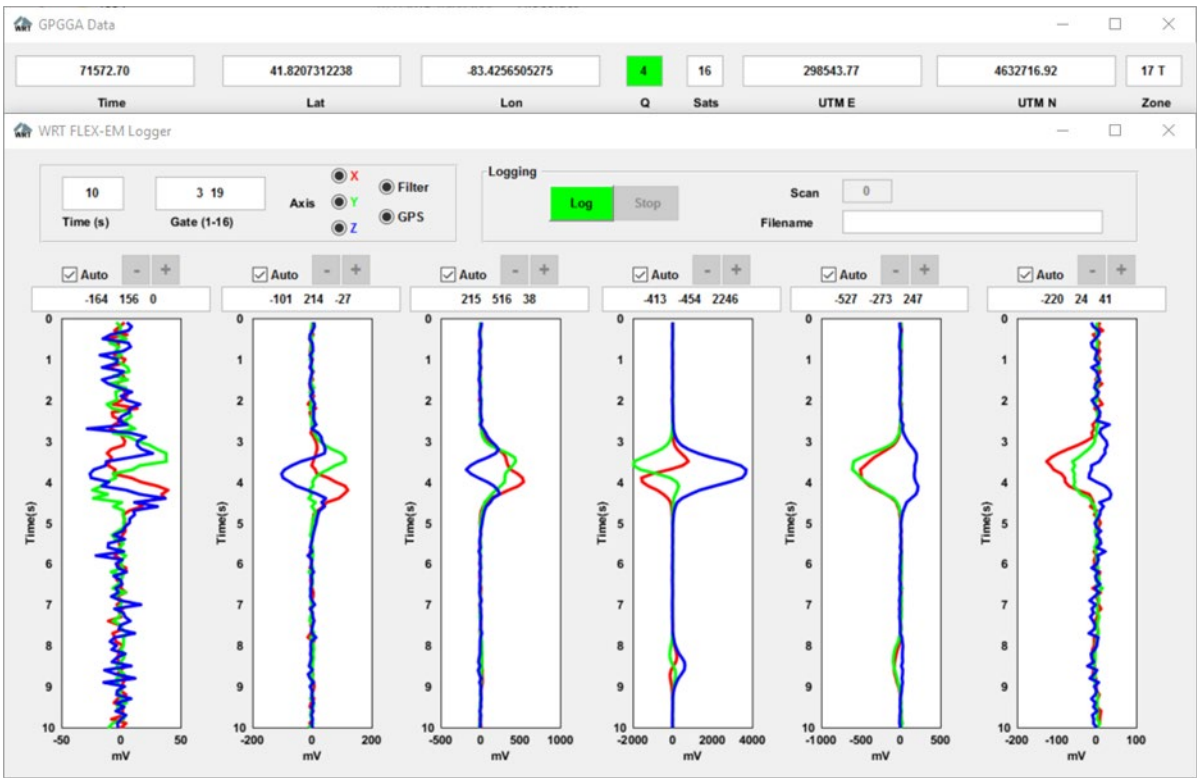

Figure 14. The Standalone FlexEM Data UI Showing Navigation Information Panel On Top and Real-time Waterfall Display On the Bottom.

Additional configuration and diagnostic feedback from the sensor system are displayed to the analyst. In this example, a clear anomaly is displayed (centered) for all axial components for the 6 receiver units across the array.

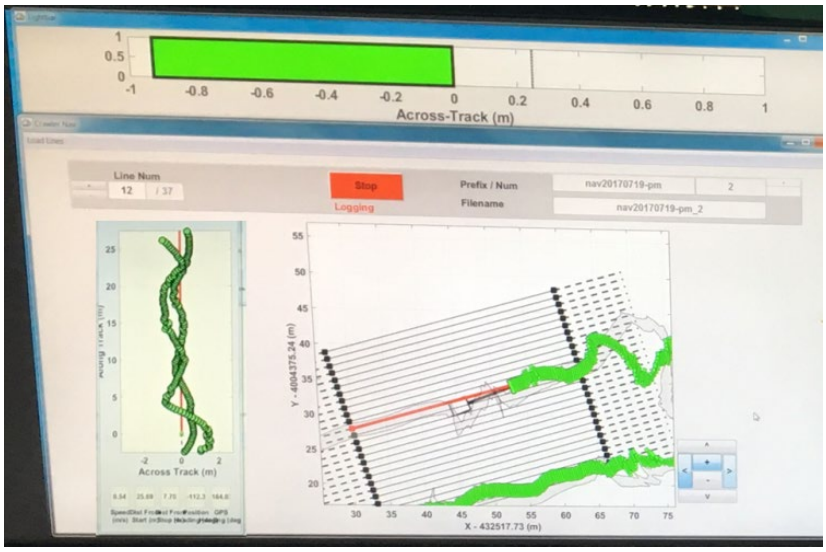

Figure 15. Photograph of the Navigation Display Used by the Helmsman Operator to Guide the Crawler and Array.

The user interface contains inputs for waypoints or automated trackline generation tools, file saving, left-right indicators, track-keeping indicators, and map view tracking of the system.

2.1.5 Launch and Recovery System

Launch and recovery of the system is relatively straightforward. The SurfROVer crawler system has been configured such that it can be hauled in a standard US DOT trailer that does not exceed the maximum of 102 inches (259 cm). We utilized two different trailers for the system during shakedown testing. The first trailer was a standard open deck car trailer as shown in Figure 16. The system is simply remotely driven on and off the trailer and tied down for transport. The second trailer used was SeaView's customized enclosed trailer that has been outfitted for marine/ROV operator workspace with up to 8 different monitors, power receptacles throughout, integrated tool chests, sink, and lighting. For transport, all workspace control station components are stowed and the SurfROVer crawler is driven into the trailer and tied down for transport. To deploy the system, the tether and operator control station is powered from ship, shore or generator and the crawler is driven from the trailer and connected to the EM array tow system.

Figure 16. Photographs of the Open and Closed Trailer Launching of the Crawler System.

The operators are able to launch and operate the crawler within minutes of arriving on site. The enclosed trailer system houses the crawler for transport and is converted into a fully functioning operator control station once launched. The OCS is completely outfitted for operations included all data displays, rack-mounted computers and data interface modules, dry and wet lab benches, and crawler control systems.

2.2 TECHNOLOGY DEVELOPMENT

Prior to this demonstration, we prepared and tested modifications and improvements to the overall system. These modifications were driven by lessons learned during prior tests in 2016 at Toledo Beach, Michigan and Duck, North Carolina. In those tests, we experienced limitations related to robustness and management of the fiber-optic tether extending from the crawler platform to the topside control unit. We also faced challenges with battery management in the form of frequent over-current faulting and associated need to reset the battery modules often during operations. Additional improvements were also made to the sensor array including replacement of the incremental encoder on the tow point with a high-accuracy absolute encoder. Lastly, changes to the power supply filtering and power isolation circuitry were performed to reduce the impacts of noise emanating from the relatively large electric motors on the platform.

2.2.1 Wireless Radio Link

During our tests and demonstrations at Duck in 2016, we utilized a thin fiber-optic tether connecting the crawler fiber-optic modem to a top-side transceiver located in the operator control station. While the tether and related subsea topside-subsea communications system functioned without exception during our prior tests, the tether required constant management and often got wrapped around the GPS mast during turning maneuvers. To ensure robust operation and reduce potential damage to the tether, we decided to utilize an improved Kevlar-reinforced tactical fiber-optic tether, although eliminating the tether altogether was deemed the most desirable improvement. Because the operational concept and mission plan for the system in nearshore areas always requires the GPS mast extending above the sea surface, we decided to investigate replacement of the tether with a wireless radio link.

To assess the potential of operations using a set of wireless radios in place of the tether, we replaced the subsea fiber-optic modem with a serial to ethernet converter. After a brief assessment of radio alternatives, we selected a pair of Ubiquiti M5 "bullet" radios that are capable of up to 600 mW power and 100+ Mbps TCP/IP data throughput. The radios are powered via power-over-ethernet (24 VDC), which made cable integration simple as both data communication and power were supplied through a single cable. At the power levels specified, we estimated over 5 km of range over nominal sea surface conditions. The radio link was propagated at 2.4 and 5 GHz using a pair of outdoor omni-directional dual band antennas (TRENDnet 5/7 dBi kit). A photograph of the antennas on a short mast are shown in Figure 17. The peak gains at 2.4 and 5 GHz for antenna are compatible with standard 802.11 ac/n/g/b/a routers and access points.

Figure 17. Photographs of the SurfROVer System Before (2016) and After (2017) Modification to Extend to Wireless Control and Data Transmission.

The short mast shown on the 2017 version of the system on the Right is prototype for testing. The wireless radios were subsequently retrofitted on the tall operational mast for our demonstration

This system was integrated with the crawler platform and tested at ranges of up to 2.5 km over land using simulated full-scale data throughput from the crawler to the topside control station. Subsequent to this, the EM sensor array and auxilliary sensors were fully integrated and validated using the wireless radio link at a land-based test site in Michigan.

2.2.2 Battery Management System

The second improvement that was developed prior to our 2017 field demonstration was related to robustness of the battery management system (BMS). During previous trials, when both battery modules simultaneously faulted due to over-voltage or over-current conditions, there was a potential for the power supply to critically shut down (thus being unable to restart itself remotely). To remedy this potential issue, we implemented an additional auxiliary power supply for resetting and/or maintaining asynchronous management of the, otherwise, independent power supplies. This allowed for resetting of power supplies under any condition, which provided needed back up for outages of any kind while remotely operated at sea.

In addition to battery management improvements, we also improved the usability of the system by installing pass-through connectorization at power supply bulkheads. This allowed for recharging of the battery systems without breaking any O-ring seals.

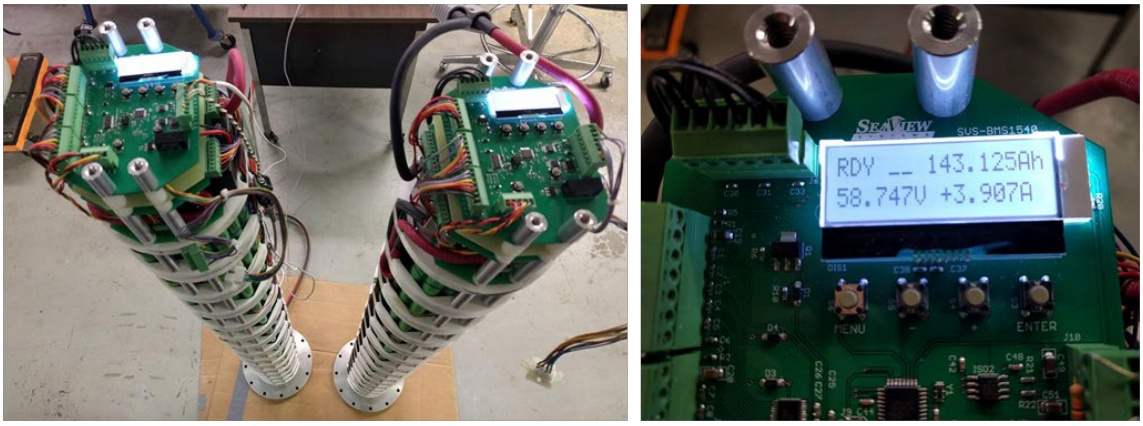

Figure 18. Photographs of the 14.5 kW-hour Battery Modules and Smart Battery Management System Electronics.

The system was improved and tested in 2017 prior to our demonstration to prevent automatic shutdown when overvoltage or overcurrent warning thresholds are exceeded.

Upgrades were also made to the configuration of the BMS functionality. It can now manage and distribute multiple functions related to managing the charging processing and monitoring and optimizing the batteries during operations via Columbe counter and current/voltage management and limiting control circuitry. The total energy available on the crawler is over 14.5 kiloWatt hours, thus the BMS also provides a means of controlling and managing the potential rapid dissipation of the power over time. In addition, monitoring each of the 40P cell packs wired in series, the BMS maintains cell balancing and monitors for overcurrent and short circuiting.

2.2.3 Tow Point Encoder Improvements

Among the more critical information supplied by the system is the crawler tow bar angle from an encoder at the tow point. Prior to this demonstration, we utilized a quadrature incremental encoder with a high degree of accuracy. This incremental encoder proved difficult to calibrate and baseline in order to provide useful angle information to support array positioning estimates. Therefore, we installed a new shaft-less absolute encoder (Northstar HDN58 series). This new encoder is completely sealed for marine use and has 0.1-degree accuracy. To accommodate the CANBUS interface, we developed and implemented an integrated circuit unit that converts the native CANBUS to serial RS232 output. The encoder was encased in a new azimuthal orientation unit that included an attitude heading reference sensor, and isolated power supply, CANBUS transceiver, and peripheral interface controller (PIC microcontroller).

Integration and validation of this unit was performed on the system during shakedown activities in Michigan and New Hampshire. Initial testing uncovered the need to filter and isolate power in order to provide consistent and robust functionality. Subsequent validation testing involved repositioning the encoder unit in various locations around the crawler platform and investigating for data dropouts or drift. Initial calibrations of the encoder were also conducted using the measured hard stop points on the machined metal tow point (as shown in Figure 9). A final full-scale test was performed in which data were collected during two independent experiments, each approximately an hour long. During the experiments the crawler and tow sled were operated over land while performing multiple maneuvers such as those used in surveys. Between the two experiments the encoder unit was power cycled many times. At the end of each data collect, the tow tongue was pushed all the way to its hard stop point at each extrema. As shown in Figure 19, no drift was observed during either of the data collects. The angle reported for the two hard right stop tests were the same (difference of 0); while the difference between the two hard left stops was 0.71 degrees. The small angular error observed during the left stop test was thought to be due to repeatability of the test procedure and not the accuracy of the encoder or any bias imparted during the test.

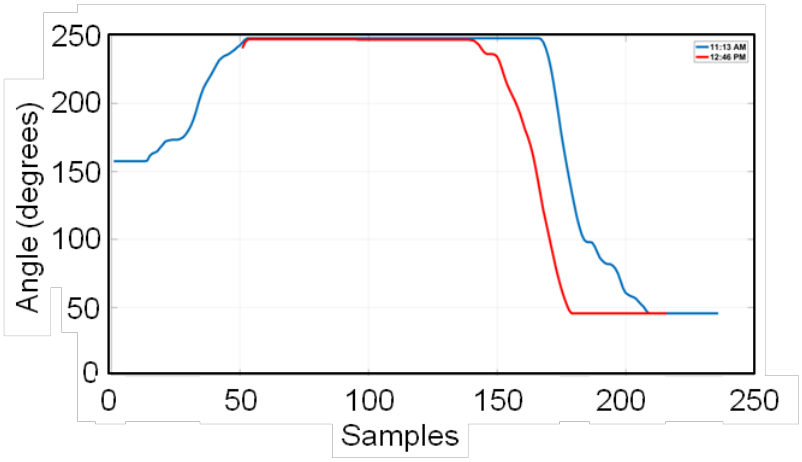

Figure 19. Plots of Two Independent Encoder Calibrations Where the Tow Tongue Was Rotated to the Port and Starboard Stops.

The total difference between the two separate port hard stops was 0.71 degrees while the starboard hard stops difference was 0.0 degrees.

Initial validation testing revealed an induced noise issue that resulted in complete failure of data transmission from the encoder. Once appropriate power filtering was in place, this issue no longer manifested, and data were output consistently without exception. Additional validation testing indicated that the encoder output was no longer affected by power noise regardless of the mounting placement or configuration of the encoder and no drift was observed.

2.2.4 Motor Noise Mitigation

During previous tests in 2016, we noticed noise pick-up, from time to time, directly to our receivers while the crawler motors were operating. Noise was isolated to inductive pick-up while only the motors were running, and the EM transmitter was not on. Additional optical isolation was introduced to prevent any directly coupled (galvanic) electrical noise from propagating through to the receiver and controller electronics. This greatly reduced the noise issues, but occasional wideband noise spikes were still observed at random yet very infrequent intervals during operation. Chokes were added to the motor output in attempt to reduce noise.

Additionally, a completely self-sufficient and independent power supply consisting of a battery pressure vessel (PV) and interconnection cables was constructed, implemented, and tested. The independent power supply also necessitated the fabrication of an electronics pressure vessel that multiplexed and managed power and data coming from the crawler, the encoder, the battery PV and the EM array. The combination of the common-mode choke coils added to the motors and the complete separation of input power from the crawler platform mitigated the motor noise issues we observed.

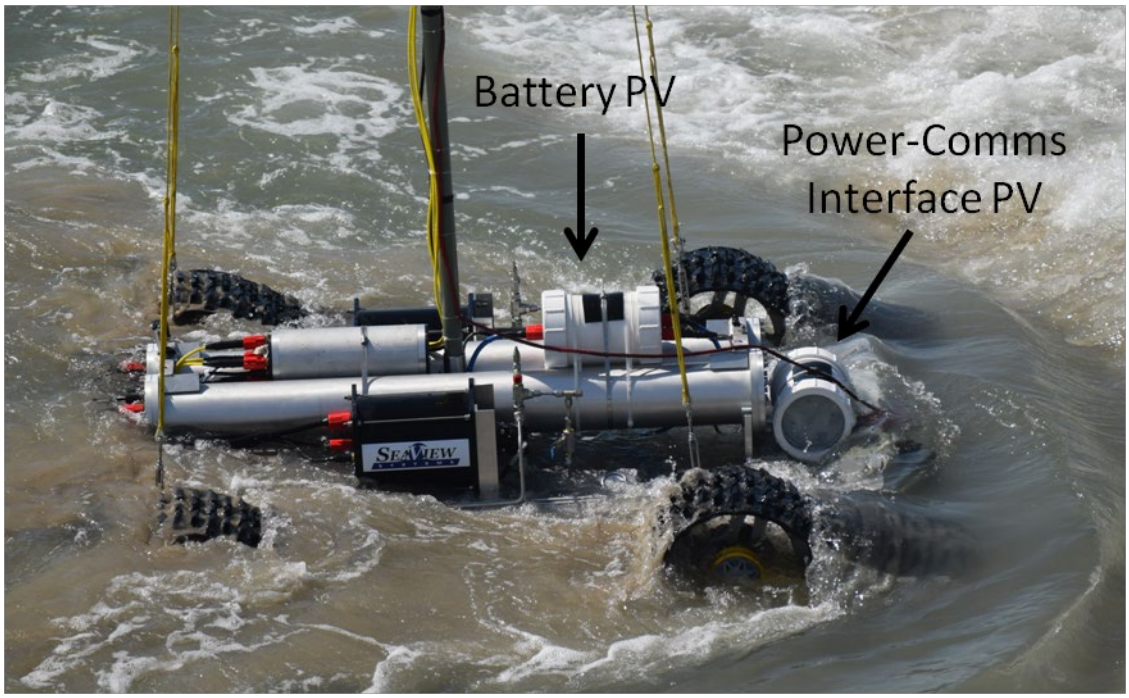

Figure 20. Photograph Showing the Two (white) PVC Pressure Vessels Added to the System to Accommodate the Fully Modular and Independent Power Supply and Power-communications Interface Pressure Vessels (PV).

2.2.5 FlexEM Array Improvements

In addition to crawler system and interface improvements implemented prior to our demonstration, we also assessed modifications of the FlexEM array for enhancing classification performance in one pass. The array configuration utilized in prior demonstrations consisted of two transmitters that were excited in series to form one effective transmitter across the array. To achieve ample multi-angular illumination of targets below the array, we aggregate data from consecutive soundings along the transect line (i.e., line methodology). As the transmitter passes over the target, any offset of the sensor from directly over the target produces a different angle of incidence between the impinging transmitter field and the target. For optimal classification results, we have found that it is best to include soundings from adjacent transect lines in the composite data set to ensure complete three-axis characterization of the target. Greater overlap in adjacent transects will produce higher quality classification; however, it is possible to achieve effective clutter rejection (discrimination) without overlap in sensor coverage.

To reduce the reliance on point-to-point positioning accuracy and increase the overall classification capability of the array, we assessed alternative multi-transmitter configurations. These included various excitation of three transmitter coils: port (left side) 1.0x0.5 m transmitter, starboard (right side) 1.0x0.5 m transmitter, and full array 2.0x0.5m transmitter (also configured as left and right in series). The configuration is depicted in Figure 21.

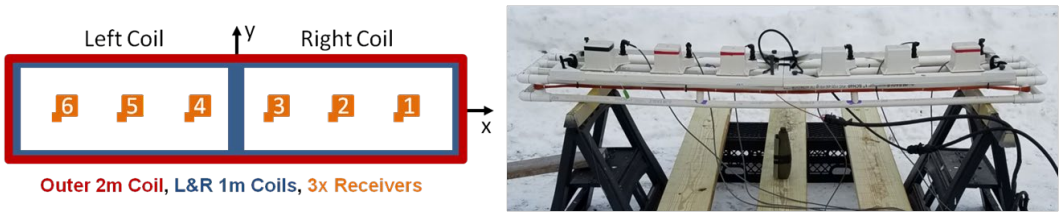

Figure 21. Left: Configuration of the Three-coil Modification of the FlexEM Array. The Red Outline Denotes the Outer Coil or Both Left and Right Coils Applied in Series to Form a Single Full-array Transmitter; the Blue Outline Denotes the Left and Right Coils Individually; and the Orange Indicates the Location of the Triaxial Receiver "Cubes". Right: Photograph of the Experimental Set Up for the Assessment. Pictured Here Is the Array with Transmitters and Receiver and a Test UXO Object (81mm mortar body) Used for Investigations.

This configuration enabled two primary types of multi-angular illumination of targets; (i) three transmitter "aiding" sequence, and (ii) two-transmitter "aiding/opposing" sequence. In the former the (t1) left, then (t2) right, then (t3) both transmitters are fired in a sequence as the array traverses forward. In the latter, the left and right transmitters are (t1) fired with opposing polarity (direction of current flow opposing) then (t2) fired in series with left and right transmitter in the same polarity or "aiding" each other.

Among the important considerations is the primary magnetic field distribution across the array. This is shown in Figure 22 for independent left and right transmitter coils compared with opposing transmitters in series. While the z-axis receiver data is nearly identical overall across the array for both configurations, there are some notable differences in the x-axis receive data. Namely, that overall the opposing configuration yields slightly greater signals across the array except for at the very center of the array, where the independent transmitters appear to have more aggregate signal.

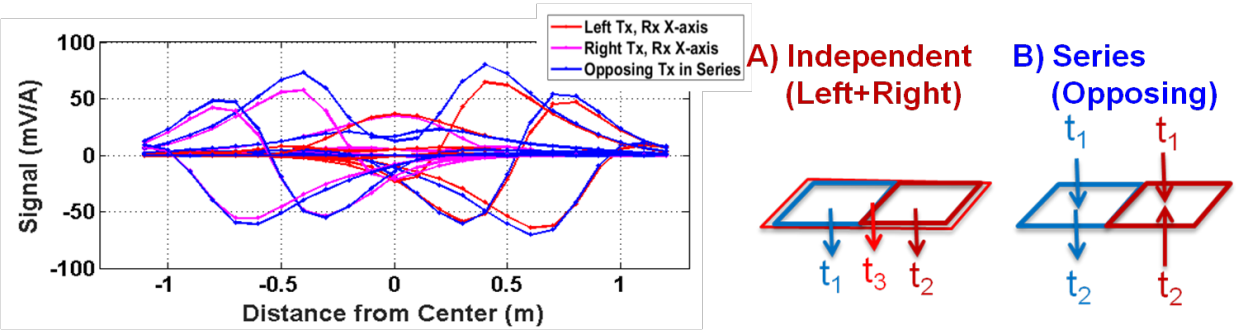

Figure 22. Comparison of the x-axis Received Signal Data Across the Array for Independent Left and Right Transmitters (Red and Magenta Curves) and Opposing Transmitters in Series (Blue Curve).

Similar signal envelope coverage is evident with the exception of the area beneath the centermost part of the array where the independent arrangement yields stronger signal.

After assessing the illumination coverage beneath array, we investigated the differences in resulting inverted magnetic polarizability curves as a function of turn-off time. For these tests, we utilized an 81mm mortar as a surrogate UXO test object under the array. The UXO was placed 50 cm beneath the approximate center of the transmitter. We first analyzed and compared the resulting polarizabilities to see what differences may exist between the independent and opposing side-by-side transmitter configurations. Figure 23 shows the resulting polarizabilities are of high quality for near the entirety of the 10 ms time window. The library match to the 81mm UXO library was 0.975 for the independent configuration and 0.970 for the opposing in-series configuration.

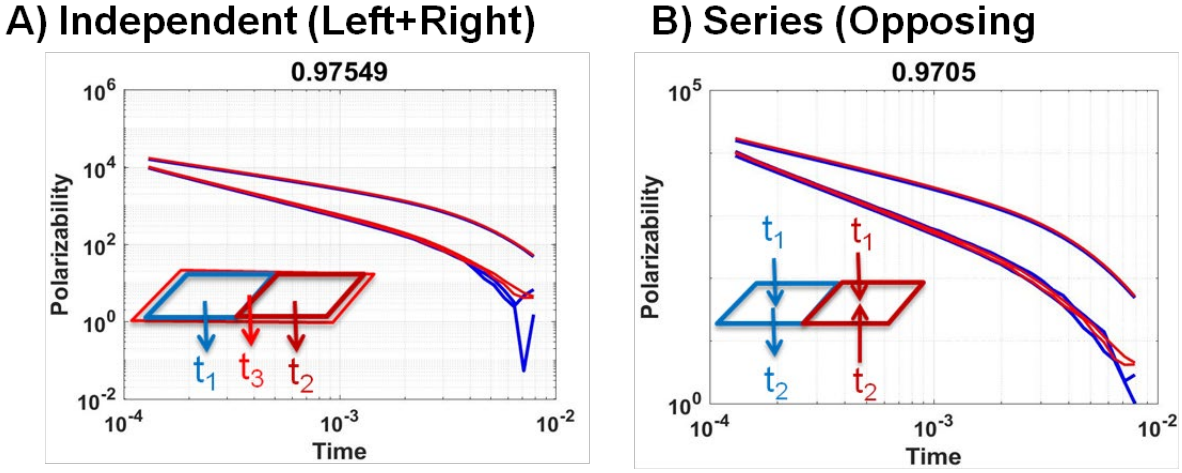

Figure 23. Inverted Polarizability Curves Comparing the Independent Left, Right, and Both Transmitter Coil Configuration to the In-series Opposing Left and Right Transmitter Coil Configuration.

The red curves are the 81mm UXO libraries for X, Y, Z and polarizability evolution and the blue curves are the respective inverted polarizabilities from data collected in land-based test stand tests. The library match to the 81mm UXO library was 0.975 for the independent configuration and 0.970 for the opposing in-series configuration.

The final element of our analysis of the improved switching transmitter capability for the crawler-based FlexEM array involves quantifying the effects of positioning error on the polarizability library fit metric. Here we look specifically at the in-series opposing (aiding-opposing) configuration. Using the data acquired with the target in a known position (i.e., "zero" positional error), we can synthetically add positional error and assess the resulting misfit between library and inverted polarizabilities. Figure 24 shows that this configuration is mostly robust to positional errors of up to 5-10 cm before match fit statistics fall below acceptable levels for reliable classification. At 20 cm of positional error, the mean fit metrics are approximately 0.50 and not supportive of single-shot dynamic classification.

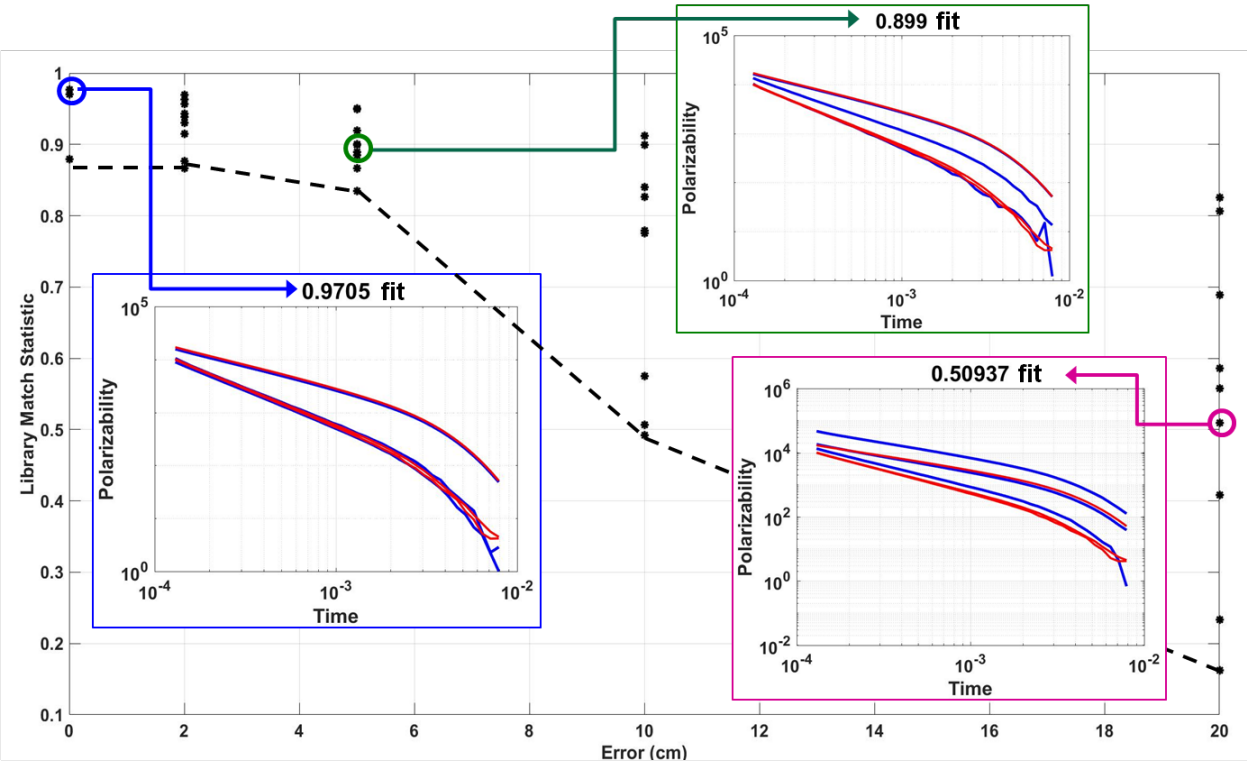

Figure 24. Results of Simulated Positional Offset for In-series Opposing Side-by-side FlexEM Transmitter Coil Configuration.

In this experiment, we placed a test UXO object below the array at multiple positions and added varying levels of error to the data prior to inverting for the triaxial magnetic polarizability curves shown. The inverted polarizabilities RMS fit error to an independently acquired and "perfectly" positioned set of library polarizabilities are shown for the 3 particular cases: 0 cm positional error (blue), 5 cm positional error (green), and 20 cm positional error (magenta). The match fit statistic appears to degrade below acceptable levels (0.85 fit) between 5 and 10 cm of positional error.

2.3 ADVANTAGES AND LIMITATIONS OF THE TECHNOLOGY

The crawler-based EMI technology has particular advantages over surface-towed or ROV-based deployment methods in challenging nearshore areas such as surf-zones and strong tidal channels.

Divers are highly constrained in terms of their mobility, depth and duration during dives due to strict health and safety regulations. Surface towed systems as well as fully autonomous unmanned undersea vehicles (UUVs) place sensors 2-5 m above the sea floor, and thus restrict detection capabilities to large UXO only. The crawler-based EMI technology demonstrated has particular advantages that can be leveraged for marine UXO operations:

- Stability and mobility in challenging high-energy nearshore environments
- On-shore / off-shore capability
- Integrated crawler and high resolution active-source EMI array.
- Tele-operation
- Tightly integrated vehicle position and control with high resolution active source EMI data. This leads to improved detection and a reduction in false alarm rate through improved classification resulting from high resolution EM sensor data collected synchronously with high resolution position data.
- Real-time operator situational awareness and dynamic repositioning capability. This provides operators both dynamic mapping mode and detailed reacquisition or static characterization data collection over suspected targets.
- Precise navigation and positioning of the sensor array in close proximity to the seafloor. This provides accurate positioning, tracking, and bottom following, which leads to improved survey efficacy and efficiency. Because signal levels drop off quickly with range from a target, it is critical to accurately and precisely position the sensor in varying conditions.
- Tele-operation removes the operator from the water column and allows for accurate operations in both shallow (<3m) and deep water (>10 m).

Limitations of the technology to be demonstrated include:

- limited high-end speed (<5 kph)
- loss of positional accuracy in water depths greater than the height of the GPS mast
- transportability
- tether system
- seafloor obstructions and tight area investigations (due to turning radius required)

Page Intentionally Left Blank

3.0 PERFORMANCE OBJECTIVES

The performance objectives are focused on demonstration of integrated system (crawler and EMI array tow platform) mobility, stability, and precise system positioning and control required for execution of UXO detection and characterization missions. The functions to be demonstrated include stability in surf zone conditions, mobility and area coverage, on-shore / off-shore traverse over varying bottom substrates, EMI array positioning, UXO detection performance, and clutter rejection capability. These objectives are summarized along with their respective success criteria in Table 1.

Table 1. Performance Objectives

Performance Objective	Metric	Data Required	Success Criteria
Quantitative Performance Objectives			
Surf-zone Stability	Average error between desired and true roll, pitch, yaw, horizontal position, and altitude of system, standard deviations during 10 m long shore-parallel and shore-normal traverses in water depths of approximately 0 m, 1 m, and 2 m below MSL	• Desired tolerances on orientation and translation of the sensor array • Current velocity data from an ADCP array • Orientation and translation position data from the navigation and control system	$\Delta R < \pm 6°$, $\sigma R < 3°$ $\Delta P < \pm 6°$, $\sigma P < 3°$ $\Delta Y < \pm 4°$, $\sigma Y < 2°$ $\Delta X < 0.20$ m , $\sigma X < 0.15$ $\Delta Y < 0.20$ m , $\sigma Y < 0.15$ $\Delta A < 0.10$ m , $\sigma A <$ 0.15
Area Coverage	Average forward advance rate over 5 adjacent (100% coverage) shore-parallel traverses in water depths between 1 and 3 meters	• Position, time, and orientation reports from the navigation and control system	100% Coverage Rate $\geq$ 0.2 hectare / hour
On-shore / off-shore Mobility	Average forward advance rate over 5 adjacent (100% coverage) shore-normal traverses in water depths between 0 and 2 meters	• Position, time, and orientation reports from the navigation and control system	Advance. Rate $\geq$ 0.30 m/s
Detection of all munitions greater than 60 mm	Signal to Noise Ratio (SNR) of signal produced by munition in EMI sensor to noise in EMI sensor	• Signal received during anomaly interrogation • Noise estimate during anomaly interrogation • Position reports from the navigation and control system	SNR > 9 dB
Detection Location Accuracy	Average error in northing and easting between true position and estimated target position	• EM array data • Navigation data • True Target Locations	ΔTN and $\Delta TE < 1.0$ m σTN and $\sigma TE < 0.5$ m
Classification of all munitions ≥60 mm	Number of munitions (≥60mm) identified as such out of total number of TOIs detected (Pclass)	• Signal received during anomaly interrogation and resulting inverted polarizabilities • Ranked anomaly list • Ground truth target positions	Probability of Classification, Pclass>0.75 with at least 50% of clutter ranked below the UXO

Table 1. Performance Objectives (continued)

Performance Objective	Metric	Data Required	Success Criteria
Qualitative Performance Objectives			
Ease of use	Operator observations	• Field notes recorded during setup and testing	Ease of use compared to alternate standard marine surveying procedures
Launch and recovery	Operator observations	• Time to launch/recover • Observational notes	Time to launch, time to recover, mean down time

3.1 OBJECTIVE: SURFZONE STABILITY

3.1.1 Metric

Compare the measured roll, pitch, yaw, and translational motion of the crawler and the sensor tow sled over time periods consistent with the relevant sensor measurement bandwidth (approximately 0.3 to 3 Hz). Changes in roll, pitch, yaw, longitudinal, transverse and vertical motions over measurement intervals between 300ms and 3s will be averaged over 1-2 minute periods and the standard deviation will be calculated.

3.1.2 Data Requirements

Orientation data will be derived from the IMU systems mounted on the crawler (in the control system pressure vessel), on the EM tow platform (forward of the center of the array), and in the GPS rover antenna (embedded in the V320 dual heading system). We will also acquire pressure depth and acoustic altimeter data for the crawler platform. We will calculate the stability metrics for experiments in which the system is traveling perpendicular to the shore in water depths between 0 and 2 meters. This will test the stability of the system through a range of dry sandy beach, saturated sandy beach, swash and surf including the wave breaking zone where hydrodynamic forces are extreme. We will record roll, pitch, and yaw directly from the IMUs and estimated translational motion will be derived from double integration of measured accelerations. All data will be acquired at 10 Hz or faster rate. Each test will be repeated to estimate variability.

3.1.3 Success Criteria

Our objective is to achieve roll and pitch stability to within ±6° and yaw stability within ±4° for both the crawler platform and tow sled platform over the frequency range relevant to EM array sensor measurements. Translation motion should remain within the tolerance envelopes specified over the duration of each test: less than 20 cm of sway and surge motion, and 10 cm of heave motion.

3.2 OBJECTIVE: AREA COVERAGE RATE

In our demonstration, area coverage refers to the system's ability to maintain an adequate advance rate for efficient surveying while operating parallel to the shoreline. The ability of a crawler-based system to cover a nearshore area is an important criterion in determining its survey efficiency relative to comparable methods. This is a function of the advance rate, maneuverability, and stability. These tests will be conducted in shallow water areas in water depths averaging between 0 and 2 meters.

3.2.1 Metric

Compare the measured coverage rate of the platform to the success criteria. The key metric is the areal coverage rate with as close to 100% coverage as possible. The resolved forward motion of the sensor sled will be determined by combining information from the GPS position, orientation, and velocity measurements with relative yaw measurements of the tow sled given by the tow point encoder. The average advance rate will be calculated as the average over all traverses. The total coverage area should be approximately 1375 m2 if 100% coverage is possible and average production rate would then be the total coverage area divided by the total time including turn-arounds.

3.2.2 Data Requirements

To demonstrate the area coverage or advance rate, we require data from the GPS and the tow point encoder. We will also record pressure depth and altimeter height of the crawler platform. Data will be recorded at a rate of 1 Hz or higher.

3.2.3 Success Criteria

Our objective is to achieve a 100% coverage rate of 0.2 hectares per hour. This equates to approximately 0.22 m/s or 0.4 knots of averaged forward advance rate if 1 m line spacing is used (150% overlap of the 2-m wide array).

3.3 OBJECTIVE: ON- AND OFF-SHORE MOBILITY

The system's ability to operate in survey mode while traversing on-shore to off-shore and vice versa is an important mission feature. Effective operations perpendicular to the shoreline requires stability of both the crawler and sensor platform to maintain a suitable advance rate. This allows for continuous surveying in an out of the water and over areas of very shallow water such as the swash zone.

3.3.1 Metric

Compare the measured average forward velocity of the platform moving from dry land to submergence under 2 meters of water to the success criteria. The resolved forward motion of the sensor sled will be determined by combining information from the GPS position, orientation, and velocity measurements with relative yaw measurements of the tow sled given by the tow point encoder. The average advance rate will be calculated for at least 5 traverses extending from on-shore to off-shore and 5 traverses extending from off-shore to on-shore in approximately the opposite direction. Multiple traverses in the same direction will be averaged and advance rates will be computed separately for shoreward and seaward directions.

3.3.2 Data Requirements

To demonstrate the area coverage or advance rate perpendicular to the shore, we require data from the GPS and the tow point encoder. We will also record pressure depth and altimeter height of the crawler platform. Data will be recorded at a rate of 1 Hz or higher.

3.3.3 Success Criteria

Our objective is to achieve an average forward advance rate of the system for shore-perpendicular traverses of at least 30 cm/s (1.1 kph or 0.58 knots) regardless of direction (seaward or shoreward).

3.4 OBJECTIVE: UXO DETECTION PERFORMANCE

The ability of the crawler-based EM system to detect relevant UXO simulant objects yields quantification of a key system metric. To produce detections the EMI array must be functioning properly, data must be processed in order to improve signal-to-noise characteristics, and positioning of receivers must provide the resolution required to delineate individual targets of 60 mm diameter or larger.

3.4.1 Metric

Compare the total number of target encounters to the actual number of targets detected. A target encounter is determined by any part of the EMI sensor have an easting and northing coordinate within 0.5 m of the recorded position of a seeded test item while at a reported altitude less than 0.5 m. The metric that we will measure will be the Signal to Noise Ratio (SNR) of the signal produced by a munition in EMI sensor to the noise in EMI sensor.

3.4.2 Data Requirements

Georeferenced EMI sensor and navigation data correlated in time are required for input into custom detection algorithms.

3.4.3 Success Criteria

Our objective is to achieve an average SNR of 9 dB or greater over all target encounters against targets that are 60 mm in diameter or larger at CPA ranges of 10 times or less the diameter of each object (e.g., 60cm for a 60mm projectile).

3.5 OBJECTIVE: UXO DETECTION LOCATION ACCURACY

The ability of a crawler-based EM array to produce accurate anomaly locations is critical to UXO survey and detection missions. To produce accurate detection locations, the estimated position of the EMI sensor must be accurate during target investigations.

3.5.1 Metric

Compare the estimated position (northing, easting) of each target detected by the EM sensor to the true position of each target. Average northing and easting error, defined as the mean of reported position minus the true position, will be calculated. Separate metrics will be reported for detection surveys along shore-parallel and shore-perpendicular transects in order to segment any potential directional biases.

3.5.2 Data Requirements

Georeferenced EMI sensor and navigation data correlated in time are required for input into detection algorithms.

3.5.3 Success Criteria

Our objective is to achieve an average northing and easting error less than 100 cm and standard deviation of less than 50 cm.

3.6 OBJECTIVE: UXO CLASSIFICATION

Our objective is to successfully classify emplaced UXO as such.

3.6.1 Metric

We will apply a Probability of Classification (Pclass) metric. Pclass will be determined from the ratio of the number of UXO correctly identified as such to the number of UXO detected.

3.6.2 Data Requirements

We will apply classification to all regions-of-interest (ROIs) generated from the detections identified in the dynamic survey data. Each ROI will contain a subset of soundings from the dynamic data that correspond to an anomaly. Base on the results of inverting these data, we will generate a ranked list of likely UXO. This list will be scored based on the emplaced target ground truth list. The scoring results will quantify the classification performance.

3.6.3 Success Criteria

Pclass>0.75 with at least 50% of clutter ranked below the UXO will indicate success.

3.7 OBJECTIVE: EASE OF USE AND OPERATOR INTERFACE

The ease of use of the integrated system including control of the crawler system, EMI sensor, topside control system, and navigation and mission planning/lane following is important to determine the level of training required for use of this equipment in a production environment. Ease of setup, calibration, and operation will be determined.

3.7.1 Metric

There will be no specific quantitative metric for this objective. The qualitative metric will be determined based on notes and observations from operators and crew.

3.7.2 Data Requirements

Observations and field notes taken by test personnel will be reviewed to determine the qualitative ease of use of each component in the system and identify any shortcomings of each component's operation.

3.7.3 Success Criteria

Success will be relative to other similar survey systems in the experience portfolio of the operators. If the system is considered significantly more complex, difficult, or unwieldy relative to similar or comparable marine survey systems, it will not be considered successful.

3.8 OBJECTIVE: LAUNCH AND RECOVERY

Launch and recovery encompasses all resources and processes required to mobilize and deploy the integrated system to and from the survey area. We also include required maintenance or other standard procedures for keeping the system operating efficiently during operations. For example, we will assess the time and effort required to stabilize the system using ballast, if needed. This may be necessary when moving from one operating area (e.g., freshwater to saltwater; or high to low energy hydrodynamic environment) to another.

3.8.1 Metric

There will be no specific quantitative metric for this objective. The qualitative metric will be determined based on notes and observations from operators and crew.

3.8.2 Data Requirements

Observations and field notes taken by test personnel will be reviewed to determine the effectiveness of launch and recovery (e.g., shore- versus ship-based), battery charging and endurance, tether management, system stowage, and required maintenance of mechanical components such the hydraulics system.

3.8.3 Success Criteria

Success will be evaluated relative to nominal remotely operated marine systems. An evaluation of shore and (hypothetical) ship launch and recovery and general system maintenance will be conducted and reported on.

4.0 SITE DESCRIPTION

The primary site for this demonstration comprises beach and nearshore areas at the USACE Field Research Facility (FRF) in Duck, North Carolina. This site provides a mix of conditions and excellent support infrastructure for engineering evaluations with thorough testing under representative conditions. The following sections describe the site selection and site areas in more detail.

4.1 SITE SELECTION

This demonstration was the first field data collection of the combined crawler-based EMI technology. This data collection was intended as a thorough shakedown and evaluation in preparation for follow-on demonstrations. As such, the site should contain a wide range of features and conditions to provide the most thorough assessment as possible. The test-site preferably has: (i) hydrodynamic challenges such as currents of 1 to 3 knots and surf/breaking wave conditions; (ii) a range of different water depths; (ii) variable bottom type and topography; and (iv) both large (155mm) and smaller simulant munitions (60mm) or munitions surrogates (ISOs). This demonstration was also intended to test extended capability from beach and shorelines areas to deeper water (>2m) coupled with challenging hydrodynamic environments. Amongst the most difficult and potentially interesting nearshore environments are those with high energy surf encompassing a range of wave heights and types, substrates, and water depths (from dry to 2-3 meters submergence).

Given the range of conditions desired and support infrastructure available, we proposed the nearshore areas at the USACE FRF for both engineering tests and more comprehensive site demonstrations. This facility is managed by the USACE Environmental Research and Development Center (ERDC) and houses an on-site permanent staff of about 13-15 scientists, engineering, and technicians. It resides in the northern portion of the outer banks barrier island chain near the North Carolina - Virginia border. An overview map of the outer banks and general site location are shown in Figure 25. The FRF site also provides water conditions and support logistics that are supportive for the timeframe and desired operations for demonstrations.

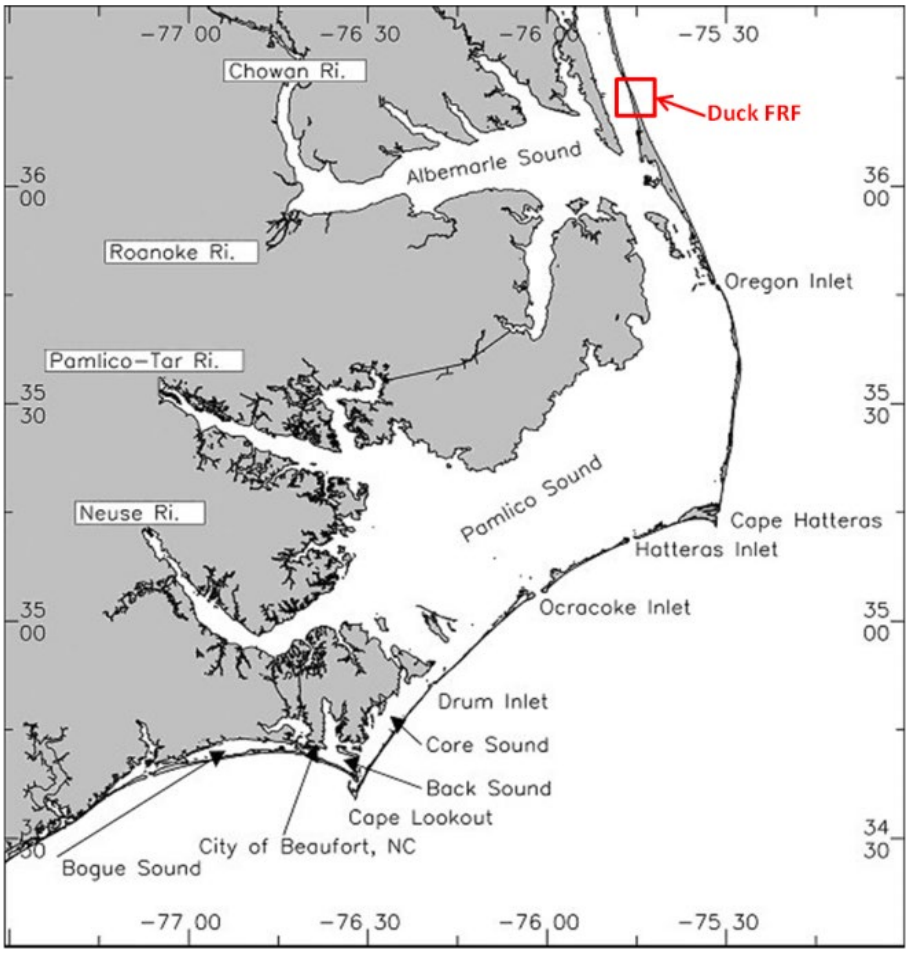

Figure 25. Regional Map of the North Carolina Outer Banks and General Site Area Location at the US Army Corps of Engineers (USACE) Environmental Research and Developmental Center (ERDC) Field Research Facility in Duck.

The demonstration is along the beach and seaward shore of the barrier island adjacent to the FRF pier.

The general test area is located within the USACE FRF site approximately 100 km south-southeast of Norfolk, Virginia. The FRF was established by the USACE in 1977 to support coastal engineering research. The facility consists of a 560-meter-long research pier (see Figure 26), a main office building, large high-bay field support building, and a 40-meter-high observation tower. Since its creation, the FRF has maintained long-term monitoring records of coastal oceanographic information including waves, tides, local meteorology, and concomitant beach response. The USACE monitoring program is supported by a field staff and several unique vehicle platforms that permit successful operation in the turbulent surf zone and adjacent nearshore environments.

Figure 26. Photograph of the FRF Pier Extending 560 Meters into the Atlantic Ocean.

Note also the extensive surf zone at the site that extends out many 100's of meters from the shoreline.

The selection of the particular survey areas was determined in conjunction with FRF staff. The area just south of the FRF pier has been well studied and is the area we selected for conducted on-shore and off-shore data collection. The criteria for selecting data collection areas represent a tradeoff between desired site conditions and access and availability. Preferred site conditions contain a range of water depths and variety of bottom types and current conditions. The site was amenable to access by USACE vessels such as the CRAB to support seeding of surrogate targets and standard test objects (e.g., ISO's). This part of the site has had extensive prior marine surveying conducted to help pre-characterize site conditions and survey areas.

Shallow water areas of interest are 0-3 meters deep with seafloor conditions that ranges from relatively flat sandy bottom to gravely sand to more complex bottom types and hydrodynamics. The use of these sites allowed us to configure, test, and assess system validation results from realistic conditions without incurring logistics and DoD intrusive site investigation expenses that would be required for demonstration at a live site during this stage. An example bathymetric profile acquired just north of the FRF pier during preliminary testing at the site is shown in Figure 27.

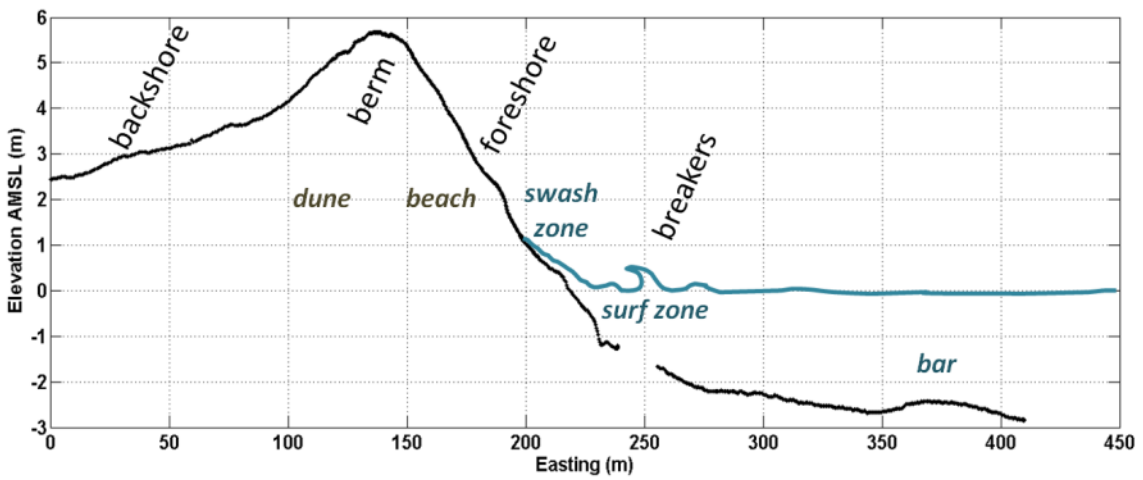

Figure 27. Annotated Bathymetric Profile in 2015 During Preliminary Testing at the Site.

This profile was acquired along a shore-perpendicular transect from the CRAB platform approximately 75 meters north of the FRF pier.

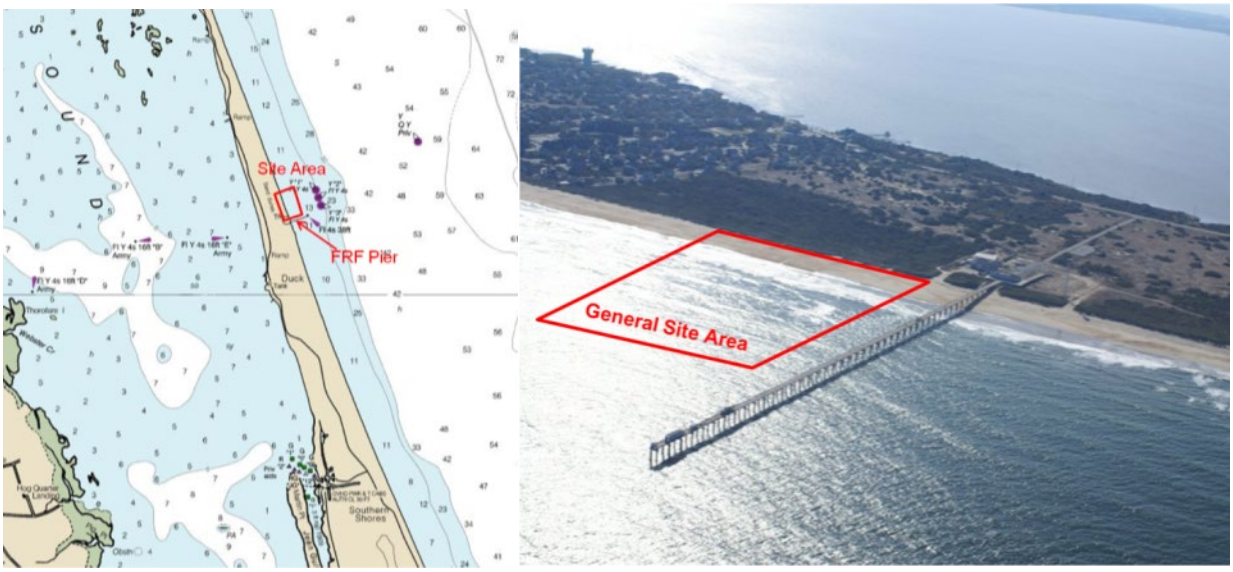

Figure 28. Left: Location of the FRF Site and Pier Annotated Over the NOAA Nautical Chart for this Part of the Outer Banks. Right: An Aerial Photograph Looking West Over the FRF Site with Pier in the Foreground and Facility Buildings Beyond the Dune Ridge.

The Currituck Sound is the background part of the photo. The general site area is outlined in red.

At FRF there is an array of permanently installed instruments to measure wave heights, currents, and water conditions at the site. There is also an extensive historical database that is continuously being updated with meteorological and oceanographic information. Near real-time data from on-site instruments are made available through the site data portal (navigation.usace.army.mil/CHL_Viewer/FRF).

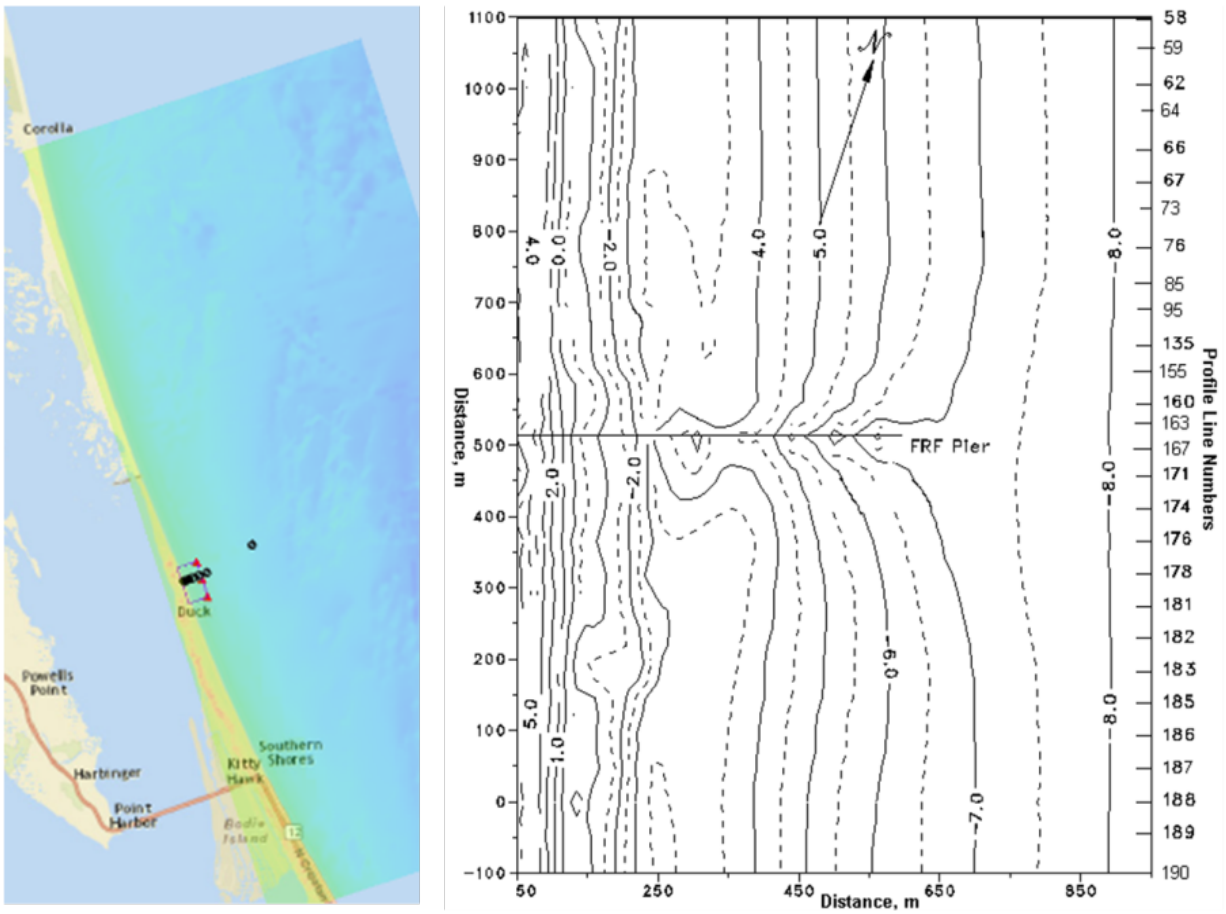

Figure 29. FRF Site Data Showing Detailed Very Near-shore Bathymetry Maps for the General Area Offshore of Duck (Left) and Areas Directly North and South of the FRF Pier (Right).

We identified both NOAA tidal water level stations and National Geodetic Survey benchmarks in the area that may be used for baseline information (Figure 29 and 30). Confirmation of the existence of geodetic benchmark stations was performed during our previous engineering proveout demonstrations in 2016.

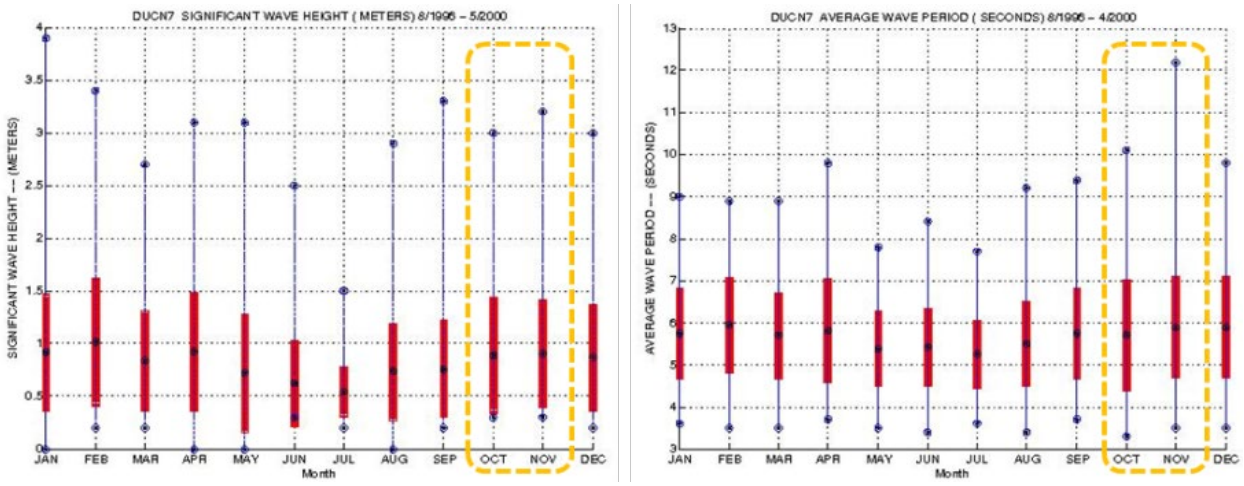

Figure 30. Significant Wave Height Statistical Data Compiled Over the Period from June 1995 to April 2000 at the FRF Site.

Wave heights for October and November are highlighted.

4.2 SITE HISTORY

Duck, North Carolina is the northernmost incorporated town within Dare County and previous to 2002, was unincorporated. Duck is located at approximately at 36° 10' N, 75° 45' W with a maximum elevation of 45 feet above sea level. The town is situated between Corolla at its northern boundary, Southern Shores at its southern boundary and by the Currituck Sound to the west. The FRF site is located approximately 1 mile north of the current town of Duck. Prior to the establishment of the Army Corps of Engineers FRF in 1977, the area was used as a naval training range.

During and subsequent to World War II, squadrons of pilots from the Norfolk Naval Yard utilized the area to conduct bombing and rocket practice launch sorties. The entire area of the bombing target range was transferred in 1973 to the Department of the Army Civil Works Division by the General Services Administration. Soon after, the Army Corps of Engineers established the FRF on the target range to conduct marine research. They constructed the 600-foot long pier on concrete pilings to extend out into the Atlantic Ocean to water depths of 20 feet or more. Present operations at the site are under the purview of the US Army Corps of Engineers Environmental Research and Development Center in Vicksburg, Mississippi.

4.3 SITE GEOLOGY

The general study area encompasses onshore and offshore areas of the northern Outer Banks. The Outer Banks are a chain of transgressive barrier and spit island features that span approximately 250 km from the Virginia-North Carolina border south to Shackleford Banks. The FRF site is located on a relatively narrow part of the sandy barrier between the Atlantic Ocean and the Currituck Sound, which separates the barrier beach from the mainland.

Coastal areas, such as those around the Outer Banks, are significantly influenced by the surficial geologic framework that exists beneath and seaward of the shoreline. In areas such as these with limited sand supplies, any accretion is derived from erosion and transport of sediment from adjacent coastal areas. This also leads to relatively thin and dynamic accretion zones of sand perched upon pre-existing geology. Current features on the Outer Banks are beaches, dunes, and marsh landforms, typical of Holocene and Pleistocene barrier island complexes. On the nearshore seafloor there are submarine scarps, shoals, and bars.

A number of studies have been undertaken to evaluate offshore sand barrow resources for beach nourishment (Dolan and Lins, 2000; Coastal Planning and Engineering of North Carolina, 2014; 2015). These studies highlight that the inshore zone along this part of the Outer Banks has free circulation of oceanic waters with little direct input of fine-grained material from inlets or estuaries. The surf zone is devoid of fines because of relatively high, wave-energy characteristics of the beach environment. The combination of low amounts of fine-grained sediments and frequent, high-wave energy off the coast tends to inhibit the accumulation of silts and clays (USACE, 2014). As part of some recent beach nourishment studies geophysical and geotechnical surveys have been conducted over approximately 230 miles in the summer of 2014. An example of high-resolution bathymetry is shown in Figure 31.

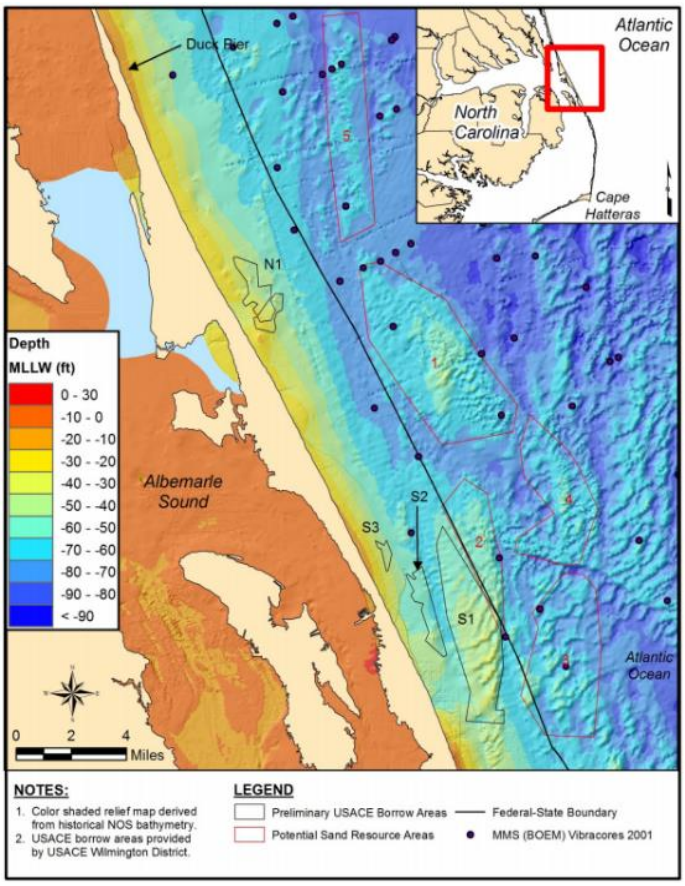

Figure 31. Bathymetry Focus Map Near the Study Area (from USACE, 2000).

The Town of Kitty Hawk in cooperation with the state of North Carolina, USACE, and BOEM conducted studies on sand barrow areas and beach renourishment in 2005 and a comprehensive study was undertaken in 2014 by the towns of Duck, Kitty Hawk, and Kill Devil Hills.

The general northeastern North Carolina coastal system is within the Albemarle Embayment complex and contains a 90 m thin Quaternary stratigraphy. The structural basin it forms is bounded to the east by a relict inter-stream divide (at the location where the current Outer Banks barrier islands reside) with Pliocene and Quaternary sequences dipping and thickening toward the center of the seaward basin (Mallinson et al., 2005). The barrier islands are constructed from sediment sourced from paleofluvial channels, shoal complexes, and sand-rich Pleistocene sedimentary deposits. Most of the region is characterized by overwash barriers while less area is covered by wider segments.

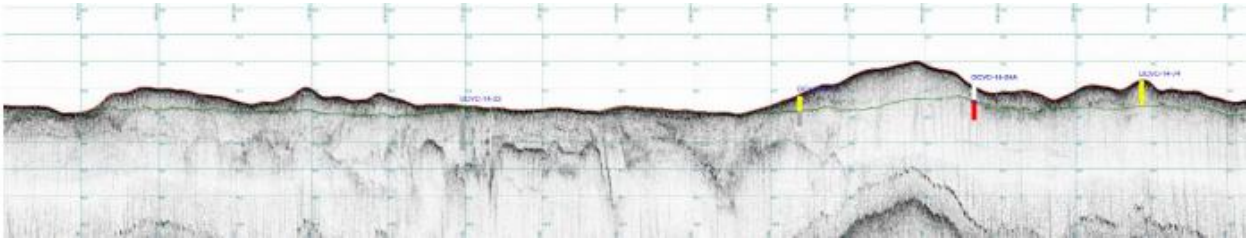

Figure 32. Shallow Chirp Seismic Cross-section Acquired Approximately 3 km Offshore from the FRF Pier and Extending to 5.5 km (from Walsh and Piatkowski, 2014).

The physical processes that drive the morphology of the general study area are well known and expected in this type of nearshore environment: tides, waves, currents, and storms. Tides are semidiurnal with a mean range of approximately 1m. Mean significant wave height over the period from 1997 to 2012 was 1.0 ± 0.6 m with mean periodicity of 8.7 ± 2.8 seconds (http://www.frf.usace.army.mil). The predominant wave direction is from the south to southeast in the spring and summer and from the north to northeast in the fall and winter.

Figure 33 presents a wave rose chart from Wave Information System (WIS) station 63221 located offshore and near Duck in 17 m of water. Examination of hindcast data shows the majority of waves higher than 0.5 m come from the northeast and the east northeast. Currents and mean flows form an important part of the shelf circulation including those from the Gulf Stream. Storms prevail in the fall, winter, and early spring (Birkemeier et al., 1985) with tropical and extratropical storms mobilizing the most significant portions of shelf sediment.

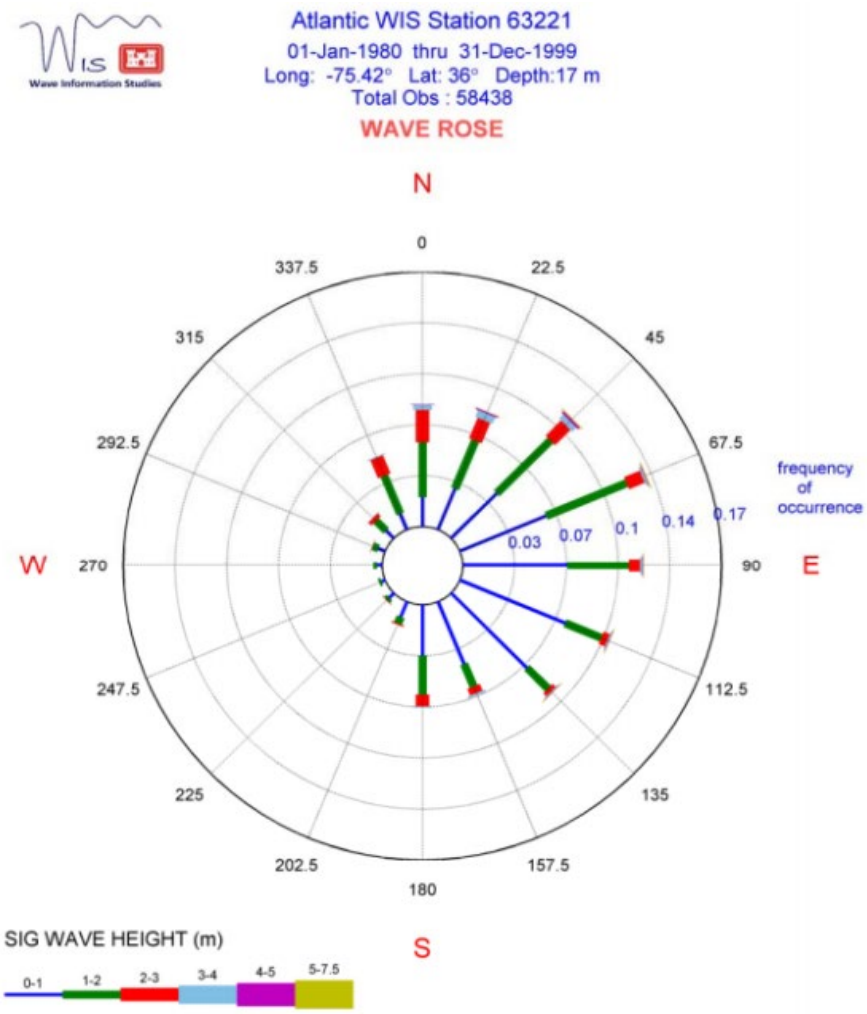

Figure 33. Wave Direction Rose Diagram from the Wave Information System (WIS) Station 63221 Aggregating Offshore Winds Between 1980 and 1999.

Extensive geophysical surveying and coastal geologic characterization have been conducted in this area. A great deal of work reported appears to have been conducted by Stanley Riggs of East Carolina University, his collaborators and students over the past 3-4 decades (Riggs, 1996; Riggs et al., 1995; Riggs et al., 1992; Schlee et al., 1988; Riggs and Nash, 2003; Eames, 1983; Bellis et al., 1975; Riggs and O'Connor, 1974; O'Connor et al., 1973).

During assessments of different towed sled configurations in 2015, our team also acquired single beam sonar data using the Echologger EA400 self-logging backscatter instrument shown in Figure 34. This system operates at 450 kHz with a 5-degree beam width to acquire acoustic backscatter waveforms at 10 Hz. Figure 34 shows variation in backscattered acoustic intensity from the bottom during survey transects offshore to onshore. Bubble in the swash zone are also evident at early time (shorter ranges).

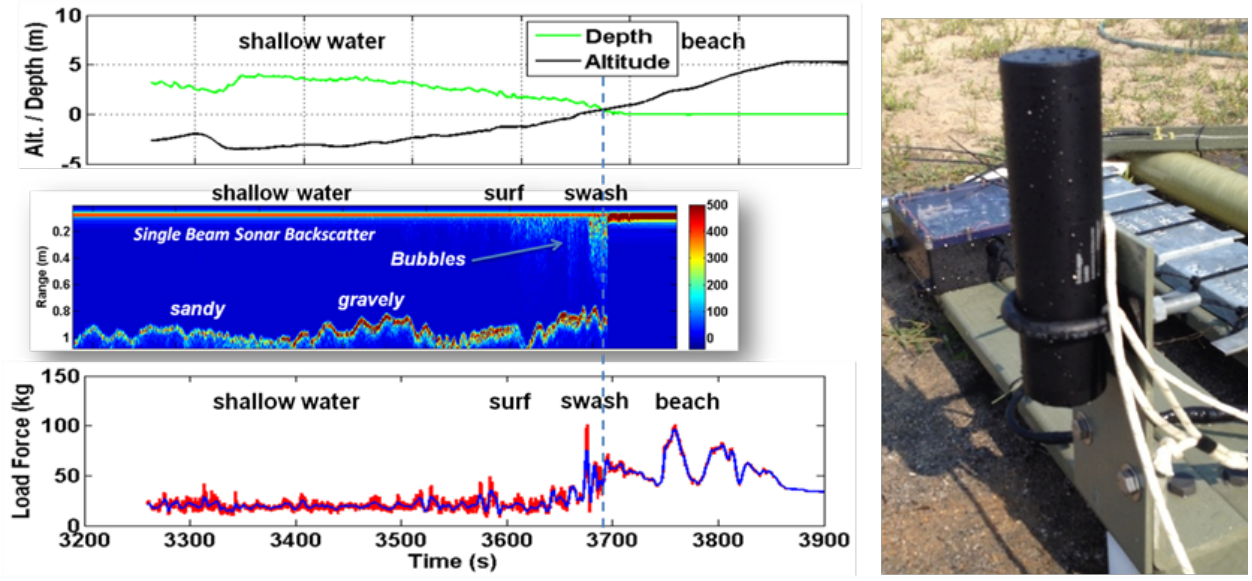

Figure 34. Left: Load Force (Bottom) and Water Depth / Altitude Off Bottom (Top) Are Correlated with Single Beam Acoustic Backscatter Intensity (Middle). Transition from Offshore Sandy Substrates to Larger Grain Size Gravely Material in the Surf and Swash Zone Are Evident in the Backscatter Range Versus Distance Profile. Right: Echologger EA400 Sonar Mounted on the Test Sled During Preliminary Engineering Data Collections in 2015.

The beach and nearshore sediments around the FRF pier have been characterized on several occasions since the early 1980's via grab samples, box cores, vibracores, and side-scan sonar (Byrnes, 1989; Haines et al., 1995; Drake, 1997). Previous long-term studies at FRF along shore-normal profiles (e.g., Duck94 and SuperDuck, 1986 studies) have characterized cross-shore grain size variability. In 2002, researchers from FRF also studied beach and nearshore morphology using repeated sub-bottom chirp and swath bathymetry surveys. The surficial sediment in this area is predominantly a bimodal mix of medium quartz sand and small pebbles. Sediment size becomes progressively fine in the offshore direction, grading to very fine and fine sands with less than 10% silt (McNinch, 2004). Sediments become finer offshore to 13 m water depth and are well sorted fine to very fine sands (0.21 to 0.07 mm). Five non-opaque heavy minerals (garnet, staurolite, edpidote, amphiboles, and tourmaline) occur with regularity and a frequency of 2% or higher (Meisburger and Judge, 1989). The dominant foraminifera found in sediment samples are Elphidium excavatum.

Dunes are dynamic geologic features that continually accrete and erode from factors such as seasonal fluctuations in wave height and storm activity (Rogers and Nash, 2003). Dune vegetation is essential to maintaining dune structure, and generally consists of hearty plants tolerant of extreme conditions such as sea oats, beach elder, and beach grasses. Other vegetation typical along the uppermost dry beach of Duck includes beach spurge (Euphorbia polygonifolia), sea rocket (Cakile edentula) and pennywort (Hydrocotyle bonariensis). The foredune includes American beach grass (Ammophila breviligulata), panic grass (Panicum amarum), sea oats (Uniola paniculata), broom strae (Andropogon virginicus) and salt meadow hay (Spartina patens) (USACE, 2000). The beach and dune community within the demonstration area is limited in extent due to development and a coastline that is receding due to storm events and beach erosion (Leatherman et al., 2000).

4.4 MUNITIONS CONTAMINATION

Although our test area was not specifically selected based on proximity to known munitions areas, the FRF is a former bombing target range. In fact, the northern part of the Outer Banks has a history of use of military munitions including the Corolla Naval Target, Buxton Naval Facility, and our study site, the former Duck Naval Target (all in congressional district NC-3; see Figure 35). The USACE Savannah District is the Program Manager for the DERP/FUDS program in this part of North Carolina with the USACE, Wilmington District acting as project manager.

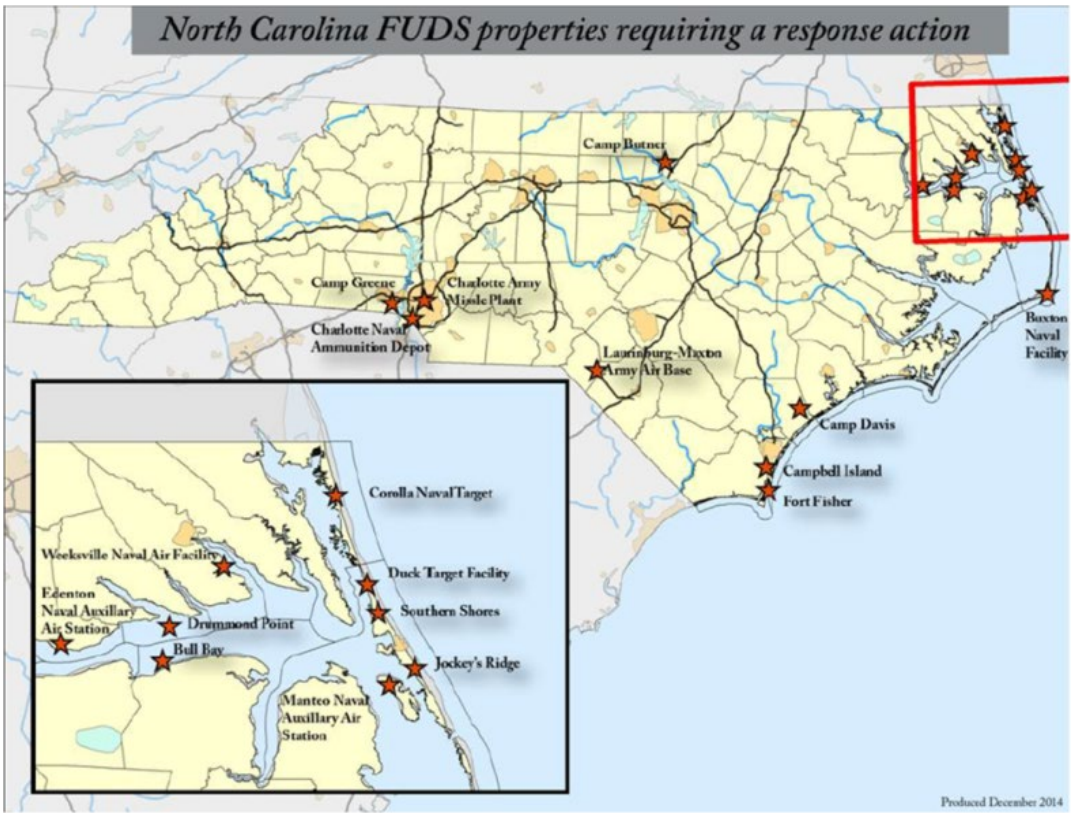

Figure 35. Map Highlighting the Locations of Formerly Used Defense Sites (FUDS) in North Carolina with Inset Showing Those in the Far Northeast Part of the Site and Along the Northern Outer Banks.

The former Duck Naval Target range site was established as a Naval training area in 1941 and constitutes approximately 175 acres. It was used extensively during the period between 1941 and 1965 by aircraft from the Norfolk Naval Yard for practicing aerial bombardments. It appears that the majority of practice runs started with pilots entering from the west and firing munitions eastward at land-based stationary targets (Figure 36 and 37). The primary objective was accuracy and precision training. Spotting charges have been reported to have been used for observations. Practice munitions used included practice rockets (2.25-11.75 inches), practice bombs (miniature - 250 lbs), and MK4 spotting charges, based on USACE historical records.

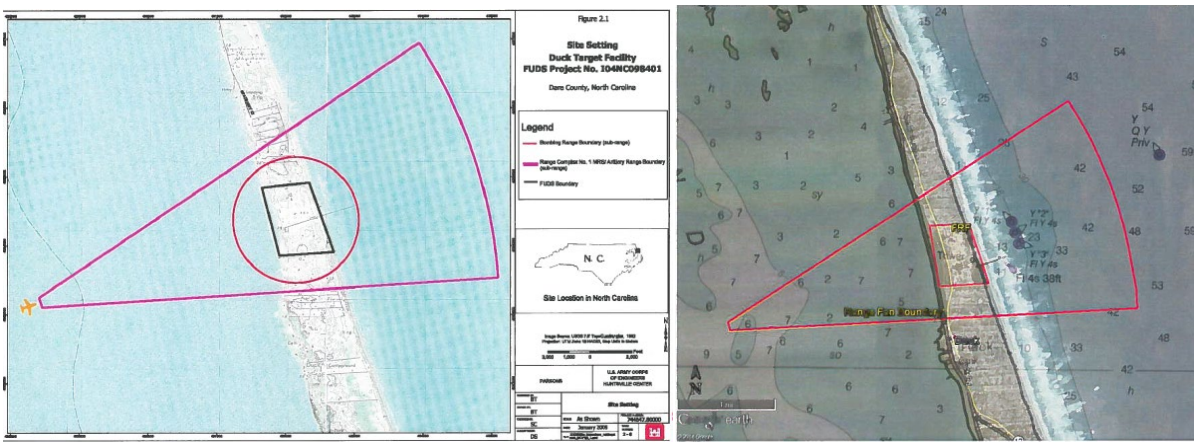

Figure 36. Maps and Overlay Diagrams Depicting the Former Duck Target Facility Range Fan and Munitions Response Site.

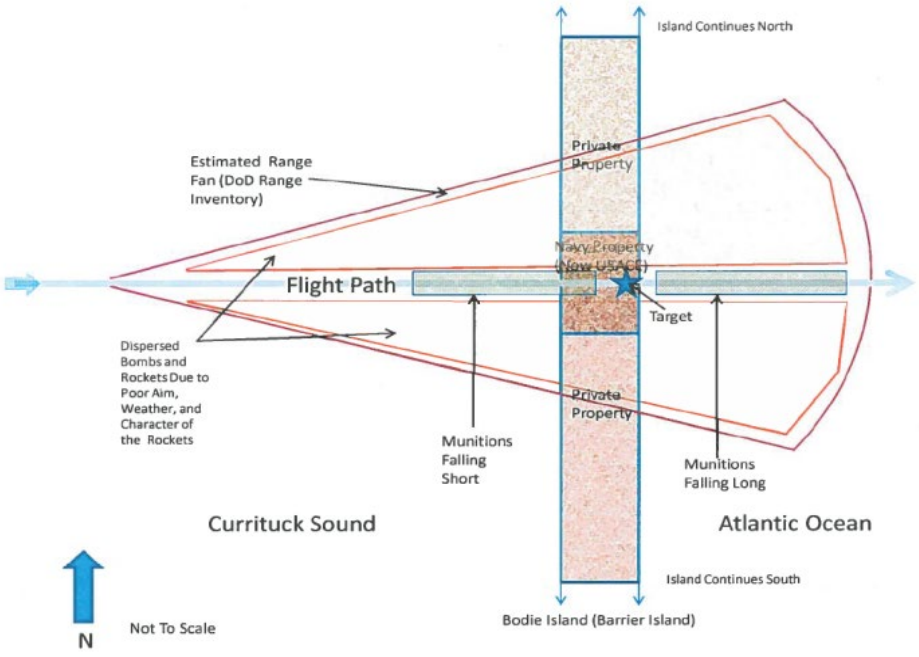

Figure 37. Overview Conception Site Model Diagram Developed by USACE.

UXO investigations and remedial actions on the site date back to 1971. Among the most significant actions are a 1972 clearance conducted before the property passed control from the Navy to the Army. An Engineering Evaluation and Cost Analysis (EE/CA) investigation was also conducted by Parsons Engineering Science and USACE in 1996 following a limited Removal Action (RA) and Archive Search Report in 1994. These activities also followed a 1993 Time Critical Removal Action (TCRA) that removed 821 total Material Potentially Presenting an Explosive Hazard (MPPEH). The 1996 EE/CA report described UXO surveys conducted using EM61 sensors that covered nearly 30 acres and identified 3,757 buried anomalies that were potentially UXO. Between 1996 and 2000 remediation activities led to the removal of over 3,500 MPPEH items. A summary of these are listed in Table 2.

Table 2. Summary of MPPEH Items Removed from the Duck Munitions Response Site.

Item	Model/Type	Body	Propellant	Warhead/Fill
2.25" Rocket (SCAR)	MK16 Mod 4, 5, 6	Steel	Ballistite (NC and NG)	No fill – Hollow or solid steel
Miniature Practice Bomb	MK5	Zinc	NA	No HE – Spotting charge
	MK23	Iron		
	MK43	Lead		
5 lb Practice Bomb	MK106	Steel	NA	No HE – Spotting charge
25 lb Practice Bomb	MK76	Iron	NA	No HE – Spotting charge
100 lb Practice Bomb	MK15, Mod 2	Steel	NA	Water or sand Spotting charge
50 lb Practice Bomb	MK89	Iron	NA	No HE – Spotting charge
250 lb Practice Bomb	MK86	Steel	NA	No HE – Spotting charge
2.75" Practice Rocket	MK2, MK3, MK4, MK5, MK6, MK7	Steel	Ballistite	No fill-hollow
3.5" Practice Aircraft Rocket	MK3	Steel	Ballistite	Solid steel
5" Practice Rocket	MK28, MK32, MK34, MK35	Steel	Ballistite	No fill-hollow
11.75" Practice Rocket	MK4	Steel	Ballistite	No fill-hollow

In 2008, USACE conducted a Site Inspection (SI) to evaluate the former Duck Target Facility munitions response site for potential release of munitions and explosives of concern (MEC). During this activity a qualitative reconnaissance was conducted, surface soil samples were analyzed, and few munitions debris items were found (some small arms cartridges, practice rocket pieces, and inert practice bombs). USACE concluded in their 2009 SI report that no MEC had ever been confirmed at the site and that the potential for unspent spotting charges is extremely unlikely. Figure 38.

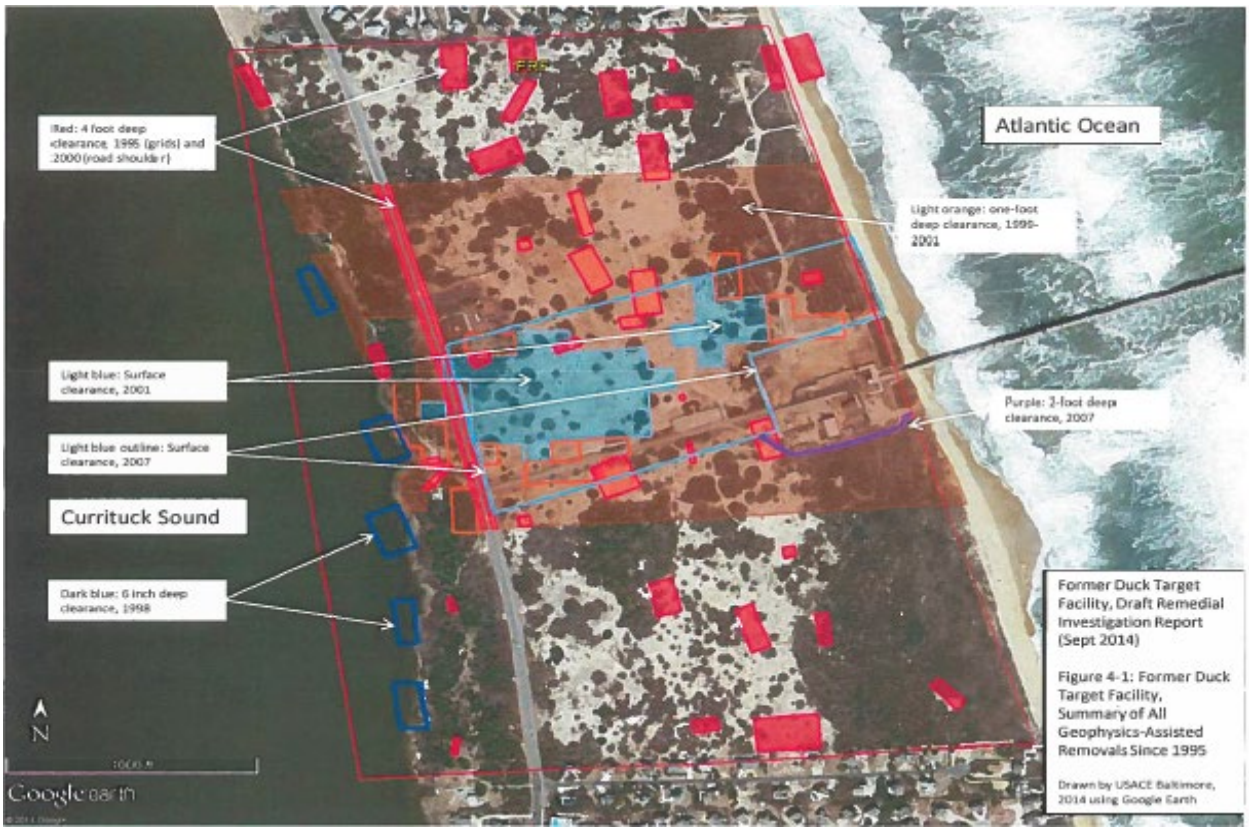

Figure 38. Previous UXO and Site Characterization Investigations at the FRF.

5.0 TEST DESIGN

5.1 CONCEPTUAL EXPERIMENT DESIGN

The Duck FRF site encompasses beach, swash, and surf zone areas that are appropriate for demonstrating the crawler towed sensor array implementation. For this demonstration, we focused on surf zone areas just south of the Duck FRF Pier. Dr. Jesse McNinch and his team at the FRF provided logistical and technical support for these tests. Hydrodynamic measurements provided by the FRF included water and wave height monitoring data, directional spectra of incident waves, offshore current profiles, tidal elevations, wind speeds/direction, and atmospheric pressure. Recently acquired high-precision bathymetric data acquired by FRF as well as historical data was also used to correlate with the measurements made on the tow sensor during testing. Environmental parameters of interest include:

- Hydrodynamics (tidal variation, wave heights, currents and pressure variations)
- Seafloor morphology (beach slope, rugosity, bedforms)
- Seabed sediment material characterization (cohesive sediment soil strength, grain size distribution and sorting, cone index, shear strength)

The FRF Data Portal (navigation.usace.army.mil/CHL_Viewer/FRF) provides access to near real-time and archived observations from the site. This includes point observations from beach, ocean bottom, or buoy-based measurement stations as well as geomorphology GIS layers (point, raster and vector data) and some limited analysis tools and raw data download capability. An example of recent beach profiles acquired from the data portal along two transects in the area near where we plan to establish our site are shown in Figure 39. We note that shoreline and beach profiles can vary depending on seasonal weather and storm influence, especially during the transition between summer and winter.

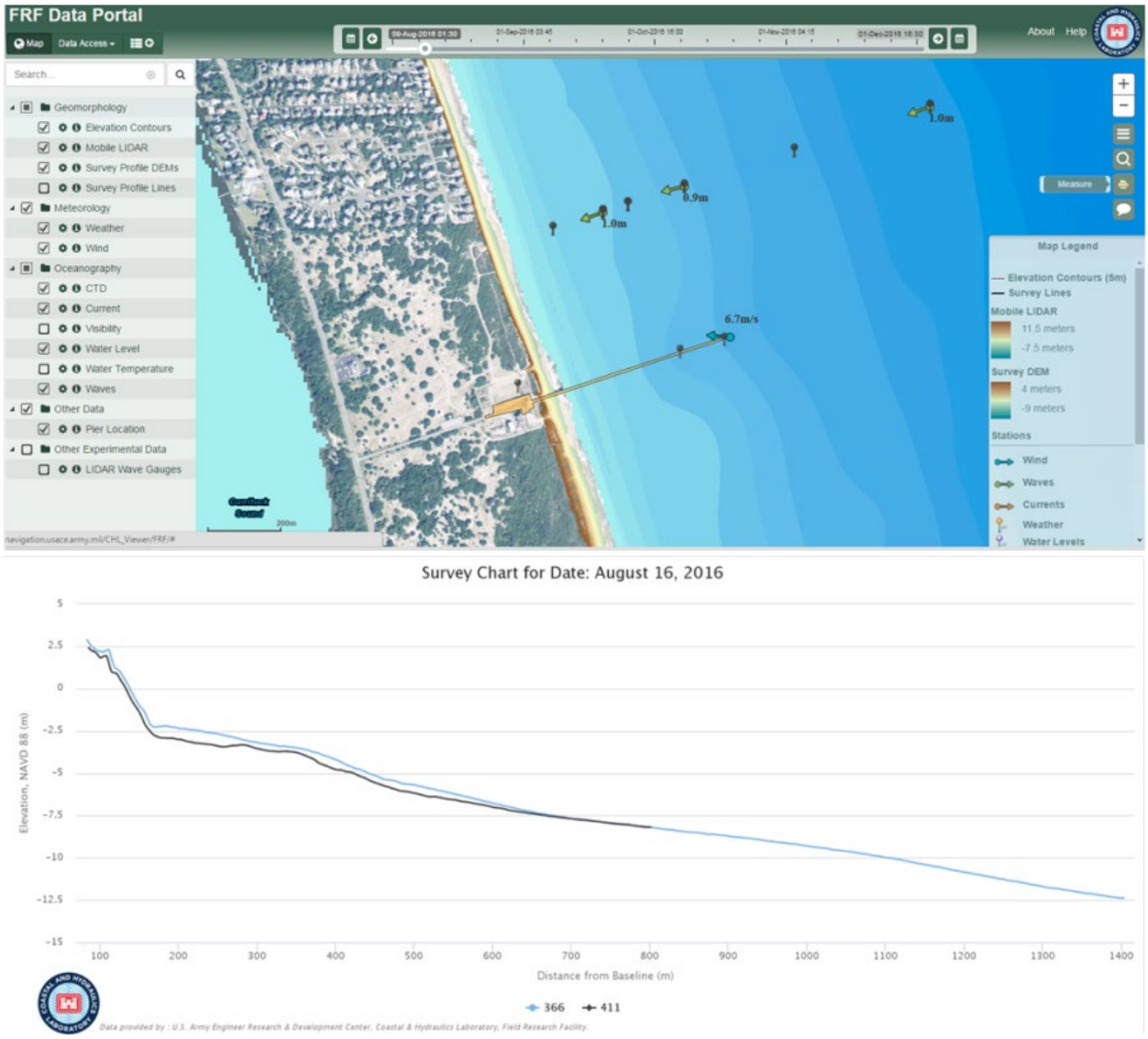

Figure 39. Top: GIS Layer Map Showing Recently Acquired (August 2016) LiDAR Nearshore Bathymetry at the FRF Site Along with Wind and Wave Vector Information from the In-shore Array. Two High-resolution Bathymetric Profiles Sampled from ~50 and ~100 Meters South of the FRF Pier Are Shown in the Bottom.

Note the beach slope extending toward a trough and bar sequence before shoaling more gradually seaward. The area 100 to 300 meters along the shore-normal baseline (x-axis) is the area targeted for our demonstration.

This demonstration focused on the collection of high-quality EM sensor and navigation data from the crawler-based tow platform in the surf zone. Specifically, we endeavored to demonstrate means of maintaining stability as measured by the following parameters; (i) altitude, (ii) X-Y position, (iii) orientation, (iv) direction of travel, or (v) speed of travel. Our focus was on determining the ability of the integrated crawler-based EMI sensor system to perform UXO detection and characterization surveys in a stable and efficient manner.

Demonstrations were planned for data collection over the beach, swash, surf zone, and shallow water areas at the FRF site. The general set up was comprised of the integrated crawler and sensor tow system connected to an operator control station (OCS) located on the observation pier via a wireless Ethernet radio link. All system functions and data acquisition were to be completely controlled from the shore-based OCS. Survey areas included transects from the lower beach area perpendicular to the shoreline through the surf zone and wave break area to shallow water (~2-2.5 m deep). In addition, survey transects were to be performed just past the wave break area in shallow water over a target grid. An instrument verification survey (IVS) strip was to be established on the upper beach for daily quality assurance checks. Figure 40 shows the basic set up including relative locations and primary test resources. Further detail on the site preparation, system specifications, and test procedures is provided below.

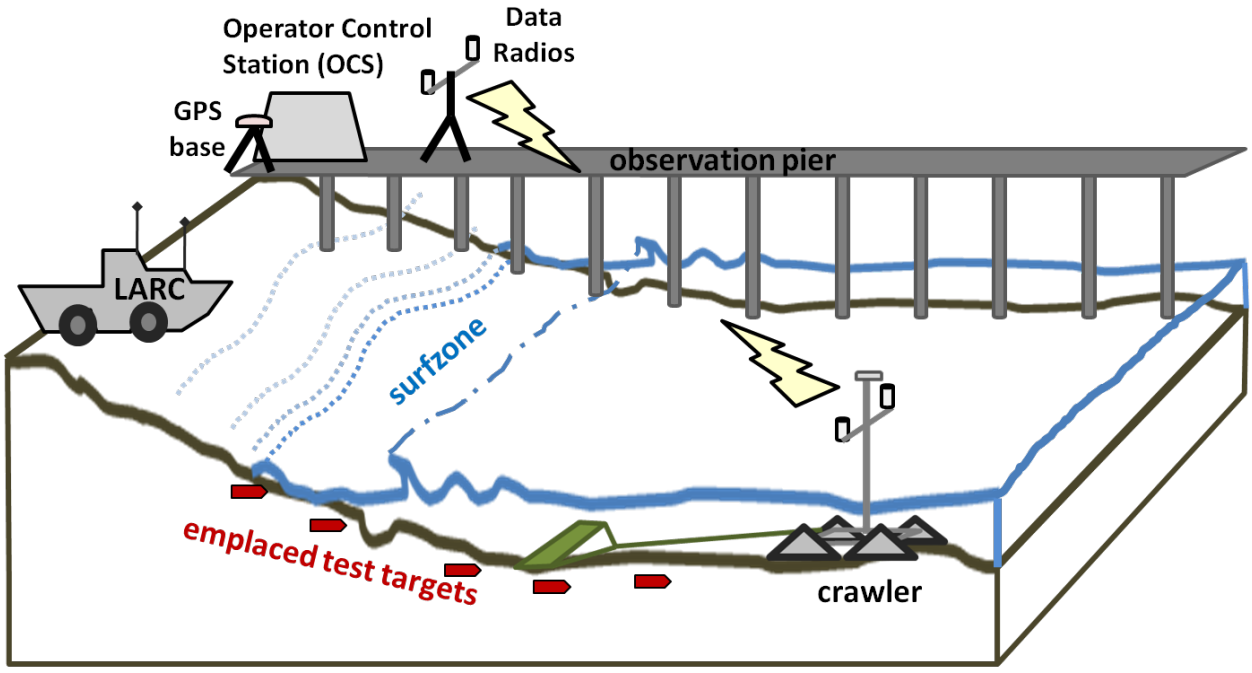

Figure 40. Conceptual Overview Schematic of the Crawler-EM Demonstration.

The operator control station (OCS) is connected to a pair of data radios that wireless transmit commands and data to/from the crawler.

Although some site preparation and coordination activities were required to take place prior to mobilization to the site, we anticipated 5 days on-site for the demonstration depending on weather and unforeseen delays. Approximately two days were planned for collecting data while the system exercises area coverage surveys in shallow water. EMI array, navigation and control data were to be recorded during all exercises. One day was planned to perform the on-shore to off-shore surveys. One additional day was planned for testing surf zone stability. Additional days were scheduled to buffer for inclement weather conditions and/or repeated tests. The final day was to be allocated for demobilization and coordination with the field project team. Figure 41 shows a representation of the scheduled test activities.

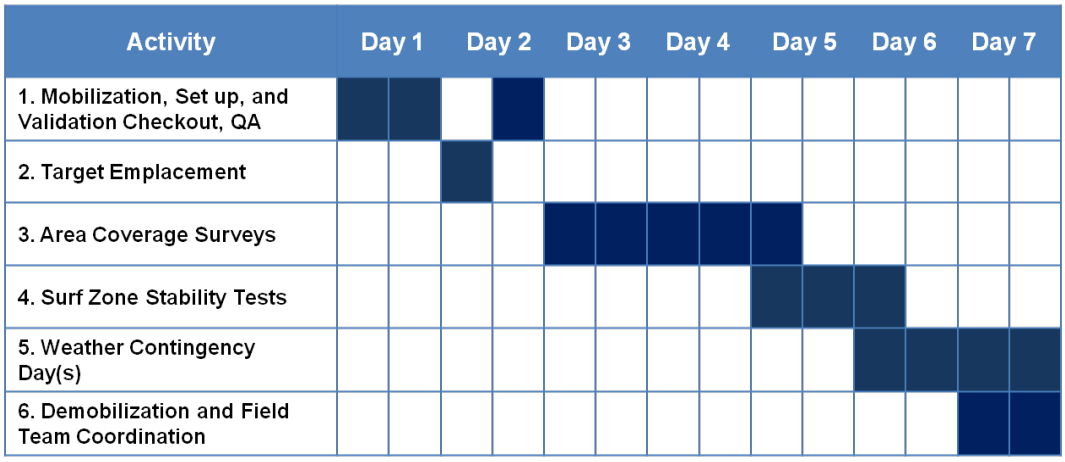

Figure 41. Timeline of Planned Testing Activities.

The first two days involve mobilization and target area set up. Days 3-7 on-site using the crawler system to conduct demonstrations and data collections. Two days have been added to accommodate repeated data collections and potential weather-related down time.

5.2 SITE PREPARATION

Our demonstration began with a day of site reconnaissance and setup including setup of auxiliary equipment such RTK-GPS and operator control station, preparation of the crawler to be used during testing, and assembly of the tow system including mounting the EMI array and GPS rover antenna onto the crawler. This was followed by preliminary integrated system deployment and data collection by an experienced system operator. The purpose of this data collection is to test the functionality of the systems, calibrate GPS and encoders, and to characterize the data collection area in terms of water column conditions, bottom types and location of EM clutter. Reconnaissance and setup took approximately four hours.

The primary tasks associated with site preparation were; (i) survey control, (ii) target emplacement, and (iii) monitoring of environmental parameters such as weather, waves, and currents. Horizontal and vertical control and datums are necessary for accurate RTK-DGPS surveys. Survey control was established through FRF's geodesy control system and used the NAD83 datum adjusted to the 2001 North Carolina State Plane for horizontal and NAVD88 vertical datum using the 2003 Geoid for elevation. We located the FRF calibrated monument points that are also frequently used for bathymetric surveys (from both the LARC and CRAB platforms). These control points have been cross-checked against the National Geodetic Survey monuments around the northern part of the Outer Banks. Crawler support equipment was located on the FRF pier. This allowed for a centralized control station and vantage point for observing operations on the beach and in the surf. Equipment established on the pier including the control station trailer and cabled connections to a radio telemetry relay tower and GPS base station. Photographs of the control station set up, radio tower, and GPS base station on the pier are shown in Figure 42 and Figure 43.

Inside the control station trailer, we set up the topside data analysis computers, user interface display monitors, and data communications router. Three computers were used for analysis; (i) one to manage crawler data controls and power systems indicators, (ii) one for navigation guidance and user interface, and (iii) one for the EM array data pre-processing and display.

We used a minimum of four display monitors that can be configured to show camera views from the crawler, battery management system and crawler motor indicators, forward-looking scanning sonar data, navigation guidance, and/or EM data and quality indicator displays. Camera displays were generally including a forward/downward-looking mast viewpoint, a forward-looking crawler viewpoint, and a backward-looking viewpoint fixed on the towed array sled.

Figure 42. Photographs of the Operator Control Station Trailer and Radio Telemetry Tower Located at the Base of the FRF Pier.

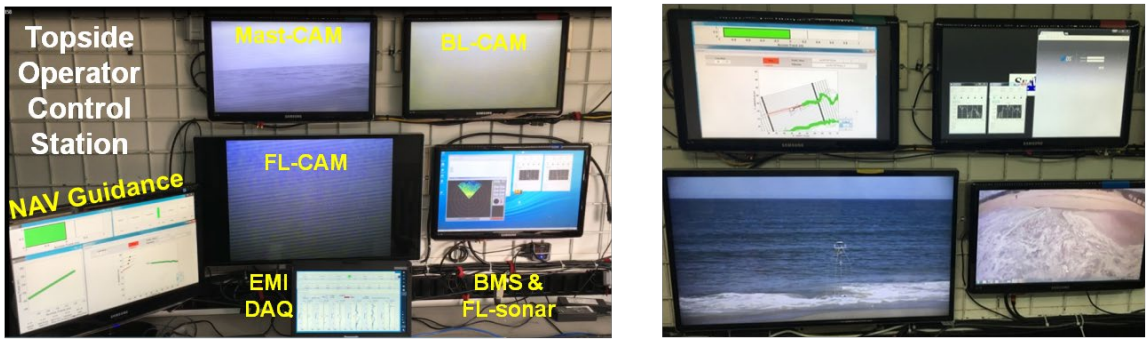

Figure 43. Photographs of the Operator Control Station Display Monitors During Demonstration Operations.

We utilized two people in the OCS: one crawler helmsman and one sensor array analyst.

5.2.1 Target and Test Area Installation

Preparation of the test area leveraged our previous demonstration work. We established two primary areas for the IVS and target grid. These areas are illustrated in Figure 44. The IVS was established on the upper beach as it was the most effective area for surveying prior to and after deployment under water. One drawback of establishing a dry IVS (not submerged) is that full operational conditions in the marine environment are not assessed during QC surveys. Given the complexity of in-water target installation at this site, we deemed this a necessary compromise.

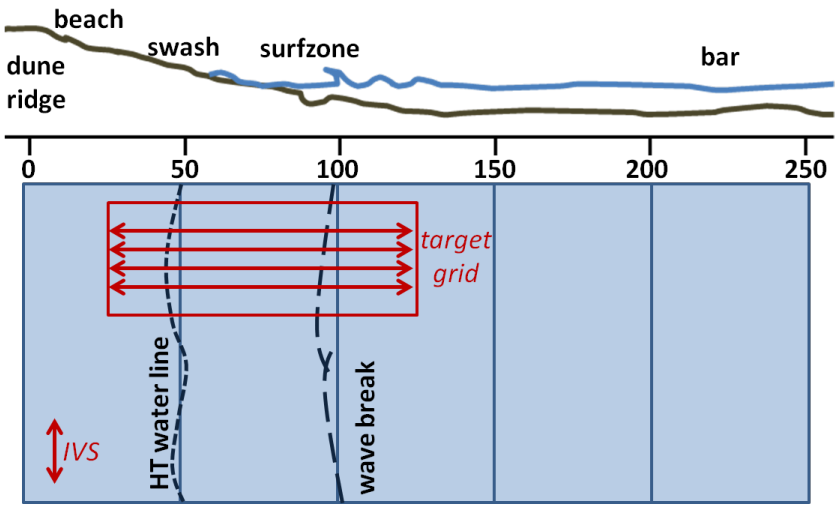

Figure 44. Schematic Diagrams of the Target Emplacement Areas at the FRF Demonstration Site: Instrument Verification Strip (IVS) and Approximately 30m X 90m Target Grid Area.

An instrument verification survey strip (IVS) was also established along the upper beach directly adjacent to the offshore survey areas. IVS seed items consisted of schedule-40 small Industry Standard Objects (large or medium ISO40) buried along the IVS line. Each of the items was placed in hand-dug holes, surveyed in using RTK-DGPS, and covered and marked with a plastic or wooden stake and labeled (Figure 45). The four IVS targets were each separated 5 meters apart and installed at approximately 25 cm below ground surface;(i) 3-inch solid steel sphere, (ii) large ISO, (iii) medium ISO, and (iv) small ISO.

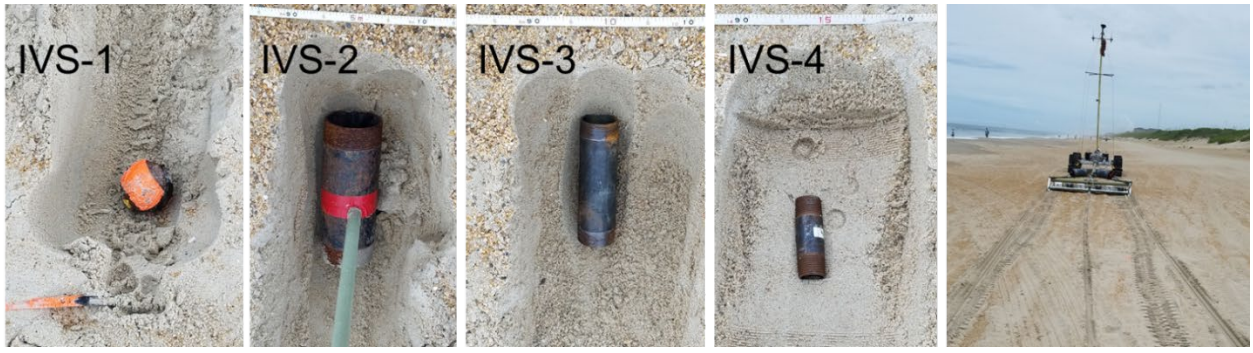

Figure 45. Photographs of the Four Emplaced IVS Targets and Crawler Passing Over Targets During QC Survey (right).

The emplaced items included IVS-1: 3-inch steel sphere, IVS-2: large ISO, IVS-3: medium ISO, and IVS-4: small ISO. Each item was separated by 5 m and buried approximately 25 cm below the ground surface.

Following setup and IVS installation activities, we emplaced and surveyed the primary target grid of inert UXO targets on the beach and in the surf zone. Target emplacement included installation of a 45m X 15m grid containing 16 items; 9 UXO simulants, 5 ISO objects, and 2 clutter items.

Placement of munition surrogates (aka, UXO targets) was focused on the most challenging regions of the nearshore – depths from approximately 0 to 1.5m – where waves shoal and break and where the seabed is most dynamic. We surveyed and emplaced targets just south of the Field Research Facility (FRF) pier between the lower beach (mean high tide water line) and the wave break zone seaward of the swash area. As expected, target emplacement was challenged by highly dynamic wave and surf conditions. Wave heights varying between approximately 0.5 and 1.1 m induced strong currents near the wave break and intermediate surf zone areas during target placement.

At low tide on the morning of 17 July 2017, we utilized prepared survey strings along four shore-normal lines. The shore-normal lines extended from the lower beach, through the swash zone, and into the surf zone. Target placement was conducted at low tide (see Figure 46 – tide gauge progression) during daylight hours in the trough region (between swash and sandbar) and just seaward of the trough in depths of 1-2 meters. Four targets were placed on the mid-section of the beach and remained dry for all surveys. Another four targets were placed between the mean low tide line and mean high tide line and thus were generally in the shallow swash region during surveys. The remaining 12 targets were fully submerged in areas from the swash zone (10-40 cm water depth) to just beyond the wave break (~120-230 cm water depth). Measuring tapes were used to guide the target-to-target (10 m) and line-to-line (5 m) spacings. Although, we timed the emplacement for the low-point in the tidal cycle, the most seaward targets were very challenging to install in the highly dynamic 0.5-0.75 meter-deep water.

Each target was installed in the seabed by a two-man team. Targets were installed and oriented in an approximately 30 cm deep hole and then backfilled quickly. Each target was attached to a small surface float ribbon (plastic flagging) that was labeled with the designated target grid number. Prior to backfilling and covering, each target location was measured with RTK-GPS antenna on a pole that was held directly above the target after placement and averaged for approximately 30 seconds. Target depth below the nominal local seafloor was measured with a simple marked staff driven into the seafloor after each target is covered with sediment. Target orientations were also noted with respect to approximate inclination and azimuth angles.

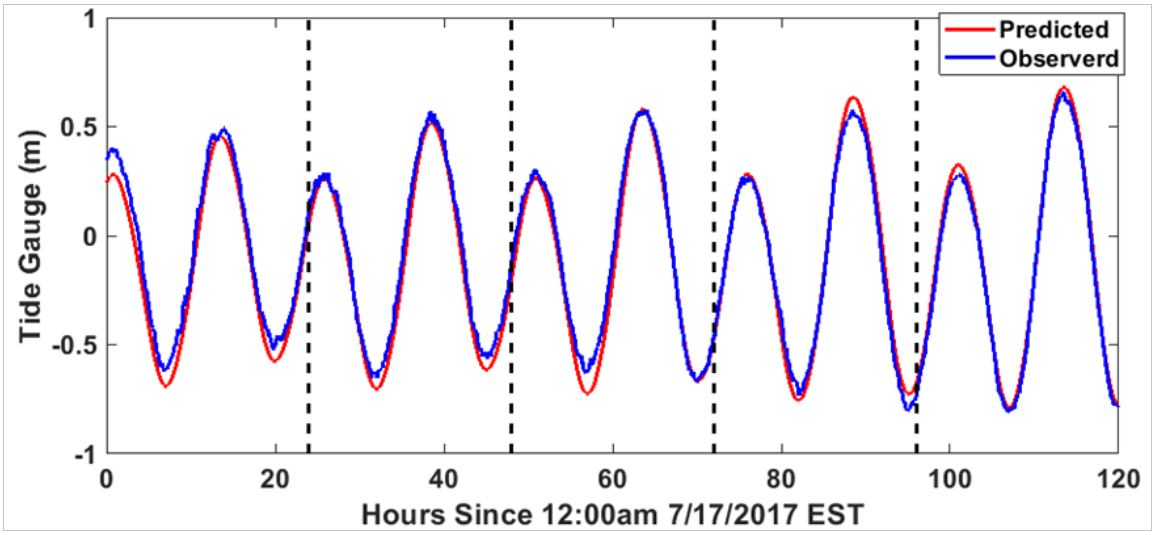

Figure 46. Tide Gauge Data and Prediction During the Demonstration Period (time since 7/17/2017 EST)

Seeded items included ferrous and non-ferrous ordnance simulants (Figure 47) of different sizes (60 mm to 105 mm). Two clutter items were also installed: (i) a 55cm piece of steel chain gathered up and (ii) a piece of broken-off angle iron approximately 28 cm long X 3 cm wide x 1 cm thick. A ground truth target spreadsheet was created containing the target's type, latitude (northing), longitude (easting), orientation, and burial depth. The emplacement team took special care to avoid emplacing seeds in the immediate vicinity of any strong geophysical anomaly sources. This was achieved by reviewing recent hydrographic, sonar, and other geophysical data sources that indicated known contacts or clutter.

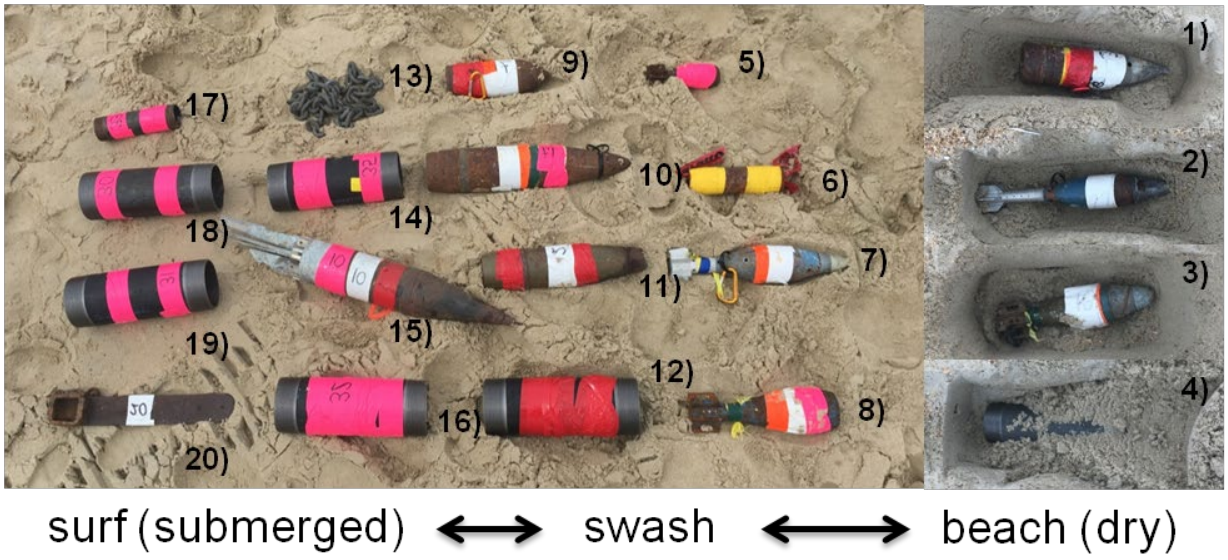

Figure 47. Photographs of the Simulant Targets Used in the Demonstration.

These include ISO's, simulant UXO from the Aberdeen Test Center (ATC) test set and Naval Research Laboratory, clutter objects, and other canonical metal objects for assessing the performance of the overall system.

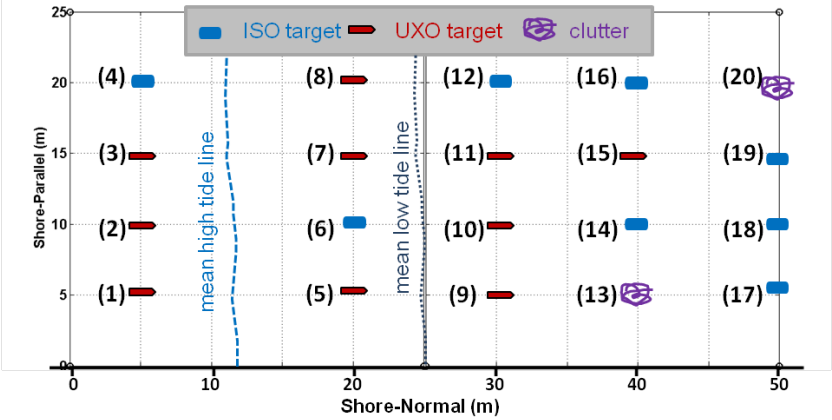

Figure 48. Left: Diagram of the Target Grid.

The Site Consisted of a 45-Meter by 15-Meter Grid with 5 Shore-parallel Target Lines Buried Below the Seafloor at Nominal Depths of 30 cm. Twenty Items Were Emplaced Including 9 UXO Simulants, 5 ISO Objects, and 2 Clutter Items.

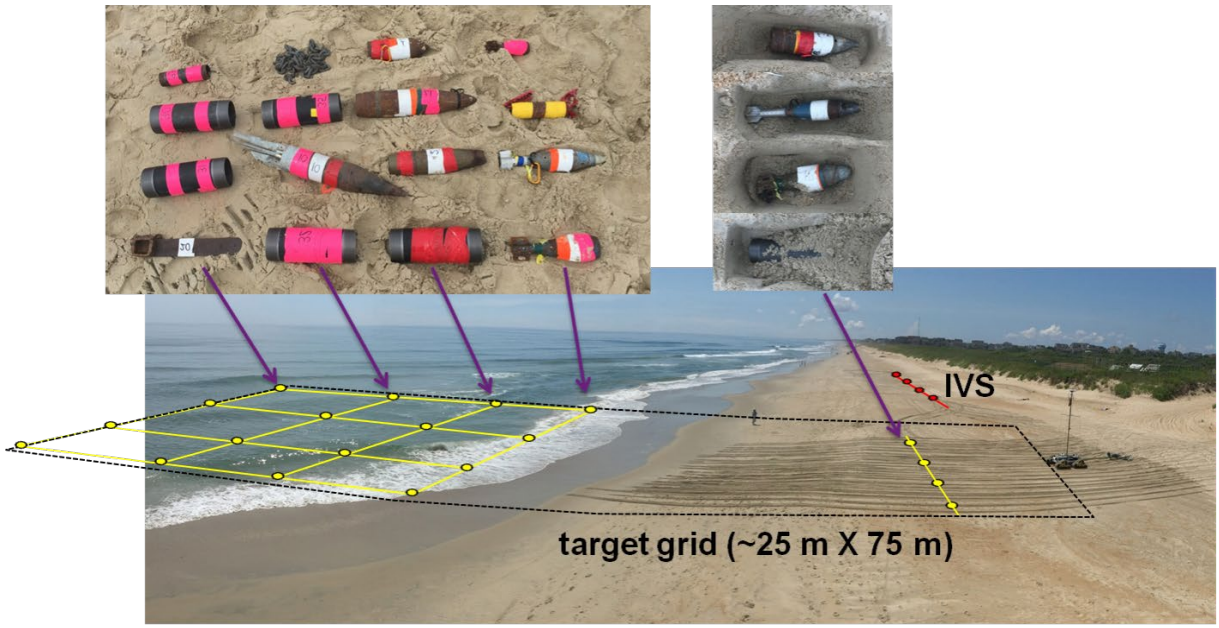

Figure 49. Photographs of the Target Test Area Shown with Approximate Locations of Targets Overlain.

An initial survey over the target area on 7/18/2017 revealed that some of the targets were suspected to no longer be present in the target grid. Four of the targets of similar size and initial installation depth to those showing high SNR signals were not evident in overpass data and there was no longer any seafloor surface expression of any of them (i.e., flagging connected to the targets that was previously visible in the surf). We determined that these four targets must have become uncovered and mobilized out of the target area during the previous tidal cycle overnight. This was partially confirmed later, when two of the munitions were found washed up on the beach approximately 60 meters south. We, therefore, decided to install two additional targets in the grid on 7/18/2017 prior to surveys on the morning of 7/19/2017. Further discussion of the target field and evidence of mobilized targets is given in Section 7.4 below.

5.2.2 Environmental Monitoring

We also utilized data from the FRF surf zone instruments to determine the relevant water characteristic parameters during our test. A CTD instrument installed at the end of the pier provided measurements of water visibility, temperature, density, salinity, and sound speed. The average conditions over the test period were as follows:

- Visibility: 1.1 meters
- Temperature: 16.7 degrees Celsius
- Density: 0.0015 g/cc
- Salinity: 28.75 psu
- Sound speed: 1506 m/s

The temperature and salinity measurements are used to compute an average water conductivity of 4.45 S/m.

Figure 50 displays time profiles of atmospheric meteorological data during our test event. Fortunately, no extreme or anomalous weather conditions occurred during our tests. Wave height and period data were also available from in-water acoustic Doppler observations buoys (ADOPP) located adjacent to the pier. Figure 57 shows data from one of the ADOPP gauges seaward of our test area in 3-4 m of water depth. Wave height, direction, and peak wave periodicity are computed.

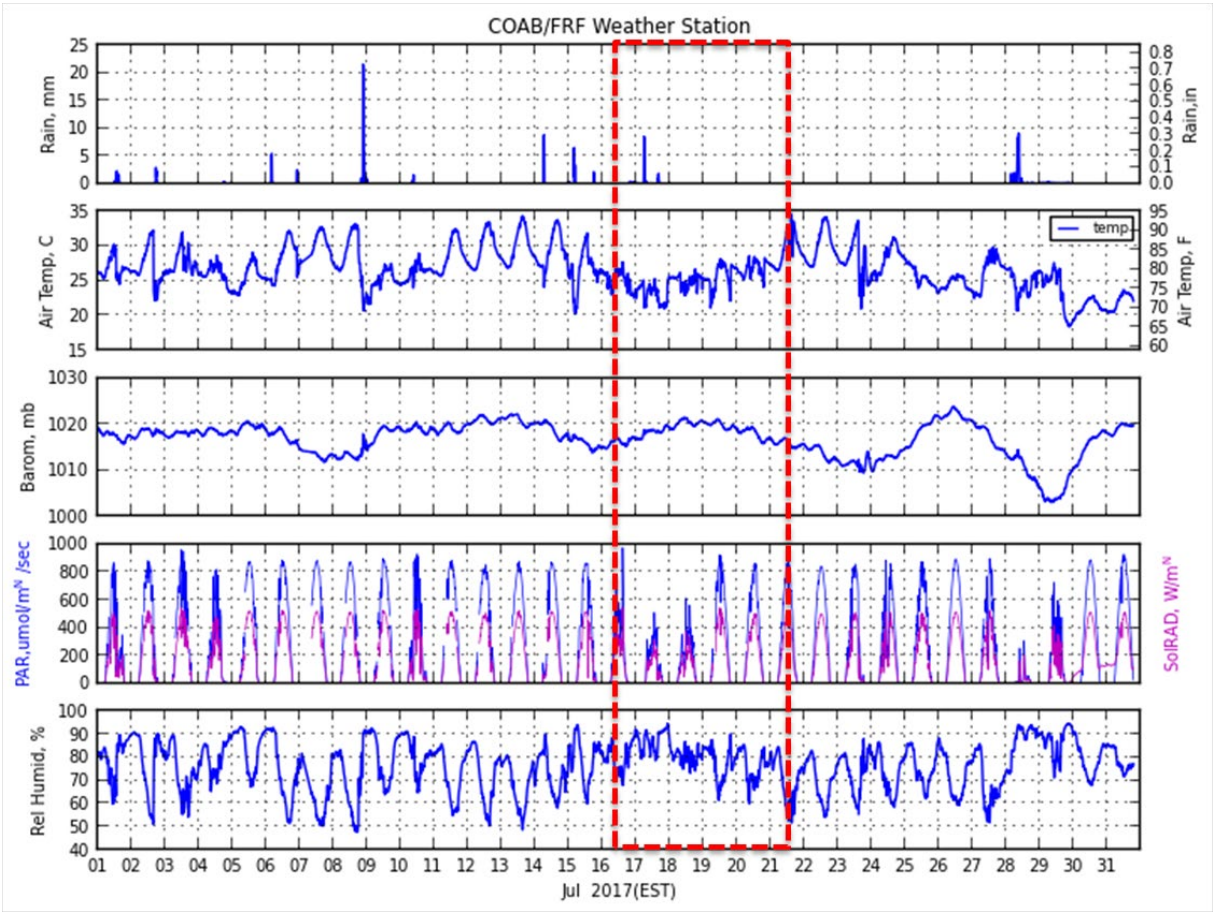

Figure 50. Atmospheric Meteorological Data Time Profiles from the Coastal Observation and Analysis Branch (COAB) Weather Station at the End of the Pier.

Data during our test timeframe is outlined by the red dashed box.

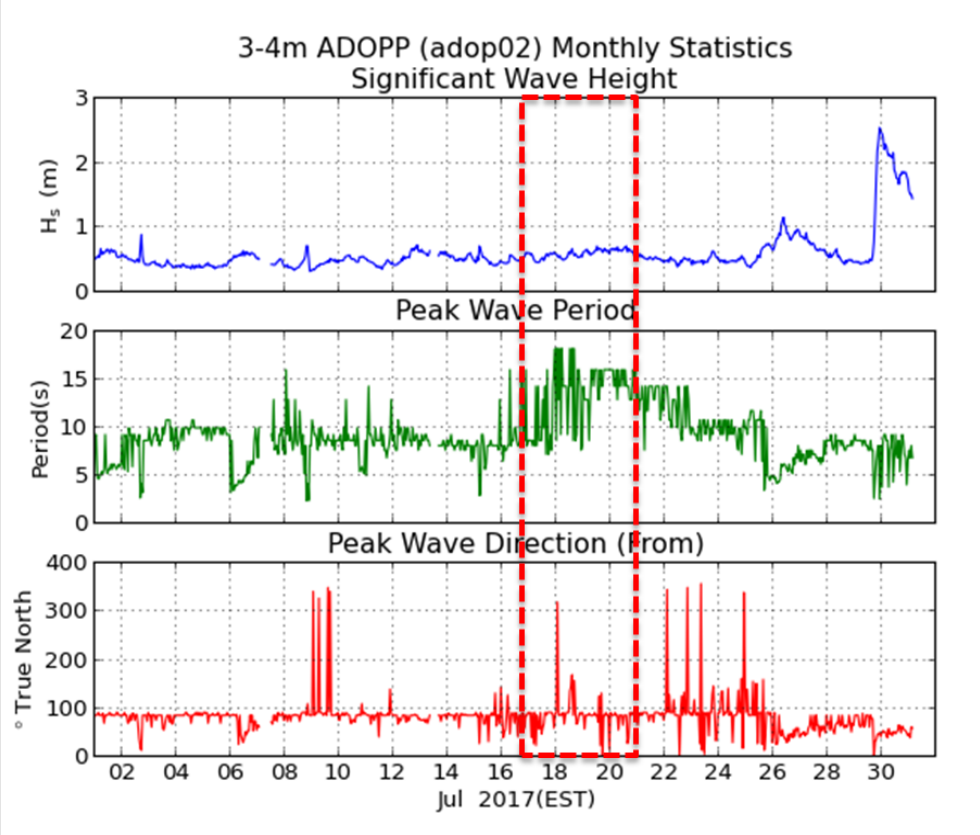

Figure 51. Acoustic Doppler Data Recorded by the ADOP-2 Buoy Seaward of Our Test Area.

Wave heights at this location remained relatively constant over the duration of our surveys. The peak wave periodicity during our test timeframe ranged from 7 to 17 seconds and was generally a little longer than the monthly average of approximately 9.2 seconds. Wave direction was primarily from the East with notable deviations that occurred over the duration of a few hours. Neither the wave period nor changes in direction were observed to significantly impact our survey operations.

In addition to data acquired from the permanent FRF oceanographic observation stations, we also temporarily deployed an acoustic Doppler velocimeter in order to better characterize currents, pressure, and flux in our specific survey area. We utilized a Nortek Vector 3D acoustic velocimeter. This unit integrates Doppler velocity measurements with temperature, pressure, tilt, and compass data to provide three-dimensional estimates of current velocities that are corrected for any motion of the unit itself by correlation of attitude and heading reference system (AHRS) data. The unit is completely self-contained in terms of battery power supply and on-board data logging. We strapped our unit to a weighted base platform that was then connected to weighted line extending to a buoy. The platform assembly was then deployed using the FRF LARC system as shown in Figure 52. Unfortunately, the unit was never recovered (along with its logged data) due to the weighted line breaking from the marker buoy. This presumably occurred during deployment and, despite several attempts (including EM and magnetometer surveys), we were unable to locate the system again.

Figure 52. Three-dimensional Acoustic Doppler Velocimeter (Nortek Vector Unit) Being Deployed for In-situ Measurements of Currents, Pressure, Temperature, and Flux During Our Experiments.

The unit was attached to a weighted base platform and deployed over the side of the LARC platform in approximately 2-3 meters of water. The unit was unable to be recovered due to the weighted line breaking form the marker buoy.

5.3 SYSTEM SPECIFICATION

The system for demonstration includes the SurfROVer crawler platform, inertial navigation and control system, integrated Hemisphere V320 dual-antenna rover and GPS mast, the Flex-EM time-domain array, and the sensor array tow sled system. In addition to the subsea survey platform and sensor components, the demonstration also utilized the topside control station with crawler video and data displays, operator control station, wireless radio transceivers, and GPS base station. Each system will be described in detail in the following section.

5.3.1 SurfROVer Crawler System

The crawler used for this demonstration is the SeaView SurfROVer crawler system designed and manufactured by SeaView Systems Inc. (Dexter, MI). The SurfROVer is a purpose-built crawler developed for shallow-water operations such as pipe and cable tracking, UXO detection surveys, and bathymetric or hydrographic surveying. It was previously demonstrated at Toledo Beach, Michigan and Duck, North Carolina in 2016 (results from these demonstrations are documented in the MR-201422 Interim Demonstration Report, August 2017). This system has four crawler tracks on independent suspensions, integrated drive propulsion and control, subsea lithium-ion battery power supply subunit, subsea lighting, a 1000-foot long fiber-optic tether, and topside operator control station. The vehicle also provides a mechanically-scanned forward looking sonar as well as a payload capacity supporting up to three additional serial sensors and three additional Ethernet sensors. The specifications for the demonstration-ready version of the crawler are shown in Table 3.

Table 3. SurfROVer System Specifications

General	
Max Operating Depth	150msw
Overall Dimensions (LxWxH)	2.6m x 2.0m x 0.9m
Composition	Low Magnetic / Corrosion Resistant / low EMI & low EMC
Weight (in air)	390kg (860 lbs) (estimated)
Weight (submerged)	Negatively buoyant: 222 kg (490 lbs) (estimated)
Ground Pressure (submerged)	0.2 PSI
Pull Force	400 kgf (estimated)
Range	4000ft from control trailer
Speed (Ground)	0.83 m/s (3 kph, 1.6 knts)
Speed (Submerged)	0.45 m/s (1.6 kph, 0.86 knts)
Propulsion	Ge-roller based Hydraulic Power Units
Turning Radius	Approx. 11 m diameter
Operating Conditions	
Current Conditions	3 knt current regardless of incident angle
Bottom Type Environments	Range of soil types (sands, muds) up to 80 kPa
Wave Action / Sea States	Up to 2 m plunging waves; Sea State 3
Traverse Capability / Obstructions	Traverse capability for obstructions 0-20 cm above flat seafloor; barriers, troughs, macro-ripples, shell reefs; etc.
Payload Capability	
Payload Allocation	150 kg; 100 L (e.g., three 20cm OD x 30 cm long pressure vessels)
Payload Power	5/12/15/24/48Vdc up to 200 W each; Capable of 5 Amp Min in-rush current per channel.
Payload Data Interface	Ethernet 10/100 (GBit available)
Topside Interface	
PC Interface	Windows or Linux User Interface for Control/Display
Motion Command	Motor % Power; Direction; Counter-rotate; Joystick or PC
Data Interface	3ch SD Video, 10/100 Ethernet, 4 x RS232, 2 x RS 485, 2 x RS485/232 onboard conversion, 2 high speed TTL.
Platform Data	10 Hz: camera awareness, direction, velocity, roll/pitch/yaw, pressure depth, altimetry, health status
Positioning	RTK-DGPS; allocation for IMU and USBL
Mechanical Interface	
Winch Tow Anchor	Four padeyes
Launch & Recovery (LAR)	2 ton winch recovery (Dyneema rope)
Tow Bridle	3DOF tow point interface
Soft Buoyancy System	Optional (desired for emergency lift to sea surface)
Auxillary Sensing	
Cameras	Two (Min) RGB or Greyscale Fixed View Cameras (e.g., 1 forward looking and 1 downward looking)
Lamps	Three sets of 10k lumen LED lights
Depth Sensor	Pressure
Sonar	Imagenex 881a imaging scanning sonar.

5.3.2 Flex-EM Sensor Array and Tow Platform

The crawler was configured to tow the 2-meter wide sensor sled and a dual-heading RTK-based DGPS system. The Flex-EM sensor electronics housing in pressure vessels is attached directly to the tow platform. The tow platform was deployed with sufficiently negative buoyancy for operation in seawater. A single cable connects the sensor head to the sensor electronics. The electronics receive power and an Ethernet connection to the vehicle data network through the central sensor manifold provided on the crawler. A topside computer running a software application interface communicates with the Flex-EM electronics through the vehicle network. The topside software application displays and logs Flex-EM sensor data and RTK-GPS data. Figure 53.

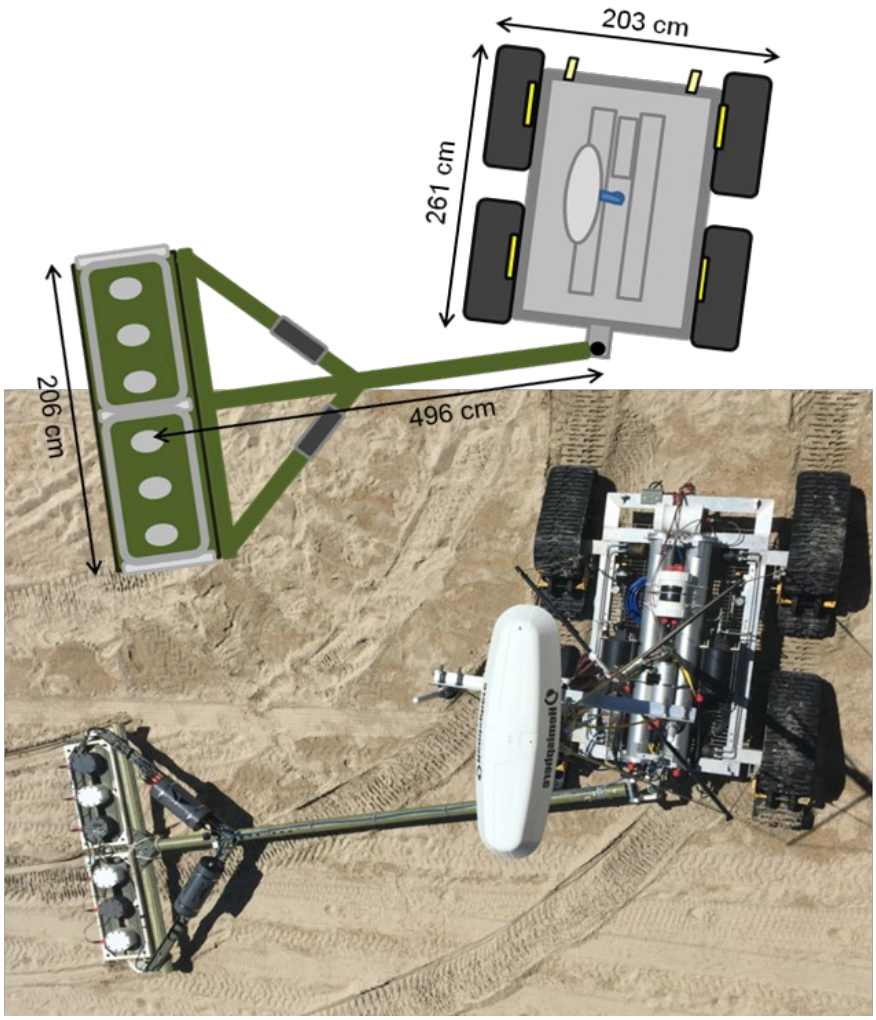

Figure 53. Configuration Diagram of the Crawler-based EM System Used for the Initial Demonstrations.

The bulk dimensions of the configuration are shown. On bottom is an overhead photograph of the system during demonstrations showing the layout represented in the configuration diagram.

5.3.3 Dual-heading RTK-GPS and GPS Mast System

The RTK-GPS system consists of a Hemisphere V320 GNSS-enabled dual-heading smart antenna and a Hemisphere R320 GPS base station. The rover outputs NMEA GPGGA, GPVTG, GPGSV, and GPHDT data strings at a rate of 10 Hz via an RS232 serial cable connected to the crawler junction box and converted to RS422 for transmission via the crawler fiber optic tether to topside. The baud rate is set to 19.2 Kbps over the GPS serial port B. RTCM RTK DGPS corrections are sent via the crawler tethered modem directly from the GPS base station to the rover unit on the crawler.

The GPS rover antenna was mounted on the top of the mast system prior to deployment. The mast system was erected manually, and the four stays were tightened using turnbuckles at their base until the system was vertical and stable. A photograph of the field team erecting the mast and stays is shown in Figure 54.

Figure 54. Photograph of the Field Team Erecting the GPS and Radio Mast on the SurfROVer Crawler Prior to Operations.

5.3.4 Environmental Characterization Sensors

Environmental conditions associated with our test data were measured with a set of self-logging sensors on the crawler platform. We mounted a single beam acoustic backscatter sonar for characterizing the seabottom and particular aspects of the water column (e.g., bubble cavitation). The single beam sonar used was the EoE Ultrasonics Echologger EA400 unit with integral power supply and data logging capability. This unit was attached directly to the crawler sled and when submerged produced full waveform acoustic backscatter data at a data rate of 1 Hz. Conductivity, salinity, and temperature of the water column were measured using an Onset HOBO U24-002 unit. In situ conditions were also observed after each mission from a set of GoPro progressive scan HERO 3+ cameras mounted on the crawler and tow sled boom.

5.3.5 Top-side Control and Display

The OCS station was in a portable trailer and consisted of the complete operator control station, data interface and networking unit, multiple displays, and the Flex-EM data acquisition and user interface laptop. For our demonstration, the control station was manned by the crawler helmsman (remote operator) and an EM system analyst. The OCS crew has access to multiple monitor systems that display camera views on the crawler as well as real-time scanning sonar and feedback from the crawler battery management system, control system, and EM array.

The follow individual displays are available at the topside OCS (see Figures 4 and 5):

1. Camera View 1: mast-mounted forward-looking live RGB camera
2. Camera View 2: crawler-mounted rear-looking live RGB camera (pointed at array)
3. Camera View 3: crawler-mounted forward-looking live RGB camera
4. Crawler Diagnostic Feedback: real-time updates from the crawler battery management, control systems, and scanning sonar view (these constitute separate windows on a single monitor display, but could be split out over multiple monitors)
5. Navigation Display: integrated system navigation and mapping location display showing the real-time track of the crawler and sled along with waypoints and lines to follow and additional marker points or points of interest (e.g., obstacles or exclusions areas to avoid)
6. FlexEM Display: this display compiles navigation information from the GPS and IMU with real-time "waterfall" traces from the EM array receivers as well system configuration, data acquisition and file logging information.

5.4 CALIBRATION ACTIVITIES

5.4.1 Encoder and GPS Calibration

The tow point encoder requires calibration to ensure its zero position and any small changes in full range and angular resolution over the course of operations. Tow point encoder calibration involves zero point and full range calibration as well as correlation with the crawler GPS rover (Figure 55). The following outlines the encoder and GPS calibration.

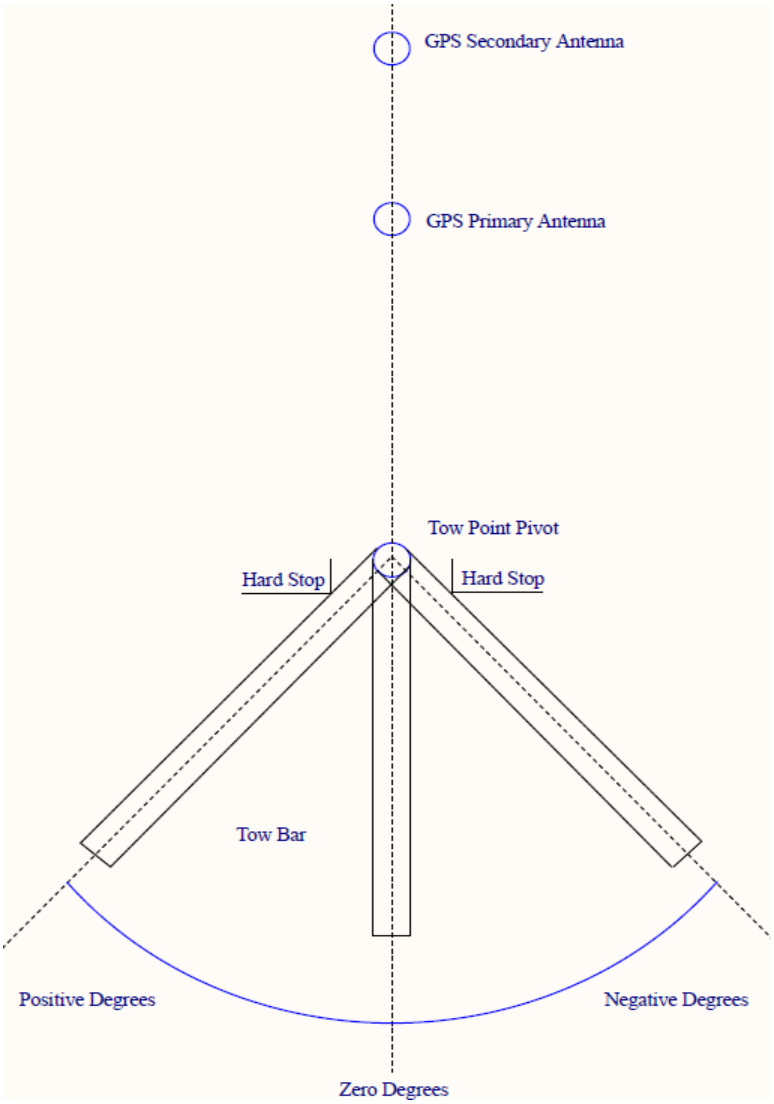

Figure 55. Diagram of GPS Rover and Tow Point Encoder Calibration.

Small yaw angles out of alignment with the crawler can cause a crabbing error effect on the heading measurements. These errors can be corrected by calibrating for the any angular bias between the in-line vehicle trajectory and the relative angle of the GPS rover antennae. The procedure is as follows:

1. Rigidly mount the GPS rover in the GPS mast receiver fixture.
2. Mount the GPS mast receiver fixture to the GPS mast using the index alignment marks and bolts.
3. Raise the GPS mast and index and bolt the fixture to the crawler.
4. Use the known towpoint fiducial mark as a reference between two know GPS survey control points. Note the deviation between true heading and measured heading from the Hemisphere V320 GPS rover. Use this heading offset as the bias correction in post-processing.

Encoder calibration:

1. With GPS antenna rigidly fixed and in-line with the crawler axis, align the towbar in-line with both GPS antennae with a long survey string.
2. Note the visual zero position.
3. Move the towbar (or towpoint) to the port side hardstop and note the positive encoder reading at hardstop.
4. Move the towbar (or towpoint) to the starboard side hardstop and note the positive encoder reading at hardstop.
5. Upon each power up, move the towbar to both hardstops and note readings.
6. Prior to each power down, move the towbar to both hardstops and note readings.
7. For each sortie, the zero position should be calculated from the hardstops using the original calibration numbers achieved from the string alignment procedure (steps 1-3).
8. Once the zero position is determined, offset the azimuth (positive or negative) should be applied to the positioning algorithm.

5.4.2 IVS Surveys

Four ISOs, separated by 5 m and contained in a beach-based survey line, were used to calibrate the EM sensor and navigation and positioning system periodically throughout surveying; at minimum at the beginning and end of each data collection day.

Background surveys were performed with the system and georeferenced using RTK GPS positions. The purpose of this step is to document the appropriateness of the location (e.g. few existing anomalies) and verify that IVS targets are not seeded near existing anomalies. Once the IVS area was deemed suitable for use, (i.e. free of significant subsurface anomalies or containing anomalies that are clearly identified so that they can be avoided during seeding), ISO targets were buried horizontally at depths below ground surface of approximately 4-8 times their diameter. These depths are intended to provide adequate signal to noise ratio for detecting the targets. Measurements of the item depths were to the center of mass of each item. On-site personnel buried the IVS targets using shovels to dig the holes to the appropriate depths for burial of the seed items.

Prior to collecting production data and each morning before beginning field operations, data were collected with the EM system moving over the IVS including the background location (blank space). The SNR of EM sensor data collected over each target is compared to the SNR of data collected previously in a controlled setting. The EM sensor passed calibration if the SNR is within +/-10% of the controlled SNR. The distance traveled using the navigation solution was compared to the known separation (5 m) of the targets. The success criteria of the navigation system ensured that the distance traveled was within +/- 5% of the known separation of the targets (25 cm). Prior to any surveying RTK-GPS accuracy was verified by capturing GPS data and confirming the rover is producing 'RTK-fixed' quality data indicative of cm-level accuracy. Standard pre-deployment functional checks of crawler motors, auxiliary sensors, and topside communication were performed prior to deployment of the crawler (i.e., pre-flight function checks).

5.4.3 Flex-EM Calibration

System Function Tests (SFTs) were used to verify consistency in data channel output on a daily basis. Static tests were performed with the Flex-EM stationed in a clean area within the IVS. Spike tests were performed multiple times each day using 2.5-inch diameter steel sphere (aka, the calibration ball). Calibration consisted of placing one of these items on, or directly above, each receiver while collecting data. The proximity of these items to each receiver yields a response in each axis of the receiver (X, Y, Z). Following these data collections, the data were quickly post-processed to determine proper functionality of each receiver and each receiver axis. Any significant deviations in the calibration ball response may be indicative of hardware faults.

5.5 DATA COLLECTION

The primary survey grid data collection activities took place on 19 and 20 July 2017. On the morning of 19 July 2017, the crawler-towed EM system was deployed to the upper beach near the test area. A roll, pitch, yaw calibration data set was acquired and then spike and IVS data collections were conducted. Subsequent to IVS surveys, data were acquired over the beach targets in a grid format using repeated adjacent passes. Similar back-and-forth surveys were conducted in the surf and deeper water in the afternoon (13 survey transects) along with additional spike and IVS data collection. Beginning in the morning of 20 July 2017, we commenced full survey coverage over the complete target grid area with continuous survey transects for 100% coverage. Twenty-seven (27) transects were completed between 9:47 AM and 11:27 AM comprising the majority of the grid coverage.

The data we acquired (and detailed in Section 3 for the creation of demonstration metrics) included: (i) RTK-DGPS data from the crawler; (ii) raw inertial navigation sensor data from both the crawler and the tow sled; (iii) raw Flex-EM millivolt count data for each of the for 16 time gates in each of the 18 channels; and (iv) the processed tow sled navigation solution including azimuth correction from the tow point encoder. These data types were time-stamped and logged with the topside data acquisition computer during testing. Unless crawler speed is the variable being tested, the operator was instructed to maintain a speed of approximately 1 knot (~0.5 m/s) resulting in 5 cm sampling of the seafloor by the EM array operating at approximately 10 Hz. Data were stored locally on the topside operator computer.

5.5.1 Scale and Sampling

Figure 56 shows the survey coverage area and transects, instantaneous speed during the survey and the ground sampling metrics. The ground sampling distances varied somewhat during our full coverage target grid surveys. This is primarily due to the platform slowing and even stopping at times and then varying speed from 0 to as much as 1 m/s at times. During the 1.75 hours of our 100% coverage surveys over the target grid, we conducted 27 survey transects with a mean instantaneous speed of 0.32 m/s. These transects aggregate to approximately 1.77 km of line km covered with our 2-meter wide array. The survey area sampled using the line-km and swath width is 3548 m^2 or 0.88 acres (0.36 hectares). The target area covered by our surveys as defined by the convex hull (or affine envelope space defined by the vertices of the survey data) is approximately 1550 m^2 or 0.38 acres. At 100% coverage, this would equate to approximately 5 hours to cover a hectare or 0.5 acres/hour. The average instantaneous speed was 0.32 m/s, which is faster than the objective of 0.3 m/s.

However, a good portion of the time during these tests were spend traversing the lower beach during when the crawler system was not submersed or only partially submersed. The average ground sampling distance was approximately 21 cm with a standard deviation over the entire survey of 6.6 cm. The largest ground sampling distance was 42 cm. Sampling distances larger than ~25 cm were uncommon and likely occurred due to sway or otherwise sudden motion of the GPS rover.

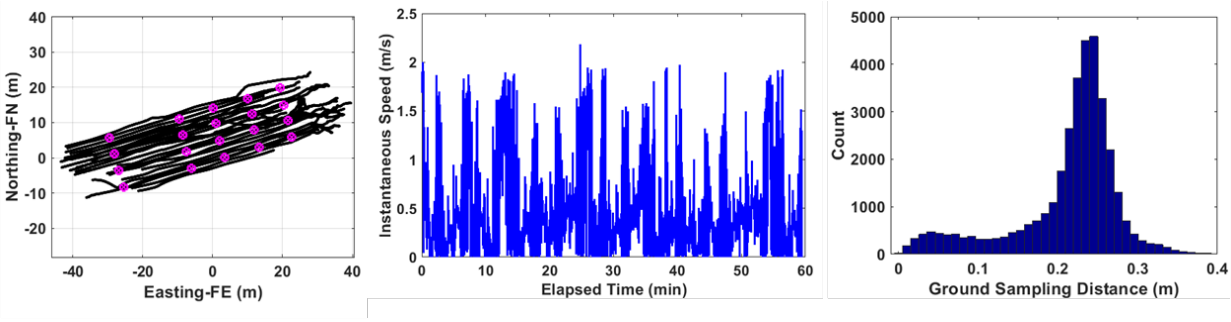

Figure 56. Scale and Ground Sampling Metrics from Demonstrated Survey Data Collection in the Surfzone.

Left-to-Right: Overview map of the surfzone transects over which the statistics were calculated; instantaneous speed of the platform computed from GPS time and position; and histogram of the computed ground sampling distance of EMI data coverage.

5.5.2 Quality Checks

Periodically throughout each data collection day crawler navigation and EM data were processed to assure data quality. Quality control metrics produced include the standard deviation of each EM channel to illuminate noisy data channels. The sample time of each data collection was also reviewed to assure no gaps in sampling. The real-time navigation display flashes indicators if data quality of any sensor is not met including loss of RTK fix quality (e.g., Q=4 for the NMEA convention).

The Flex-EM data logging software displays the raw GPS and EM sensor data in real-time. These data are monitored by the data collector to assure quality. A software indicator also displays GPS position quality. When the GPS position is of the highest quality (RTK-fixed) the software indicator is green. When the GPS position is sub-optimal, i.e. in a non-RTK fixed quality state, the software indicator will turn orange and then red to alert the operator to a degradation in position quality.

Post-processing of EMPACT data occurred shortly after each data collection to produce detection maps and EM sensor noise metrics. The maps were reviewed to assure proper position and EM sensor integration and data collection using proper line spacing. Noise metrics were reviewed to assure proper EM sensor operation.

IVS data were acquired before and after survey operations over the grid area. We generally acquired at least 2 passes (down and back) over the survey strip to ensure good coverage over the targets. The Z-axis receiver data were processed and gridded to examine data maps for general quality and position control. Then the data is post-processed using the detection and mapping software described. Figure 57 shows examples of the our IVS surveys during the full grid coverage operations on 19 July 2017. In both surveys all targets were detected with high confidence (>20 dB) and located within our data quality objectives (+/-25cm)

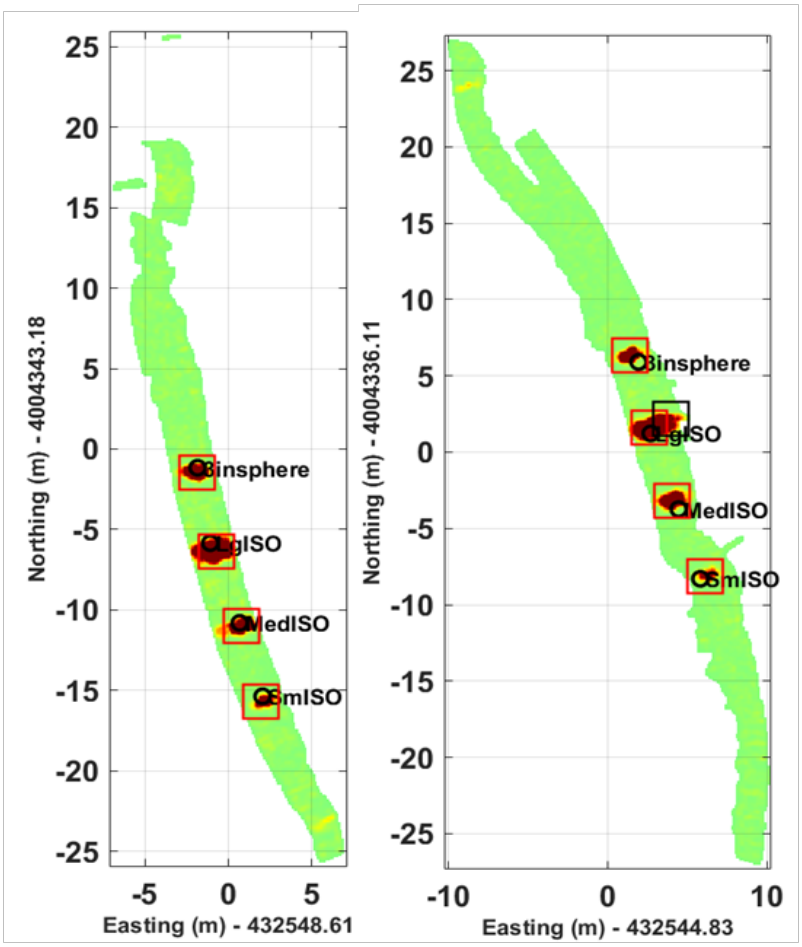

Figure 57. Gridded EM Maps Displaying the Processed Z-axis Receiver Channel Data Over the IVS Survey Area Before (LEFT) and After (RIGHT) Full Grid Data Collections on 7/19/2017.

All targets were detected with high SNR and localized within our data quality objectives. Two passes were used (down and back) to create the aggregate dataset for each IVS assessment. The red square symbols indicate detections in relation to the black circle symbols, which indicate the recorded groundtruth positions. The black square symbols indicate additional independent detections that are not within 25cm of the groundtruth location.

Accumulated IVS data are shown in Figure 58. The target detection locations are shown on a location error plot referenced to the previously acquired RTK-GPS ground truth positions. In the four cases represented the target locations are well within the +/-50 cm 100% error probability and all targets were located within a +/-25 cm (50%) circular error probability (CEP). Some deviation of the normally very accurate (<10cm) IVS positions were observed and attributed to flexing and motion of the GPS rover atop of the mast. This effect was also observed during operations and is discussed in more detail in Sections 7.1 and 7.4 below.

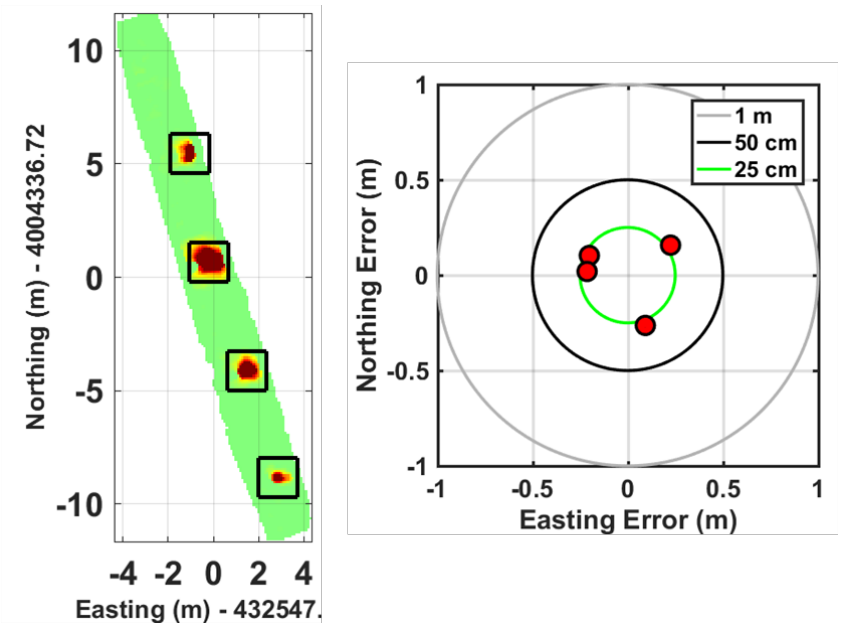

Figure 58. Aggregation of Four Survey Passes Over the IVS Area.

The Z-axis receiver data map show well- formed anomalies and detections (black square symbol) for each target. The detection locations are relatively accurate and within our performance metrics, however, they appear to be larger than expected. We correlate the relatively large position errors over the IVS to observed sway of the GPS rover atop of the mast.

5.5.3 Data Summary

All data were backed up to multiple hard drives during the demonstration. Redundant copies reside on a White River Technologies networked attached storage system raid. Data were compiled from the following survey days:

17-18 July 2017: set up, calibration, and shakedown surveys at Duck FRF site
19-20 July 2017: surf-zone target grid demonstration surveys

The primary datesets include all raw and processed system navigation and EM data. The raw data files are mixed ASCII and BINARY format. Processed data are saved in binary Matlab .MAT files. Auxiliary data from on-board and local site monitoring stations are also compiled with the primary data. These include FRF meteorological and oceanographic data from wind and acoustic doppler measurement stations around FRF as well as base station and geodetic survey control GPS data (HyPack format). On-board auxiliary data included the following:

- single-beam sonar (Echologger) full waveform data files from 19 July 2017
- self-logging accelerometer data (Hobo) and self-logging conductivity, salinity, and temperature data (Hobo CST) from 19 July 2017
- the crawler-EM mission planner Navigation lines as saved on the OCS mission and trackline guidance user interface computer
- on-board acoustic doppler velocimeter data (Vector ADV) * lost to sea without recovering data

6.0 DATA ANALYSIS AND PRODUCTS

Data analysis was performed using custom preprocessing, detection, and discrimination software developed using the Matlab software environment. Flex-EM data pre-processing, gridding, and detection work products may also be imported into the Geosoft Oasis Montaj UX-Detect software module.

6.1 PREPROCESSING

6.1.1 Navigation and Control Data

A custom software application imports the raw log files recorded during the test and analyze the data to produce statistics describing the noise and bias of the individual sensors, the vehicle navigation, and the control system performance. RTK-DGPS, GPS heading, and tow point encoder data were synchronously acquired and inserted directly into the archived EM data files. No further preprocessing of the Navigation data is required.

6.1.2 EM Sensor Data

The preprocessing of Flex-EM data included median filtering of each data channel to remove intermittent spikes found in the raw data. To remove any temporal drift, the data were sent through a linear piece-wise detrending algorithm to center the noise of the data at an amplitude of zero. Navigation and EM data were correlated in time through interpolation of the EM data with time samples that match the navigation data.

6.2 DETECTION

The Flex-EM post-processing software implements data filtering, position and EMI data merging, and detection routines to provide anomaly locations. A physics-based inversion routine determines accurate target locations as well as classification features corresponding to detected anomalies. Dipole parameters are selected to minimize misfit between dipole model outputs and the Flex-EM data. Classification features based on these dipole-fit parameters are compared to those of known library targets to determine a target or clutter classification. The inversion of Flex-EM data can be performed on-site immediately after surveying an anomaly with very little input from the analyst.

Each time channel of the Z-oriented receiver data is passed through a median filter to remove noise spikes. A 2-D map is created using the sum time decay for the Transmit-Z/Receive-Z data channels. Data are gridded, a 2-D interpolation is applied, and a 2-D spatial filter is applied to spatially smooth the data.

A peak detection algorithm is applied to the generated grid using a threshold based on the data noise floor standard deviation or site-specific TOI detection thresholds. A detection radius is applied to identify the ROI surrounding each peak. If ROIs associated with multiple peaks overlap, a combined ROI is generated that encompasses the multiple detections. Finally, across track and along track indices are generated for each alarm in an ROI. These indices correspond to the receiver cube and sounding number associated with each alarm and provide the initial starting parameters for the inversion. Each ROI is saved as a data volume (number of soundings x number of time gates x number of data channels) in Matlab binary (.MAT) format. Alarm indices and UTM coordinates are saved as part of the data structure as well.

6.3 PARAMETER ESTIMATION

Parameters are estimated using physics-based models to support discrimination of targets from potential clutter items. The primary discrimination method uses a least-squares fit to library polarizabilities. Secondary discrimination methods apply a Gaussian mixture model to the 2-D (size and rate of decay) feature spaces generated from the discrimination parameters.

All features are derived from a least-squares fit to a dipole model. The bases for the discrimination features are the object polarizabilities. Polarizabilities are estimated from a linear least-squares inversion of the dipole forward model:

$$\begin{bmatrix} H'_x & H'_y & H'_z \end{bmatrix} = \frac{1}{4\pi R^3} \begin{bmatrix} m_x & m_y & m_z \end{bmatrix} \begin{bmatrix} \frac{3x^2}{R^2} - 1 & \frac{3xy}{R^2} & \frac{3xz}{R^2} \\ \frac{3xy}{R^2} & \frac{3y^2}{R^2} - 1 & \frac{3yz}{R^2} \\ \frac{3xz}{R^2} & \frac{3yz}{R^2} & \frac{3z^2}{R^2} - 1 \end{bmatrix}$$

where mx, my, and mz are the object principal polarizabilities scaled by the transmitter field:

$$\begin{bmatrix} m_x & m_y & m_z \end{bmatrix} = \begin{bmatrix} L_x & L_y & L_z \end{bmatrix} \begin{bmatrix} H_{Tx}' & 0 & 0 \\ 0 & H_{Ty}' & 0 \\ 0 & 0 & H_{Tz}' \end{bmatrix}$$

The primed coordinates denote the target frame of reference where the magnetic field data are transformed using the Euler rotation angles φ, θ, ψ:

$$\begin{bmatrix} H_x' & H_y' & H_z' \end{bmatrix} = \begin{bmatrix} H_x & H_y & H_z \end{bmatrix} \begin{bmatrix} \cos(\phi)\cos(\theta) & \cos(\phi)\sin(\theta)\sin(\psi) - \sin(\phi)\cos(\psi) & \cos(\phi)\sin(\theta)\cos(\psi) + \sin(\phi)\sin(\psi) \\ \sin(\phi)\cos(\theta) & \sin(\phi)\sin(\theta)\sin(\psi) + \cos(\phi)\cos(\psi) & \sin(\phi)\sin(\theta)\cos(\psi) - \cos(\phi)\sin(\psi) \\ -\sin(\theta) & \cos(\theta)\sin(\psi) & \cos(\theta)\cos(\psi) \end{bmatrix}$$

The rotation angles and the target location (*x, y, z*) are estimated using a non-linear least squares inversion.

6.4 CLASSIFIER TRAINING AND DISCRIMINATION

Historic data collected using the sensor and data collected during preliminary tests performed in-air on at test stand at White River Technologies New Hampshire test facility were used to develop polarizability libraries.

6.5 DATA PRODUCTS

Data products consist of calculated metrics as well as figures to illustrate the data used to calculate the metric.

6.5.1 Stability and Mobility Data

Metrics generated from these tests result are based on the comparison of a true value to a value estimated by the navigation system. These can be represented by plots of time versus the navigation system data and time versus the ground truth data or desired data. For stability (roll, pitch, yaw) data the navigation output will be compared to the desired parameters. For northing and easting data the navigation output was compared to target ground truth of the northings and eastings of the target locations. Figure 59 illustrates an example of these data products.

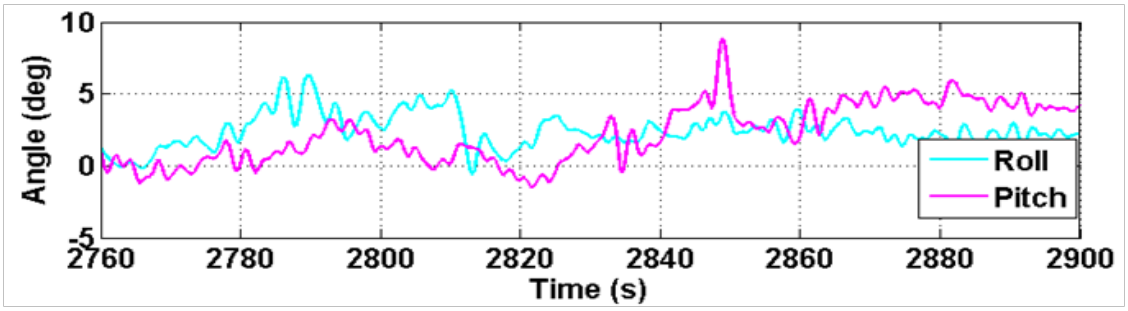

Figure 59. Examples of Stability and Mobility Data Products.

6.5.2 Detection Accuracy

The estimated detection location (N, E) were compared to the ground truth location of the target interrogated. This resulted in a two-dimensional location error plot (Figure 60) showing the location of the estimate versus the ground truth to reveal error trends and bias. Halos of different sizes are shown to illustrate scale.

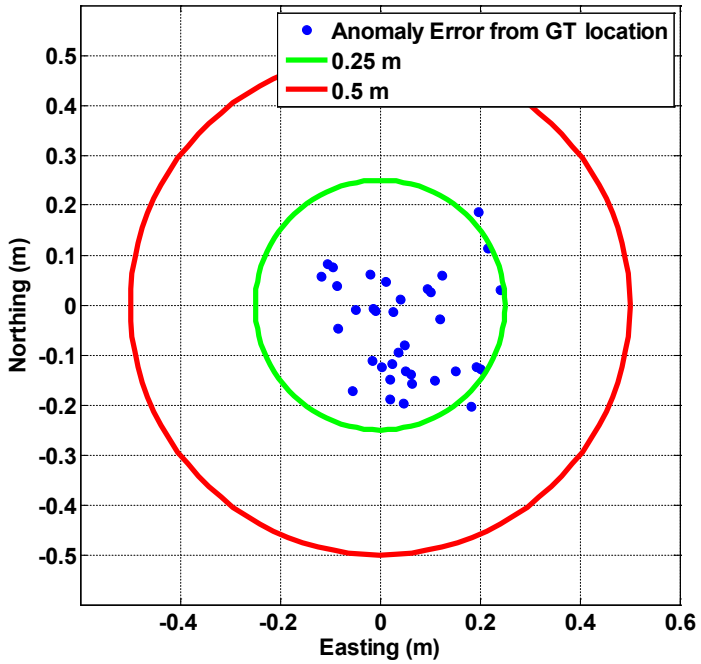

Figure 60. Data Product Illustrating the Detection Location Accuracy Metric.

6.5.3 EMI Sensor Data

Data from the Flex-EM was periodically checked including all data channels comprising 18 receivers with N time gates each. Survey data maps (Figure 61) and channel-based profile plots are used to assess data quality. An example of this is shown in Figure 62.

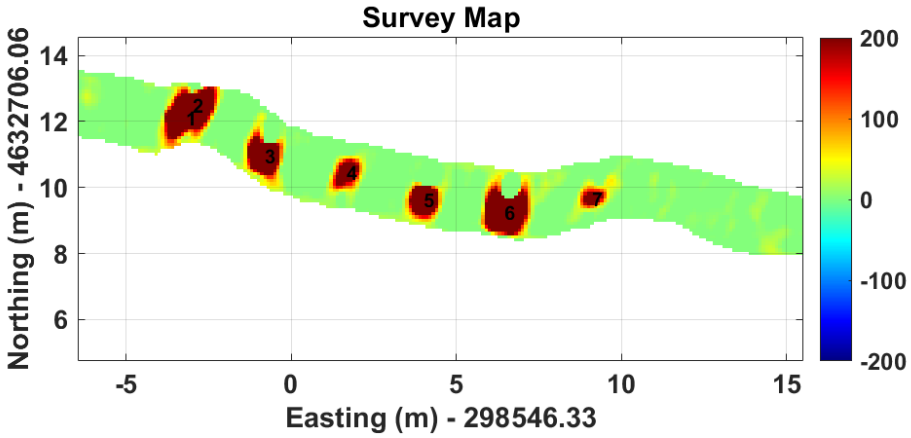

Figure 61. Survey Map Created Using a Single Pass Over Six Emplaced Targets.

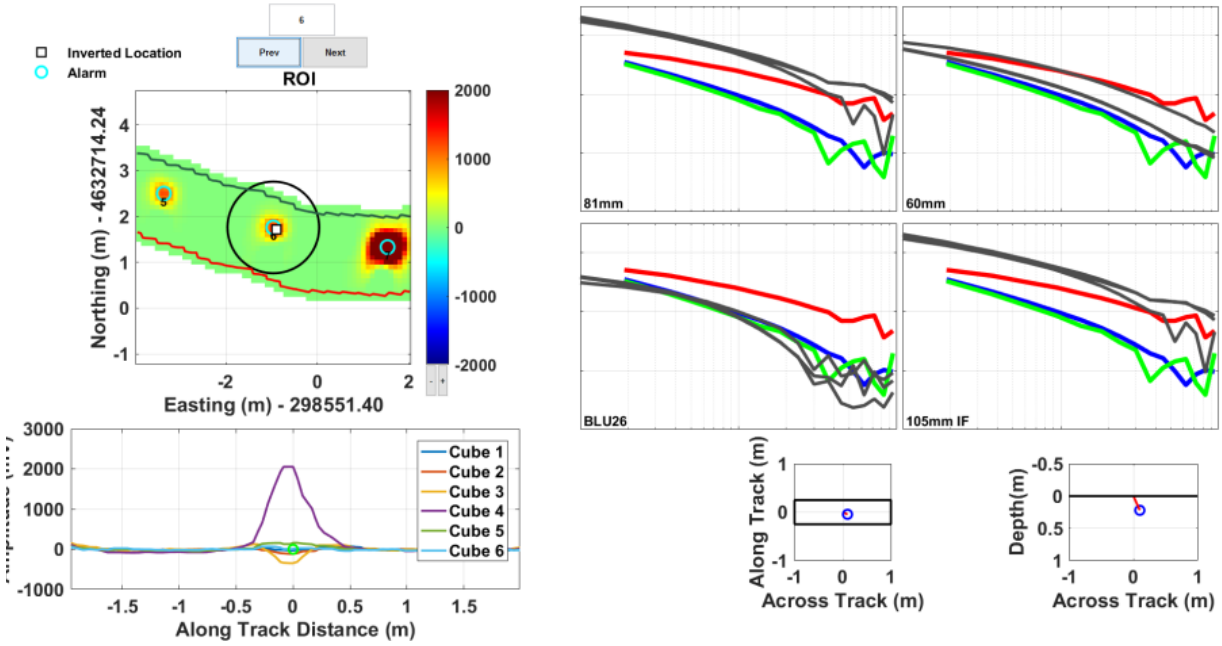

Figure 62. Example Data Product Illustrating the Map and Inverted Polarizability Analysis Information to be Supplied Along with the EMI Array Data Quality Checks.

This target comprises a relatively good match to a 60mm mortar as indicated by the library match fit in the upper right quadrant of the polarizability match display.

7.0 PERFORMANCE ASSESSMENT

We assessed performance using the previously defined test objectives and associated metrics shown in Table 4. These include quantitative metrics related to system stability, navigation and control, target detection/localization, and object classification as well as qualitative metrics such as those associated with operational use. An assessment of each objective is provided in the following sections.

Table 4. Summary of Target Objectives, Metrics, and Results.

Performance Objective	Target Metric	Observed Result
Surfzone Stability	$\Delta R < \pm 6°$, $\sigma R < 3°$ $\Delta P < \pm 6°$, $\sigma P < 3°$ $\Delta Y < \pm 4°$, $\sigma Y < 2°$ $\Delta X < 0.20$ m, $\sigma X < 0.15$ $\Delta Y < 0.10$ m, $\sigma Y < 0.07$ $\Delta A < 0.10$ m, $\sigma A < 0.15$	$\max(\Delta R) = 5.8°$, $\sigma R < 2.7°$ $\max(\Delta P) = 7.7°$, $\sigma P < 3.8°$ $\max(\Delta Y) = 8.9°$, $\sigma Y < 3.6°$ $\max[\Delta X$ or $\Delta Y] = 0.26$ m , $\max[\sigma X$ or $\sigma Y] = 0.04$ m $\max(\Delta A) = 0.06$ m, $\sigma A < 0.01$ m
Area Coverage	Shore-Parallel Adv. Rate > 0.42 m/s	Average Shore-Parallel Adv. Rate = 1.09 m/s; approximate coverage rate of 0.5 acres/hour
On-shore / off-shore Mobility	Shore-Perpendicular Adv. Rate > 0.28 m/s	Average Shore-Perpendicular Adv. Rate = 0.32 m/s
Detection of all munitions greater than 60 mm	SNR > 9 dB Pd > 0.95 (assuming a nonfluctuating target and Gaussian noise a 0.95 Pd at 9 dB corresponds to a pFA of approximately 0.01)	All target SNRs > 20.7 dB Pd = 1.0
Detection Location Accuracy	ΔTN and $\Delta TE < 1.0$ m σTN and $\sigma TE < 0.35$ m	$\Delta TN = 0.29$ m, $\Delta TE = 0.22$ m $\sigma TN = 0.42$ m, $\sigma TE = 0.51$ m
Classification of all munitions ≥60 mm	Probability of Classification, Pclass>0.75 with at least 50% of clutter ranked below the UXO	Data not sufficient to assess, but limited multi-angle illumination data yielded promising results
Ease of use	Ease of use compared to alternate standard marine surveying procedures	OCS very effective, but line of sight valuable; more robust tether or wireless tether needed
Launch and recovery	Time to launch, time to recover, mean down time	Launch and recovery very effective; no significant down time

7.1 SYSTEM STABILITY

To assess system stability, we analyzed and compared inertial data from the crawler and tow sled IMUs. We also integrate non-quantitative observations of platform and tow sled stability. The qualitative observations were made both during operations-based operator, analyst, and observer notes and live streaming video from crawler-mounted cameras as well post-mission via review of video data. Video data was acquired from GoPro cameras mounted on the crawler, on the tow sled, and on observations points (like the pier) during surveys.

Typical target area transects began on the beach and progressed directly into the surf perpendicular to the shoreline. Once in the surf, the crawler-EM system rate of forward advance would slow due to hydrodynamic resistance and possibly also due to softer sediments on the seafloor. Among the most dynamic and challenging regimes was deep swash and surf inside of the wave break where strong wave induced currents ebb and flow. Some examples of the system operation in the swash and surf from the vantage point of the pier are exemplified in Figure 63 and Figure 64. In these images we show that sometimes both the crawler and tow sled are partially submerged and experiencing similar currents and at other times one of them is fully submerged while the other is only partially submerged. In the latter case, the two "bodies" of the system may experience very different forces both in magnitude and direction.

Figure 63. Photograph of the Crawler and Towed EM Sled System Operating in Shallow Swash.

In this instance, both the crawler and sled and partially submerged and experiencing relatively light hydrodynamic loading.

In addition to video and photographs from remote vantage points, we also utilized video from on-board cameras on the crawler to assess stability under dynamic loading conditions. Figure 65 shows and example of images captured from video collected on looking forward from mount points on the crawler and on the sled, and looking down and backward from the mast.

Figure 64. Photograph of the Crawler and Towed EM Sled System Operating in the Surf.

In this case, the crawler platform is seaward of the wave break and likely experiencing a very different forcing than that experienced by the EM tow sled, which is currently being inundated by a wave.

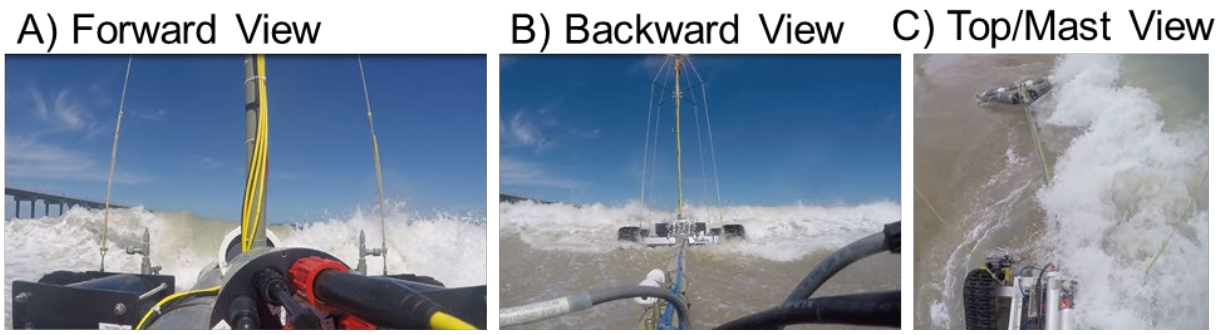

Figure 65. Photograph Captures from Video Cameras Located on the Crawler Platform During Operations.

A) forward looking camera on the crawler, B) crawler-looking camera from vantage point on the sled tow bar, and C) back- and down-ward looking camera from vantage point on the mast.

In some cases, we observed heave and sway of the tow sled relative to the crawler when operating in the surf. By far, the largest instability occurred while the array was oriented parallel to the wave break in moderately deep surf where the ebb and flow of run up wash imparted strong cross currents on the tow platform. This generally manifested as a yaw deviation with the array lifting slightly off the seabed and rotating to a new yaw angle relative to the direction of motion. This appeared to happen when the tow sled experienced significant lateral forcing, especially when shallow (0.15-0.35 m) swash impacted the tow sled or when ebbing currents strongly pulled the array back seaward. An example of this is exemplified in Figure 66, where we show a sequence of video captured still images of the system from the mast viewpoint. Here the system is traversing primarily parallel to the shoreline and swash direction. Initially the sled is tracking the crawler with a noticeable yaw deviation toward shore. After being inundated with a wave and experiencing the subsequent ebb current as water drains back seaward, the tow sled is tracking near in-line with the crawler.

We quantified EM tow system stability metrics using data collected while the crawler towed the EM array through the surf. The IMU on the tow sled provided roll, pitch, and yaw information and when used in combination with similar IMU data from the crawler, it provides relative angles and translation of the sled during surf-zone surveying maneuvers. Stability was determined with respect to relative rotational stability and translational movement of the EM array over the seabed.

A representative example of the analysis of roll, pitch, and yaw stability analyses are shown in Figure 67. This example shows the crawler rotational angles (roll, pitch, and yaw) overlain with those from the EM array tow sled. If we use the crawler as a stable reference in the surf, deviations from its rotational angles may indicate instability of the EM array. The objectives are also plotted relative to the instantaneous angle information reported from the IMU on the crawler platform. These are ±4 degrees in yaw and ±6 degrees in both roll and pitch. It is apparent that the yaw deviations exceeded our objectives in a large portion of the example transect, while the roll and pitch deviations are within our objectives.

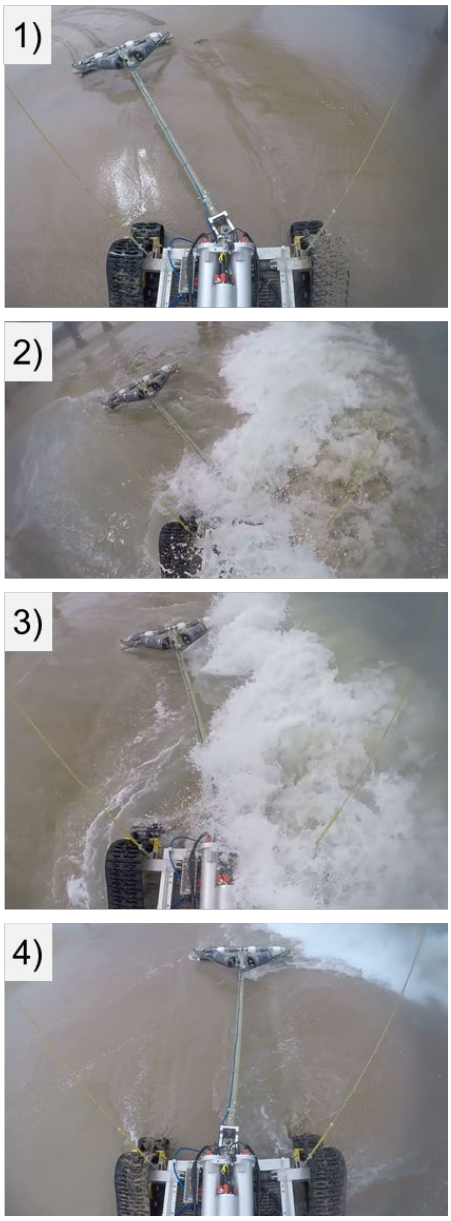

Figure 66. Sequence of Still Images Captured from Video Acquired from the Camera Mounted on the Mast of the Crawler.

The camera view is looking down and backward toward the EM tow sled system. In this case, we can see the progression of the tow sled as the crawler traverses parallel to the shoreline near the water depth of the wave break at this time. In the TOP figure (1) the seafloor is nearly completely drained between ebb and flow swash cycles, but the image of the EM tow sled reveals a noticeable yaw deviation from the crawler. In the next image in the sequence (2), a wave begins to inundate the system perpendicular to the direction of travel. The initial impact does not seem to force either the crawler or tow sled to translate or rotate (despite the warped appearance of the fisheye camera view). Between (2) and (3) the wave forcing reaches a maximum and the ebbing current from the previous wave acts to push the tow sled seaward. In the BOTTOM image (4), the tow sled has rotated in yaw to a position that is nearly in-line with the crawler and the ebbing current is nearly fully drained again.

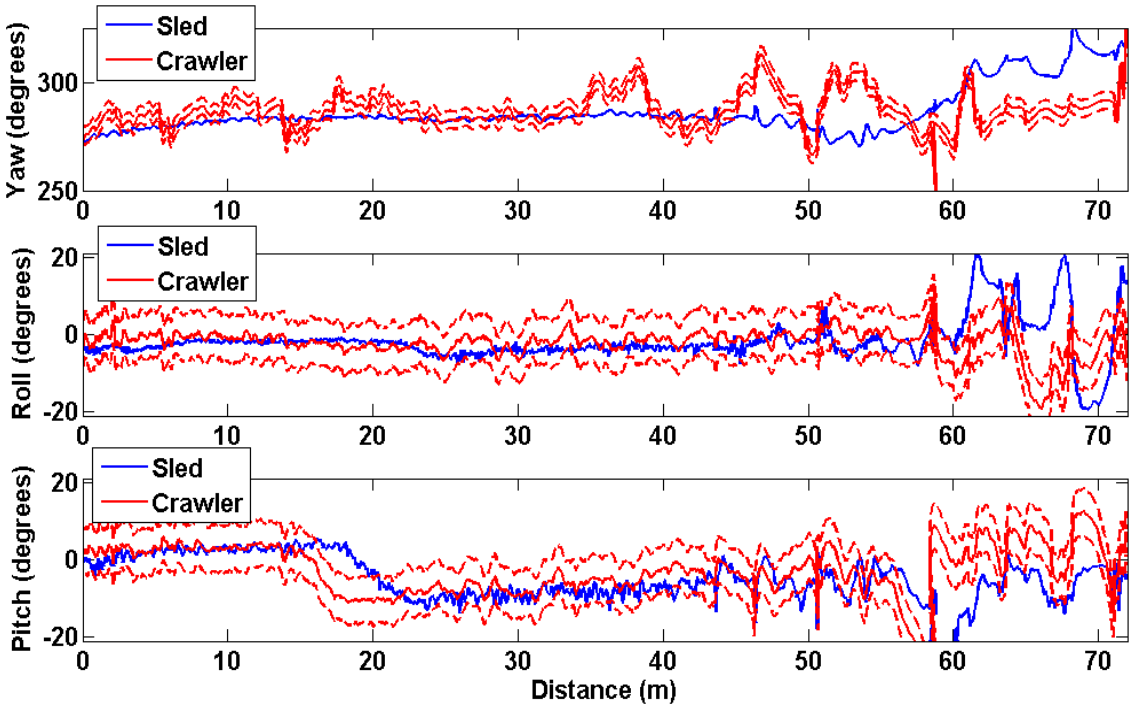

Figure 67. Plots of Measured Sled Yaw (Top), Roll (Middle) and Pitch (Bottom) Are Shown in Blue. The Solid Red Line Is the Yaw, Roll, and Pitch of the Crawler. Dashed Red Lines Indicate the Performance Objectives.

The distance is relative to the starting point on the upper beach such that the transition from dry beach to intermittently flooded swash zone occurred approximately between 25-35 meters and surfzone to wave break at approximately 50 m. Objectives were met for roll and pitch but exceeded in yaw.

To estimate the overall stability metrics, we compiled transects from 19 July 2017. Almost all of these transects were perpendicular or nearly perpendicular to the shoreline. This included nearly 2 line-km of transects. Figure 68 shows the roll, pitch, and yaw deviation histograms. The maximum roll deviation over these transects was 5.8º while the standard deviation of the roll was 2.7º. For average pitch deviation over these transects we computed a maximum pitch deviation of 7.7º with standard deviation of 3.8º. Yaw deviations were the greatest with a maximum of 8.9º and standard deviation of 3.6º.

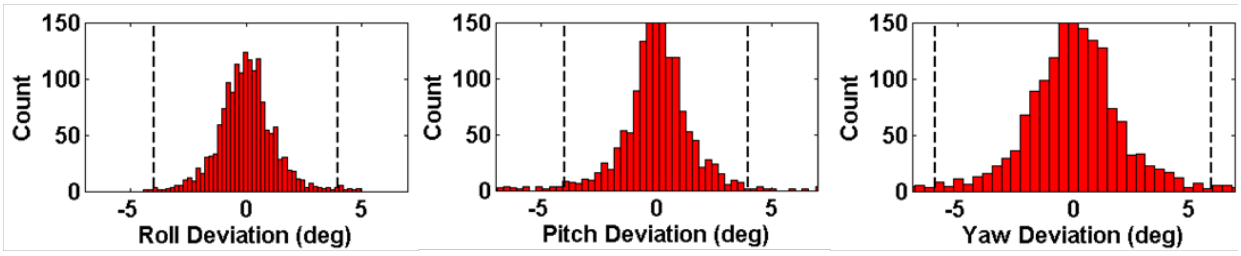

Figure 68. Example Survey Transect Roll, Pitch, and Yaw Stability Measurements During Surfzone Demonstrations on 7/19/2017.

The histograms show the distribution of deviations with the performance goal metric outlined by the dashed lines.

We also analyzed individual transects survey runs using the IMU data from the crawler in order to compare it with the IMU data acquired directly on the V320 RTK-GPS smart rover antenna on the mast. As briefly described in Section 5.2.2 (Quality Checks), observers noticed some sway motion of the GPS rover antenna at the top of the mast during IVS surveys and subsea transects. Figure 69 shows a comparison of the individual transects and accumulated statistics for pitch and roll computed from the crawler and GPS antenna. All data are from transects conducted perpendicular to the shoreline. These plots show increasing roll and pitch variability as water depth increases (or elevation decreases). The GPS roll and pitch are more variable than the crawler roll and pitch, which is expected due to the long moment arm relative to the base point of roll and pitch rotation of the crawler on the seafloor. It may also indicate accentuated motion of the GPS antenna on the mast relative to the crawler (i.e., sway and heave of the antenna mast). Roll and pitch deviations appear to be minimized over flat sandy areas in the swash zone (elevations approximately -1 to 1 m) and slightly higher in the upper beach region (elevations >1 m).

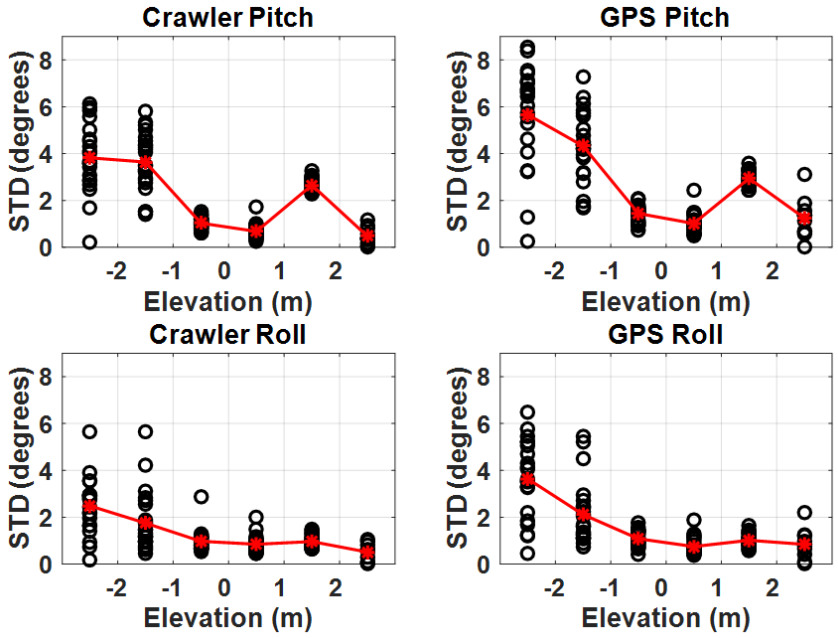

Figure 69. Analysis of the Standard Deviations of Roll and Pitch Computed from IMU Data on the Crawler (LEFT) and the IMU on the V320 RTK-GPS Smart Antenna on Top of the Mast (RIGHT).

Both IMUs indicate higher deviations in relatively deep water (elevations <-1 m). Roll and pitch deviations for the GPS are noticeable accentuated relative to those from the crawler, especially in water depths beyond the wave break and surf area (elevations <-1m).

7.2 AREA COVERAGE RATE

Originally our metric for area coverage considered the ability of the system to provide 100% coverage a nearshore area. We outlined a metric that quantified the potential to maintain an advance rate while operating parallel to the shoreline. In our full grid coverage surveys during the demonstration, we performed transects perpendicular to the shoreline. Therefore, area coverage was primarily gauged by assessing the average advance rate, cumulative distance travelled during grid coverage, and either elapsed or total time of the surveys.

During full coverage surveys the system achieved an average advance rate of 0.288 m/s or 1.03 line-km per hour. This advance rate is computed from the total distance travelled (1.77 line-km) and the total time to complete the survey (103 minutes). The rate of advance could also be computed by taking the instantaneous average speed of 0.32 m/s, but this overestimates the accumulated rate due to time in transitions and turns when the system is not moving. Some transition time was also taken up by data collection analysts needing to reset acquisition parameters, such as a new line filename prior to restarting surveys.

Using the accumulated advance rate, we estimate a maximum possible coverage rate of 2072.2 m^2 per hour or 0.512 acres per hour (0.21 hectares per hour). This assumes essentially no overlap is required and that survey lines are perfectly straight. Generally, we would require at least 20% overlap to achieve 100% coverage within some statistical sampling confidence interval (e.g., PNNL Visual Sampling Plan methods). Assuming 20% overlap, we compute a coverage rate of 0.41 acres per hour (0.17 hectares per hour). To put this in very plain language, we can consider a 100m x 50m area or the approximate size of a football field (or slightly smaller than a soccer pitch…), at an average advance rate of 1 line-km per hour, we could fully cover this area in about 2.5 hours.

Figure 70 shows a map view of the survey transects from which we computed advance rates. The average ground sampling distance was approximately 21 cm with a standard deviation over the entire survey of 6.6 cm. The largest ground sampling distance was 42 cm. The target area covered by our surveys as defined by the convex hull (or affine envelope space determined by the vertices of the survey data) is approximately 1550 m^2 or 0.38 acres. At 100% coverage, this would equate to approximately 5 hours to cover a hectare or 0.5 acres/hour. The average instantaneous speed was 0.32 m/s, which is faster than the objective of 0.3 m/s. However, a good portion of the time during these tests were spend traversing the lower beach during when the crawler system was not submersed or only partially submersed.

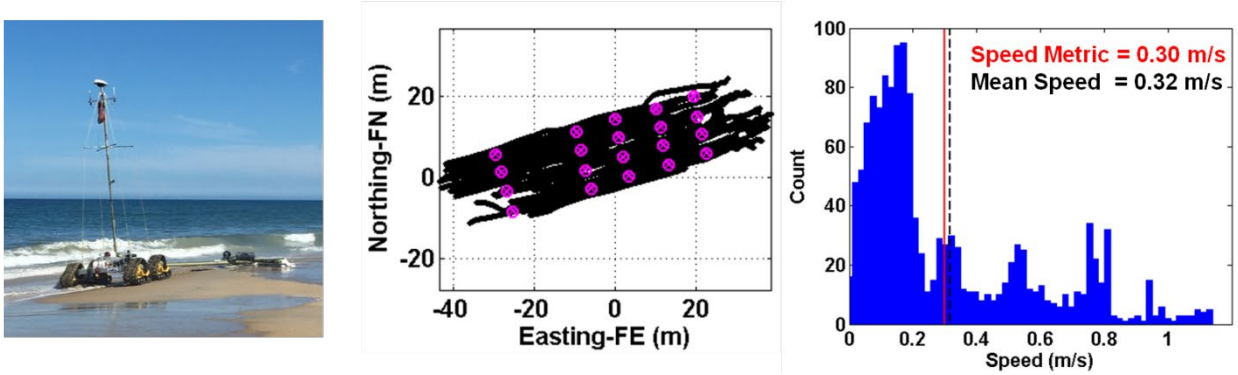

Figure 70. Compilation of Offshore and Onshore Transects Used for Computing Coverage Metrics.

Left: transects divided into shore parallel (red) and shore-normal (green) transects. Histograms of averaged advance rate for both directions of transects are shown in the middle and right. Shore perpendicular speeds were noticeable slower and had a wider variation compared to shore parallel speeds.

7.3 ON- AND OFF-SHORE MOBILITY

The mobility of the integrated system perpendicular to shore was shown in Figure 70. Because our primary metric was an assessment of the average forward velocity of the system perpendicular to the shore to submergence of 2 meters of water, we aligned our survey transects into and out of the surf. We were able to average 27 perpendicular traverses extending from on-shore to off-shore to compute an average velocity of 0.32 m/s, which exceeded our objective of 0.30 m/s (or 1 kph or 0.54 knots).

During the AM portion of these surveys perpendicular to the shoreline, we also measured conductivity, temperature, and salinity (CST) with the Hobo CST self-logging instrument strapped to the tow bar extending to the EM sled approximately 25 cm above its the base (i.e., above the nominal seafloor). Therefore, the sensing elements were only fully submerged when the sensor was in at least 25 cm of water. Also, during these surveys we acquired data with the Echologger single-beam acoustic profiler. The data were time synchronized using fiducial markers common to both data sets (e.g., simultaneous submergence). Figure 71 shows the CST and acoustic backscatter intensity data for multiple survey passes from beach into the surf and back again to the beach. The temperature gauge on the CST meter has a slower response time due to the nature of those measurements relative to the conductivity or acoustic backscatter data. Nonetheless, we can observe ports of the data when the sensors are alternately submerged (in surf) and dry (in swash or on beach). There is also a noticeable consistency and symmetry to the form of the conductivity and backscatter data throughout the submerged time portions.

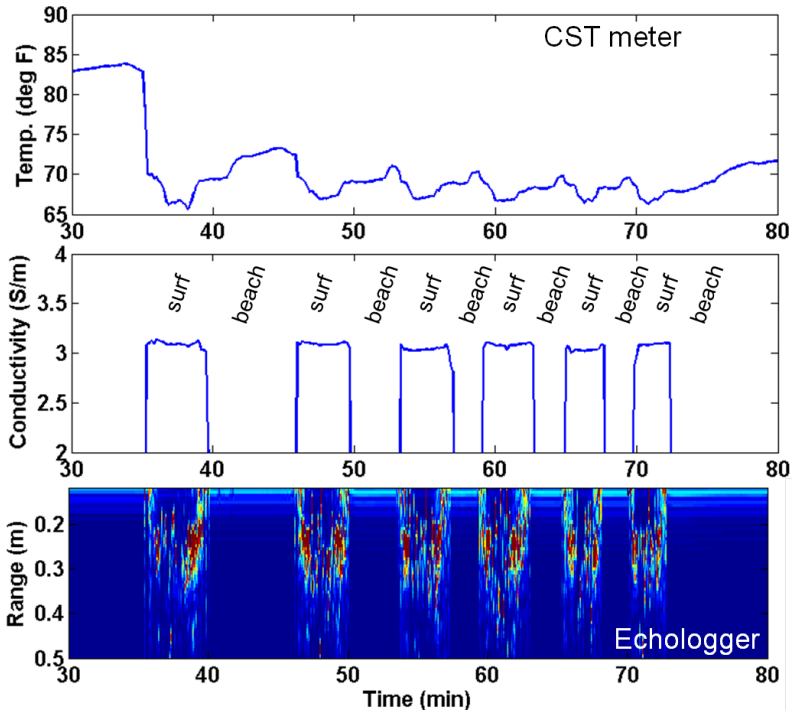

Figure 71. Synchronous Temperature (Top), Conductivity (Middle), and Acoustic Backscatter (Bottom) Data Acquired During Part of the AM Surveys on 7/19/2017.

Alternating periods of submergence and dry operations are evident in all data. Electrical conductivity of the seawater was relatively consistent and stable at just over 3 S/m during these surveys.

Acoustic backscatter gives us some indication of variability in the bottom type and thus bottom condition. We attempted to correlate the integrated acoustic backscatter intensity with crawler speed and water depth. This is shown in Figure 72 for a single out-and-back transect. Here we are primarily showing the portions of the transect while the system was fully submerged. Because the Echologger instrument (single beam acoustic backscatter) was mounted approximately 25 cm above the track base and the depth sensor was approximately 38 cm above the track base, the depth sensor was not submerged during the same period as the Echologger. Although it is difficult to observe any clear correlation, it is likely the crawler advance rate was decreased in less dense substrate as indicated by a lower overall integrated acoustic intensity. Other maneuvers such as the turnaround and adjustments also contributed to changes in the speed, making a direct correlation between backscatter and speed indeterminate.

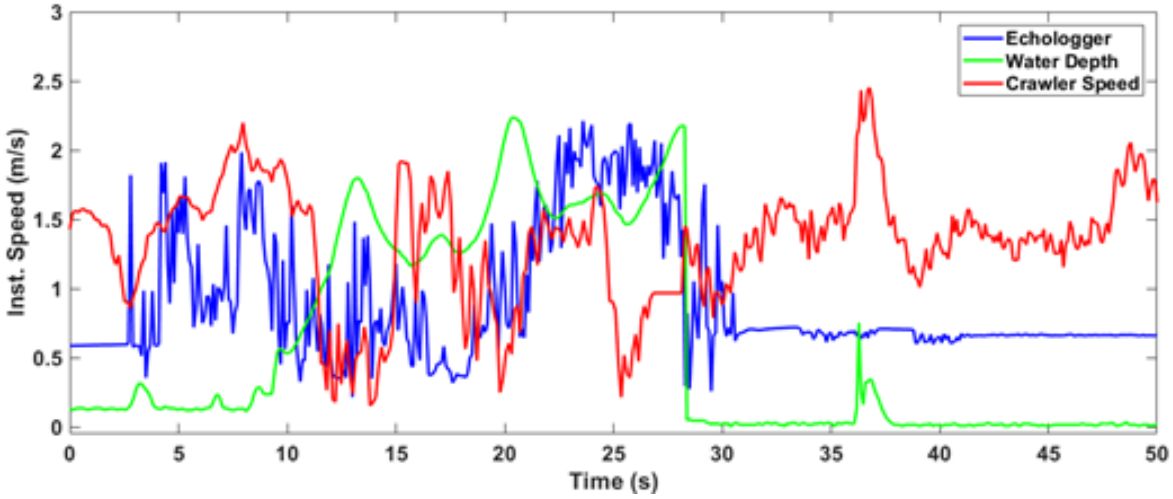

Figure 72. Comparison of Instantaneous Crawler Forward Advance Rate (Speed; Shown in Red) and Integrated Acoustic Backscatter Intensity Recorded by the Echologger Single Beam Acoustic Instrument (Blue). The Water Depth Measured on the Crawler (green) Shows That This Portion of the Crawler Onshore-to-offshore Transect Was Primarily While the System Was Submerged.

Slowing of the crawler system at ~20 seconds was likely associated with the turnaround for return to the shore. Water depth and acoustic backscatter data <3 seconds and >30 seconds is not valid due to the measurement devices being elevated out of the water.

7.4 DETECTION

Detection metrics were calculated using the SNR and location of detections output from the detection processing and ground truth information. The target detection objective was target SNR greater than 9 dB for all targets greater than 60 mm in size (diameter). We achieved the objective with SNR greater than 36 dB for all targets. The largest detection SNR value was 69.6 dB for the 105mm projectile (target #17) and the smallest was 38.9 dB for the medium ISO object (target #21).

Figure 73 shows the SNR and offset from the estimated target location to the ground truth location for all of the TOI. All IVS passes yielded SNR values that exceeded 40 dB. For target detections in the surf-zone, we found a greater variability and generally lower SNR values.

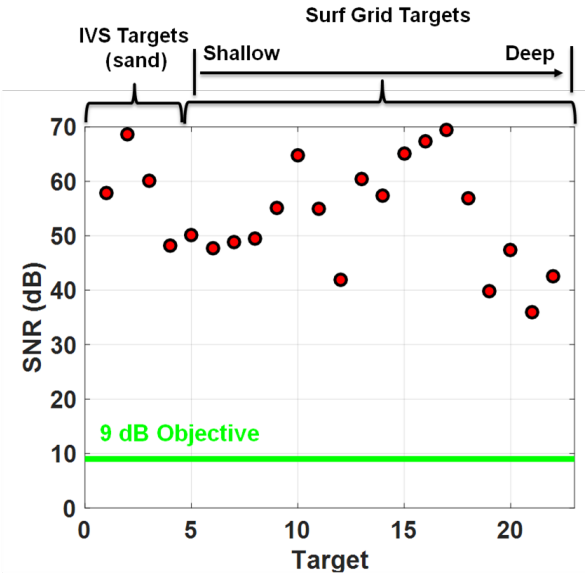

Figure 73. Detection Performance Results.

The signal-to-noise ratio (SNR) is plotted against target index showing that all detections exceeded the 9 dB SNR objective. Targets in the surf yielded lower SNR values as might be expected. We attribute this to the targets extending deeper below the seafloor than originally planned. In addition, lack of horizontal control prevented multiple passes for full coverage surveying.

A map of the Z-oriented integrated time decay data for the receiver array is shown in Figure 74. This survey consisted of the 27 shore-perpendicular passes over the target grid. The standard deviation of Z-oriented receiver data signals was slightly lower in the surf than on the beach: 1.4 mV on beach IVS surveys and 1.1. mV over all surf zone transects. All targets were successfully traversed, although it was apparent that some of the targets had mobilized out of the target area overnight, as was discussed earlier in Section 5.2.1. Very few natural clutter (non-emplaced targets) items were observed. These can be seen in the map further out into the ocean. There was also a particularly challenging area in the northeast part of the grid where the system did not obtain 100% coverage.

The original target set was installed on 7/17/2017, but four of the targets were no longer generating observable signals. We also searched for the flagging that was attached to targets and extending above the seafloor, but could find any evidence of it. On the morning of the next day (7/18/2017), we found two of the targets washed up on the beach 50-60 meters south of the target grid area. Two targets were installed to replenish these mobilized targets between first and second row of submerged targets in the grid. They did not appear to wash away (mobilize out of the target area) and were observed in the survey data from 7/19/2017.

In addition to mobilization of some targets, it is suspected that some of the remaining installed targets may have buried further into the seabed. We believe (but were not able to confirm) that the rough surf produced conditions that accelerated burial of the deepest row of targets over the duration of our surveys and thus modified their original burial depths. We estimated that the total sensor standoff (from receiver measurement point to center of the target) varied between 45 and 65 cm. In some cases, the sensor array may have been closer than the 20 cm nominal standoff from a hard base – this is due to the EM array sled scouring into the seabed.

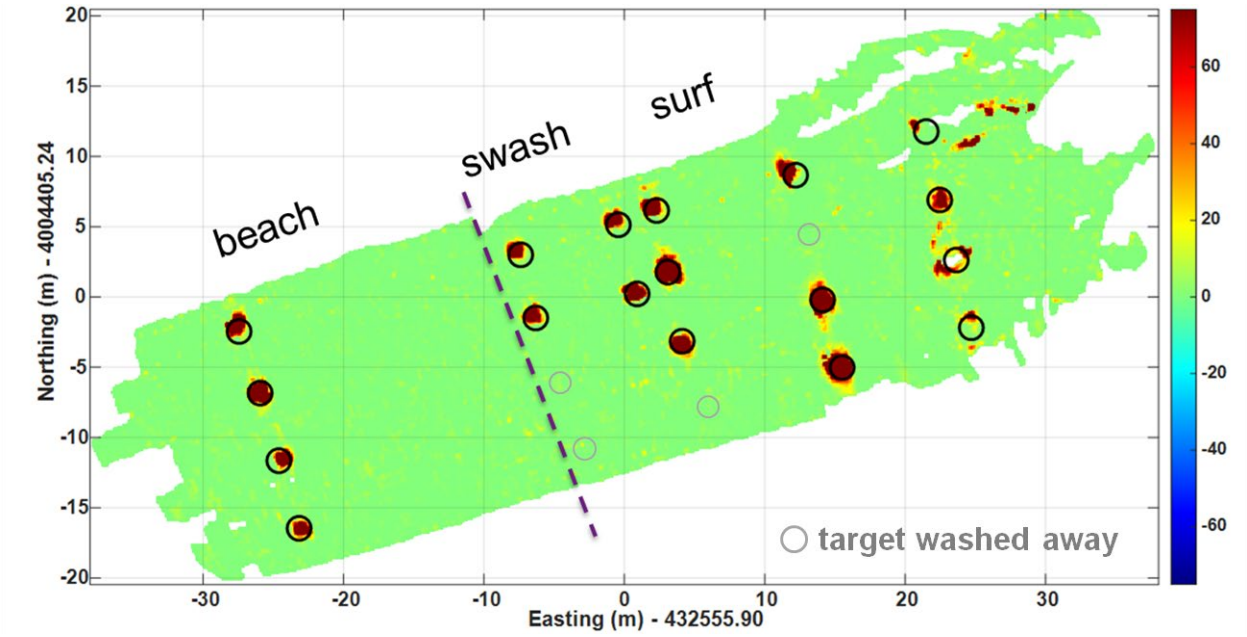

Figure 74. Example EM Data Map from Z-oriented Receiver Data During Shore-Parallel 100% Coverage Surveys in the Surf-zone.

Four of the previously emplaced (installed on 7/17/2017) targets mobilized and washed away prior to surveying. Two additional targets were subsequently added between the second and third shore-parallel target lines on 7/18/2017 and prior to data collection on 7/19/2019.

Detections were scored as TOI detections if the detection location was within a radius of 0.5 m of the TOI ground truth location. Eight non-TOI alarms were generated at SNR values greater than 9 dB; two were from emplaced clutter targets (angle iron and chain) and the others were presumably from native clutter (assumed but not confirmed) within the survey area.

7.5 LOCALIZATION ACCURACY

Detected anomalies from the surf-zone surveys were used to estimate target locations. The estimated detection locations were compared with those from GPS-based surveying of groundtruth locations.

Overall, the performance objective of mean and standard deviation of emplaced target locations (Easting and Northing estimates) less than 100 cm was achieved. All but three of targets were located within a 50cm radius (86%). The detection location errors for both IVS (beach) and surf-zone grid targets are show in Figure 75. The "bullseye" plot shows no particular statistical offset bias to the location errors. The maximum RMS average error in either northing or easting was 29 cm with a maximum standard deviation of 51 cm. The maximum standard deviation exceeded our objective of 35 cm.

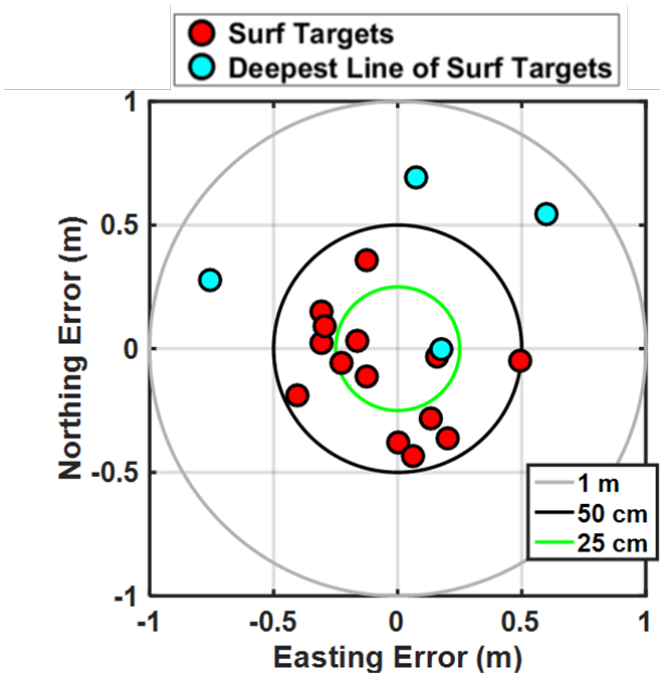

Figure 75, Target Localization "Bullseye" Plot for All Targets Detected During Surf Grid Surveys.

All targets were detected within a 1.0 m radius of the recorded groundtruth locations. 86% of the targets were located within a 50cm radius.

Further analysis revealed that there were significant differences in localization errors between those on the beach, this in shallow water (<1m), and those in deeper water (>1m). The deepest set of surf targets, which were generally in 2 meters or more of water had the greatest location error (see light blue symbols in Figure 75). In the aforementioned analysis of the surf-zone targets, we processed the RTK-GPS data along with data acquired from the encoder at the tow point for correct for angular offset of the trailing EM sled (since the GPS rover was on the crawler). We also utilized data from the IMU on the crawler to help correct EM receiver positions for roll, pitch, and yaw deviations of the EM sled relative to the crawler. Overall, the encoder-based corrections obtained better results. A comparison of the effect of the two types of corrections on target localization error are illustrated in Table 5.

Table 5. Comparisons of Location Errors and Location Deviations for Different Regimes and Analysis Methods.

Method	Error ΔNorthing(m)	Deviation σNorthing(m)	Error ΔEasting(m)	Deviation σEasting(m)
IVS Area (Encoder-based)	0.01m	0.13m	-0.06m	0.20m
Surf Zone Grid (Encoder-based)	0.02m	0.31m	-0.04m	0.33m
Surf Zone Grid (IMU-based)	0.34m	0.42m	-0.17m	0.45m

As stated, we observed a decrease in localization accuracy for the deepest line of targets in the grid. Deviations also increased noticeably. This was mainly attributed to stability of the GPS rover on the mast. One particular observation associated with positioning helps to understand the cause of the increased errors and deviations. Associated with the zone in which the waves break is a significant shore-parallel trough. This trough is evident in GPS elevation as well as pressure depth sensor data from the crawler. This is shown in Figure 76. Following the sudden drop into the trough (when traversing seaward), all localization sensors show an increase in variability. This includes GPS antenna roll and pitch, crawler roll and pitch, GPS location (Northing and Easting), GPS-derived heading, as well as encoder data.

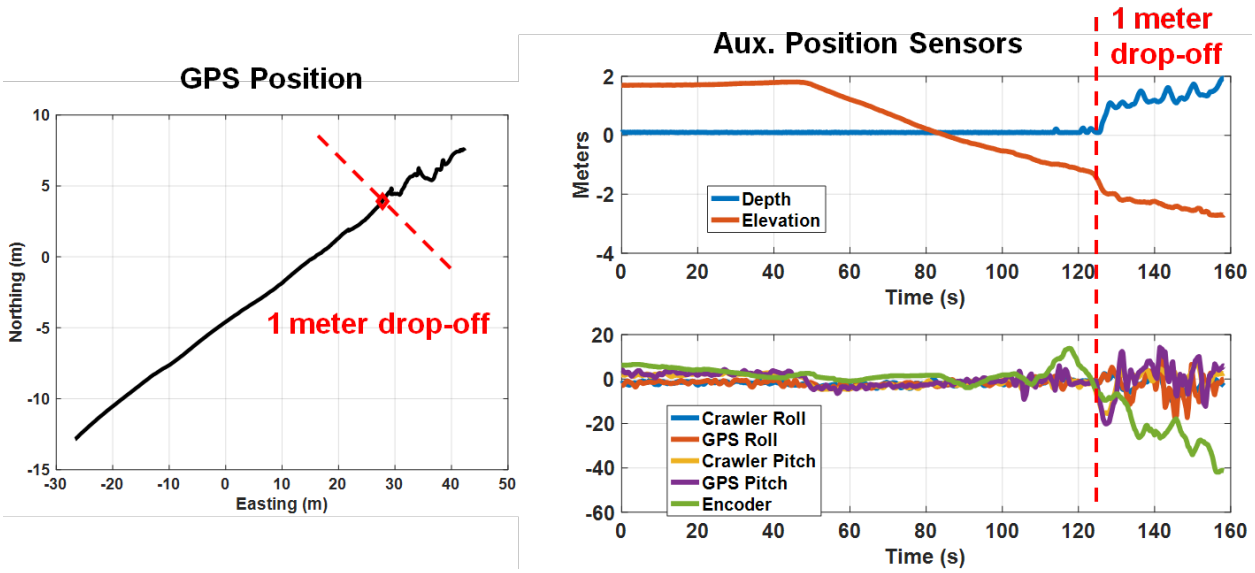

Figure 76. Example Transect Showing the Increased Deviation in Roll, Pitch, and Yaw from Multiple Sensors on the Crawler.

LEFT: GPS transect map indicating the stability of GPS. RIGHT: Seafloor bathymetry in the area of the wave break included a relatively deep trough. When combined with rough surf in this area, the GPS rover appears to have motion deviations likely due to sway of the mast.

A more detailed view of this phenomena is shown in Figure 77. Here we analyzed roll and pitch deviations between the crawler and GPS points. It appears that once the system enters deeper surf (at approximately 100 seconds), a noticeable increase in roll and pitch occurred. The GPS point appears to have somewhat accentuated deviations (~2 degrees) due to the additional moment arm and wobble of the mast. At specific times (e.g., ~121 and 129 seconds), we notice relatively large deviations in the pitch of the GPS relative to that of the crawler. These likely occurred where the crawler tumbles forward through a trough or other bathymetric anomaly.

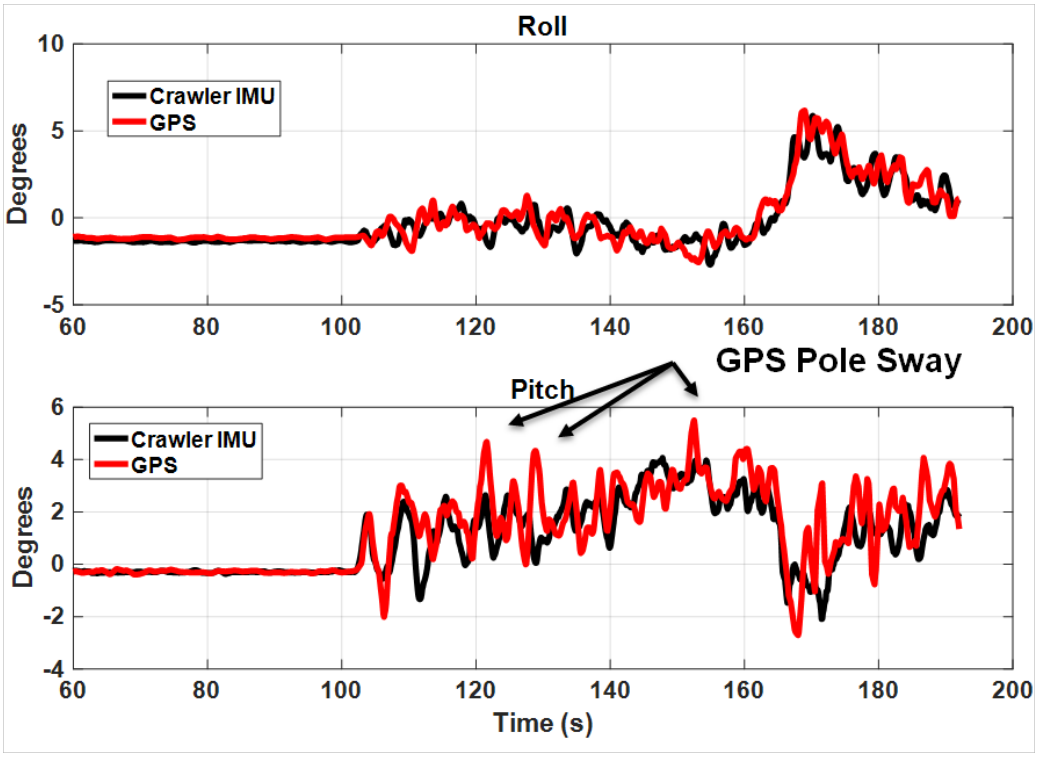

Figure 77. Detail View of GPS Roll and Pitch Deviations Relative to Those Measured on the Crawler.

Three accentuated deviations of the GPS pitch (pitched backward for positive deviations) are highlighted where the GPS mast experienced sway that imparted additional error in the GPS position estimates.

7.6 UXO CLASSIFICATION

Although only a limited number of target encounters were experienced from our grid surveys, we evaluated the potential of the system to classify targets. In our 2016 report, we showed that FlexEM system had classification capability using magnetic polarizability inversions matched to libraries. Because the FlexEM towed array sensor in our surveys only utilized one transmitter coil, we aggregate the data from consecutive soundings along the transect line (i.e., line methodology) to ensure the target receives the required multi-axis illumination from the transmitter. As the transmitter passes over the target, any offset of the sensor from directly over the target produces a different angle of incidence between the impinging transmitter field and the target. For optimal classification results, we have found that it is best to include soundings from adjacent transect lines in the composite data set to ensure complete three-axis characterization of the target. Greater overlap in adjacent transects yields higher quality classification; however, we have shown that it is possible in certain cases to achieve effective clutter rejection (classification) without overlap in sensor coverage.

Each of the 20 target encounters in addition to the 8 clutter anomalies detected in our grid surveys were analyzed. We used custom classification software modules (the MECCA modules in the EMClass software suite) to invert and analyze each anomaly. Figure 78 shows an example of the classification user interface. A combination of map, profile view and polarizability library match windows are used to assess classification information.

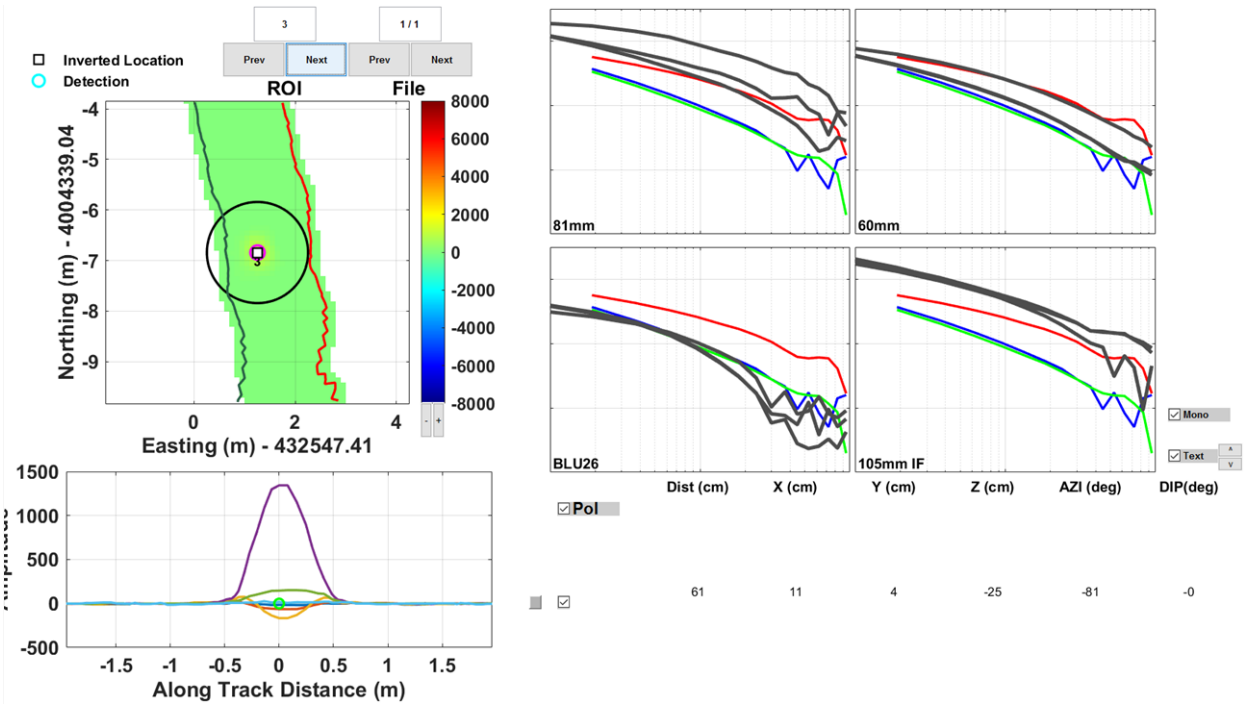

Figure 78. Example of the Classification Analysis User Interface for the FlexEM Crawler System.

The map view region-of-interest (ROI) is shown in the upper left with threshold alarm and inverted location markers overlain on the Z-axis data image. Bottom left shows the raw EM data profile over the ROI. The upper right panels show a basic set of four polarizability time evolution libraries (gray curves) with the current set of inverted triaxial polarizabilities overlain (red, green, and blue curves). The bottom right panels show map view and cross-section views of the inverted target (medium ISO) location relative to the array center.

Prior to our demonstration, we acquired library data over a subset of targets using a test stand and the FlexEM array. Unfortunately, the library does not contain all of the items used in our demonstration. Our library contains polarizability curves for the following items: 60mm mortar, 81mm mortar, 105mm projectile, BLU-26 submunition, and medium-sized ISO-40.

Magnetic polarizabilities from data acquired over the IVS area were analyzed first. Polarizabilities generated from data acquired over the IVS were consistent and matched expectations for the canonical and standardized targets: 3" steel sphere, large/medium/small ISO objects. Figures 79 - 81 show the polarizabilities generated by inverting data from traverses over the IVS. The polarizabilities generated for the 3" sphere show the axisymmetric symmetry expected for the sphere and very similar to the BLU-26 library curve. The medium ISO polarizabilities match relatively closely to the 60mm mortar library data and are consistent between realizations based on repeated passes. The small ISO curves are also repeatable and reveal the expected single primary and two closely matched secondary/tertiary polarizabilities.

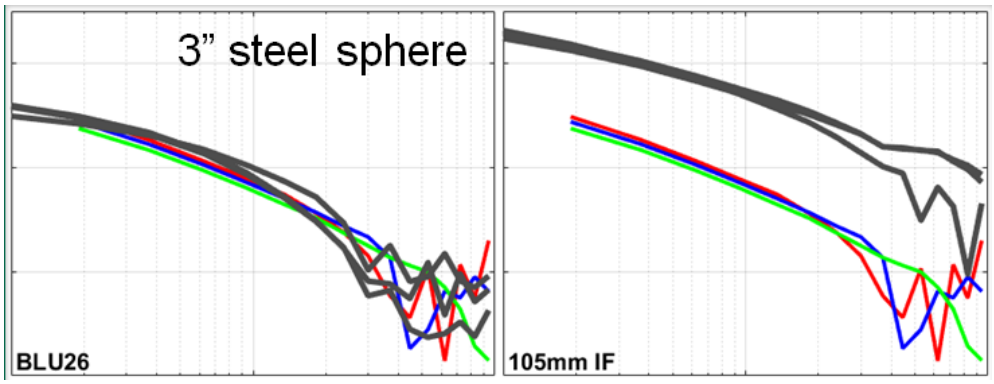

Figure 79. Polarizability Library Match for the 3-inch Steel Sphere in the IVS Area.

The inverted polarizability for this target exhibited strong triaxial symmetry as expected for a spherical object. The curves fit closely to that of the BLU-26 spherical-shaped submunition.

In Figure 80 and Figure 81, we show inverted polarizability curves for two independent set of passes over the medium ISO and small ISO targets in the IVS area. Although the curves for the respective targets are generally consistent, there are some slight discrepancies observed. In some cases, we found that the primary polarizability curve was not as consistent as the secondary and tertiary. This is more evident in the two passes over the medium ISO object as shown in Figure 91. It is unclear what the cause of this discrepancy may be, but we conjecture that it could be attributed to reduced primary field strength on the target along the primary axis of the object based on the orientation of the object relative to the axial fields produced by the transmitter.

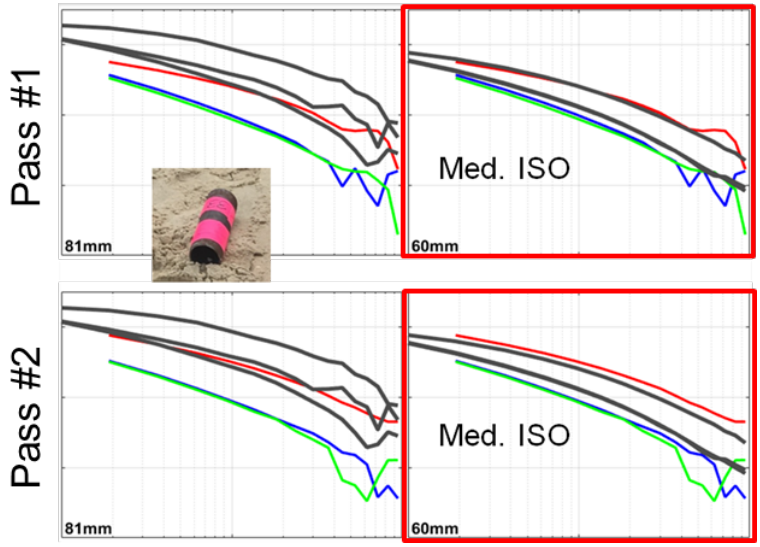

Figure 80. Polarizability Library Match for Two Different Data Collection Events (Top and Bottom Plots) Over the Medium ISO in the IVS Area.

The polarizability curves are generally consistent between to the surveys and match relatively closely to the library for the 60mm mortar. The red outlined curves indicate those that match libraries (for the medium ISO in both cases here).

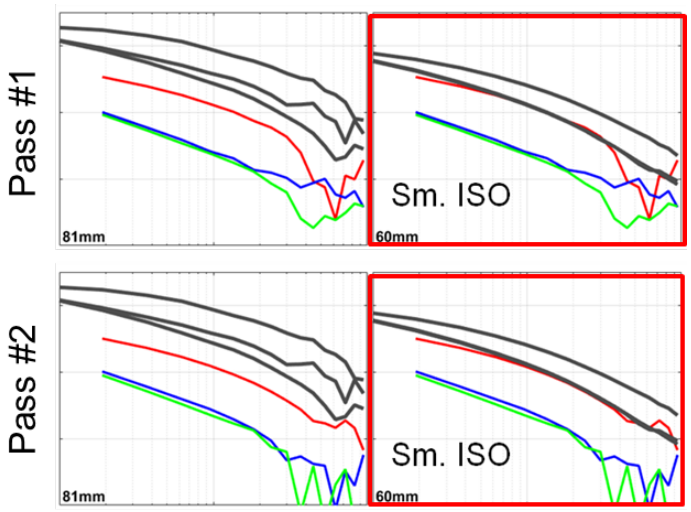

Figure 81. Inverted Polarizability Curves for Two Different Surveys Over the IVS Strip (Top and Bottom Plots).

The top set of plots compare the inverted polarizability curves from Pass #1 to the library curves for a 81mm mortar (left) and 60mm mortar (right). The inverted polarizability curves are very consistent and exhibit the size and symmetry expected for a small ISO object.

An example polarizability for an encounter over the 60mm mortar target placed in the western-most line of targets on the upper beach is shown in Figure 82. The polarizability curves exhibit a strong match to our library, especially for early and intermediate times (approximately the first half of the curve as plotted in logarithmic space). At later time, the lower SNR of the decay signals influence the quality of the polarizability and it appears noisy. The inverted X, Y, and Z locations are accurate.

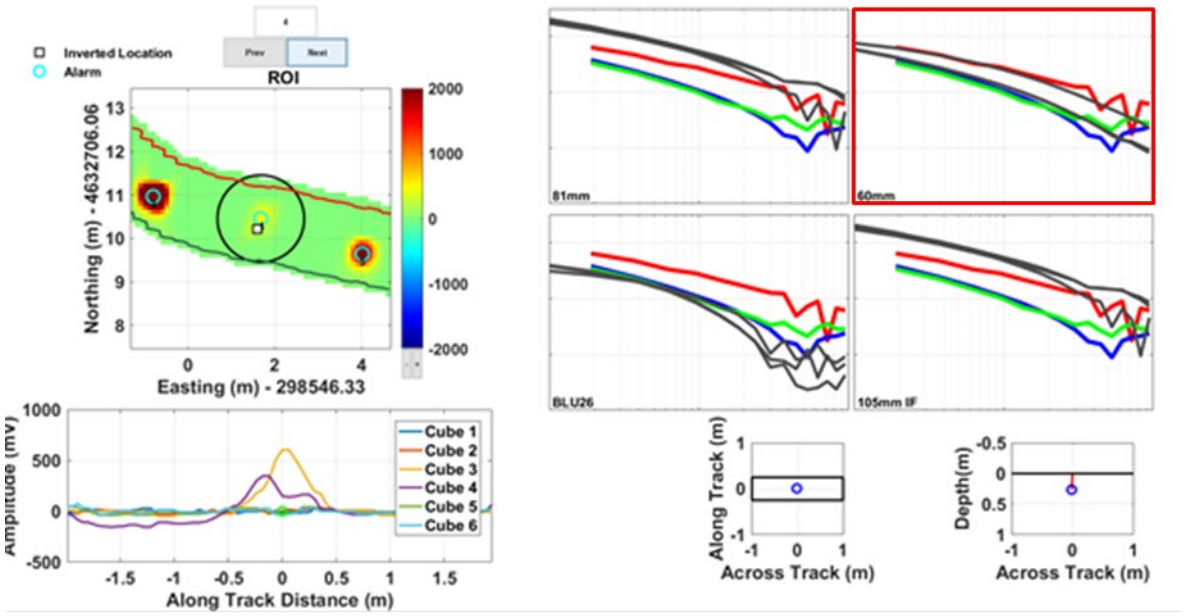

Figure 82. Polarizability Library Match for a 60mm Mortar Target from Surfzone Grid Coverage Data.

Analysis of the classification results from our full grid surveys over the beach, swash transition zone, and surf zone yielded somewhat mixed results. In many cases, inverted polarizabilities generated well-formed curves that matched our expectation for the known target or else matched our library polarizabilities. The inverted polarizabilities for the 105mm projectile in the shallow surf-zone shown in Figure 83 exemplify this. However, in some cases the triaxial polarizabilities exhibited one or more of the curves that did not match well to our libraries. In most of these cases, it was the primary polarizability that did not match well to the library.

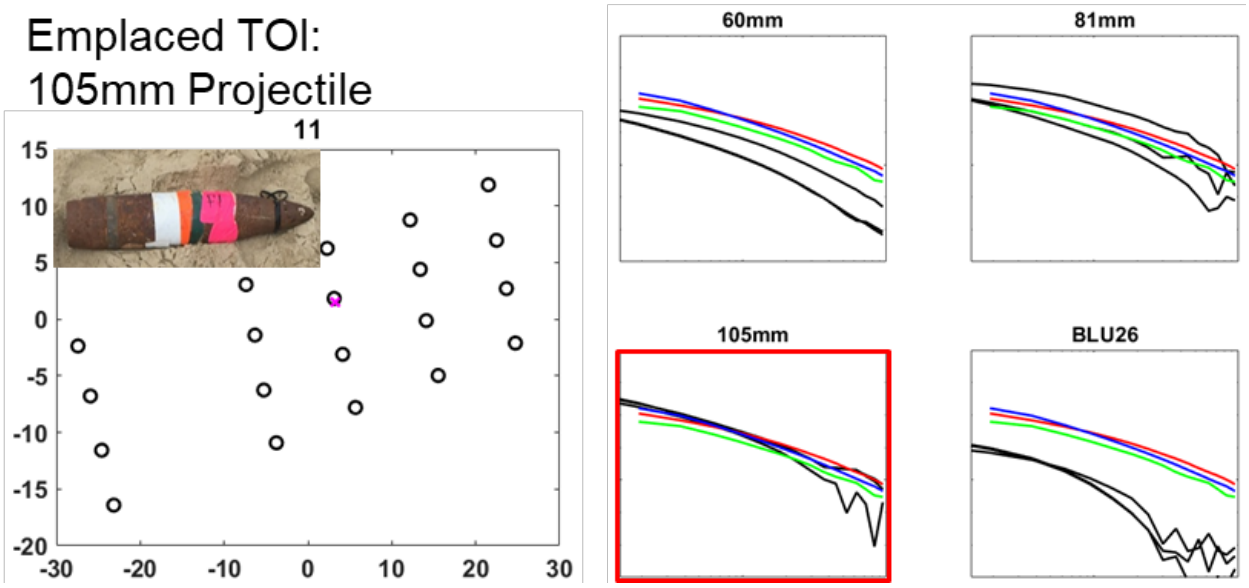

Figure 83. Polarizability Library Match for a 105mm Projectile Buried in the Surfzone.

The map view on the left shows the target grid layout (black circle symbols) with detected location overlain (magenta "X" symbol). The inverted polarizability curves (red, blue, and green curves) match most closely to the library curves for the 105mm (gray curves).

In the example in Figure 84, we show the polarizability match for the medium ISO target along the line of targets furthest seaward in the surf. The inverted polarizabilities in this case match the library well at only the earliest time gates and then deviate from the library curves. It is not clear if this is due to noise or other sources of error causing the non-optimal polarizability curve match.

Figure 85 shows the inverted polarizabilities for an encounter over the 60mm mortar emplaced in the beach. In this example, the primary polarizability does not seem to match the library very well. The secondary polarizability matches to the library primary polarizability relatively well as does the tertiary polarizability to the secondary library polarizability. We suspect that poor angular illumination along the across-track direction leads to anomalous inverted primary polarizability as it is not well constrained by the data.

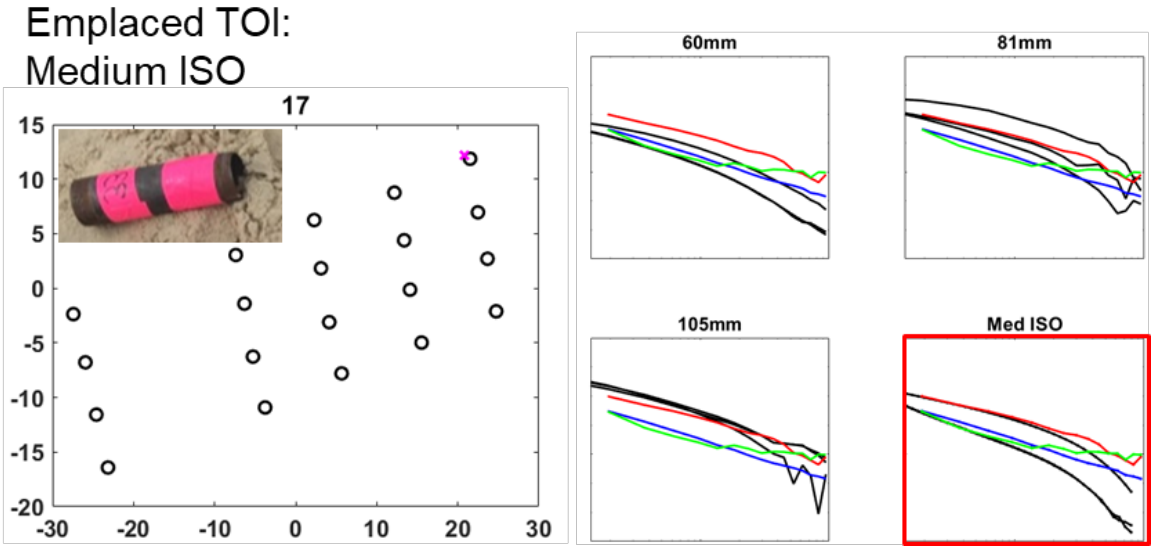

Figure 84. Polarizability Library Match for a Medium ISO Buried Along the Most Seaward (Deepest Water) Shore-Parallel Line of Targets.

The map view on the left shows the target grid layout (black circle symbols) with detected location overlain (magenta "X" symbol). The inverted polarizability curves (red, blue, and green curves) match most closely to the library curves for the medium ISO (gray curves), especially at the earliest times when the polarizabilities are well constrained due to high SNR decay data.

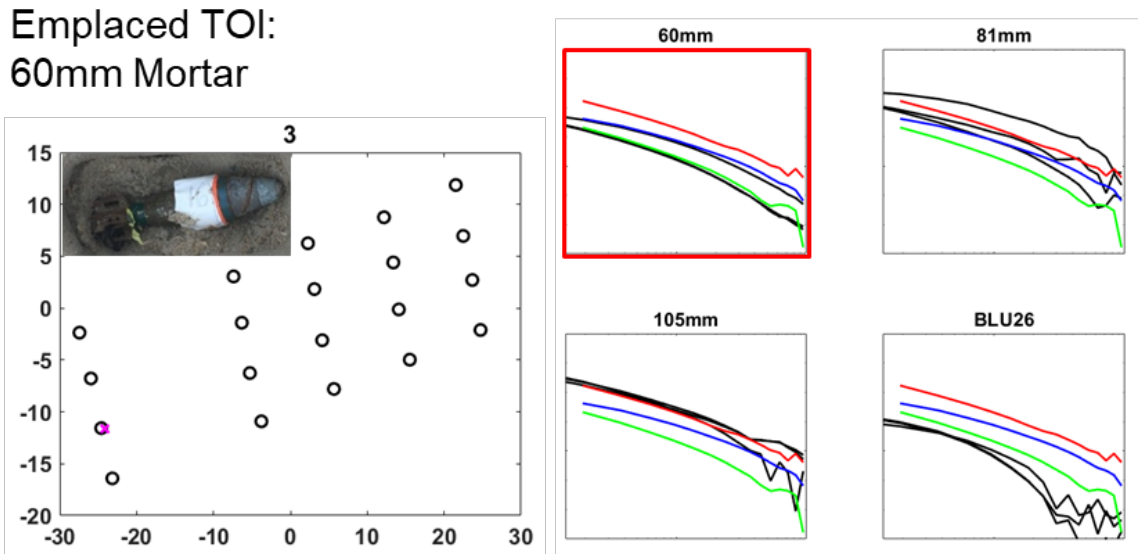

Figure 85. Polarizability Library Match for a 60mm Projectile Buried in the Beach.

The map view on the left shows the target grid layout (black circle symbols) with detected location overlain (magenta "X" symbol). The inverted polarizability curves (red, blue, and green curves) match to some degree to the library curves for the 60mm (gray curves), however, deviation of one of the secondary polarizabilities (red curve) is noted. This is likely due to poorly constrained lateral (X-directed) receiver data.

In Figure 86, we show well-formed inverted polarizabilities for the 90mm projectile. Although, we do not have a set of library curves for this target, the inverted polarizabilities form a set that exhibits the expected signal amplitude and symmetry. The signal amplitude is slightly greater than that for the 105mm projectile library and the polarizabilities have one strong primary curve and two similar and nearly equivalent secondary polarizabilities. This exemplifies the potential for an analyst to classify based on size and symmetry via the polarizabilities displayed even though a library match is not available.

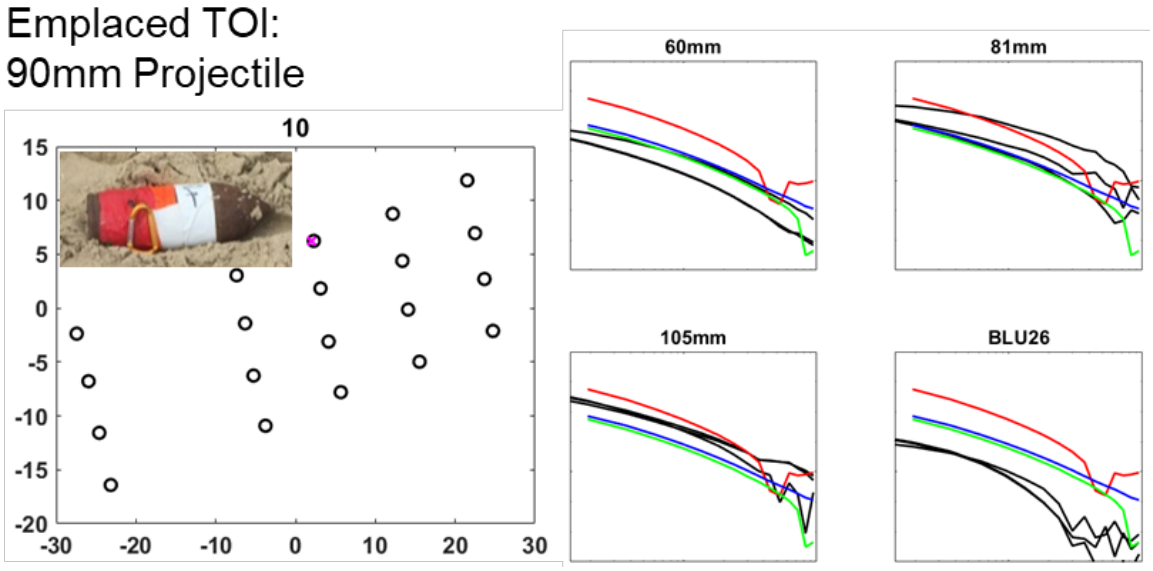

Figure 86. Polarizability Library Match for a 90mm Projectile Buried in the Surfzone.

The map view on the left shows the target grid layout (black circle symbols) with detected location overlain (magenta "X" symbol). The inverted polarizability curves (red, blue, and green curves) do match exactly to any of the curves in our library set. We did not have library curves for the 90mm projectile object.

We also analyzed classification data for encounters over the two emplaced clutter items and one non-emplaced (native) clutter item. The two emplaced clutter items consisted of a steel chain approximately 2.5 cm (1-inch) in size and approximately 60 cm (24-inches) long and bunched together as well as a piece of angle iron. Both objects produced inverted polarizabilities that appear to be well-formed and of high enough quality for classification analysis. Figure 87 and Figure 88 show the polarizability curved relative to 4 different library curves. Although both objects generated relatively large polarizabilities (i.e., size on the order of UXO), they did not have the symmetry expected for the UXO objects emplaced in our target grid. Therefore, they did not match to any of the library curves and could readily be listed as clutter by a trained analyst. Similarly, the non-emplaced (native) clutter polarizabilities shown in Figure 89 indicate a relatively large object with irregular dimensions and non-symmetry.

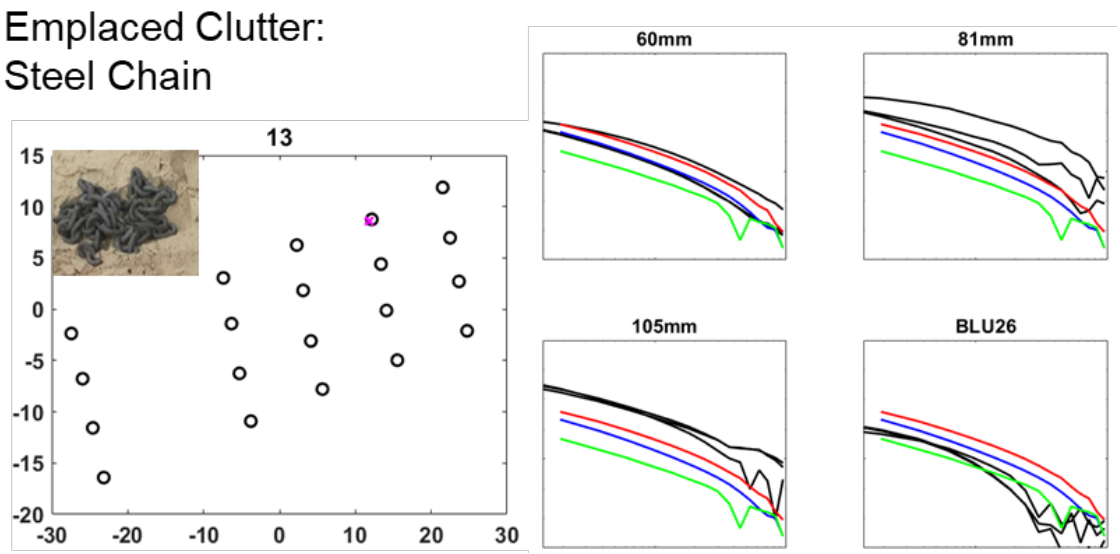

Figure 87. Polarizability Curves for the Emplaced Steel Chain.

The map view on the left shows the target grid layout (black circle symbols) with detected location overlain (magenta "X" symbol). The inverted polarizability curves (red, blue, and green curves) do not match any of the libraries shown and do not exhibit any of the expected size and symmetry features.

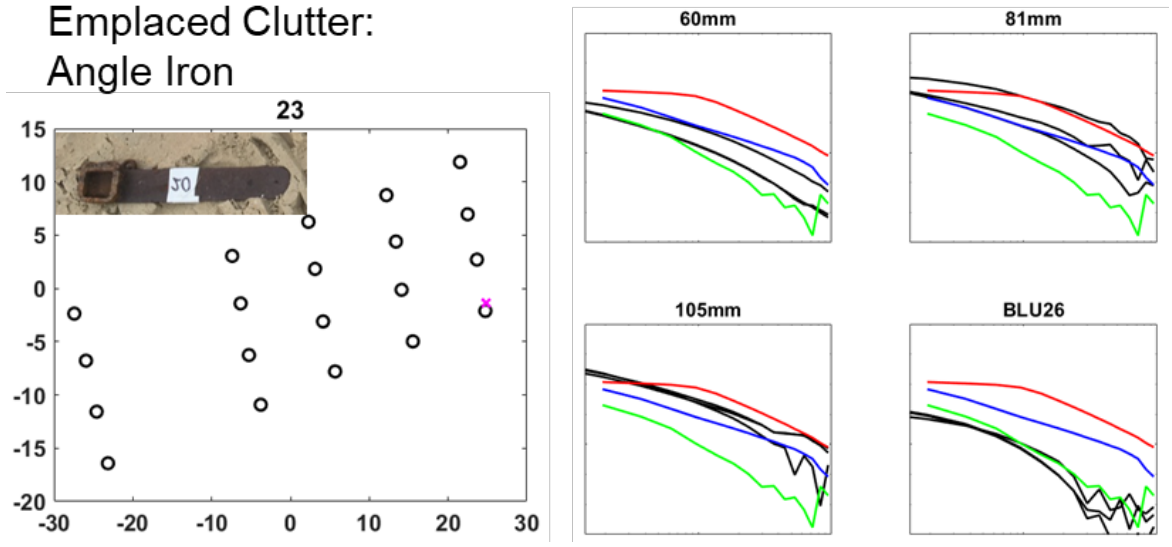

Figure 88. Polarizability Curves for the Emplaced Angle Iron.

The inverted polarizability curves (red, blue, and green curves) do not match any of the libraries shown and do not exhibit any of the expected size and symmetry features.

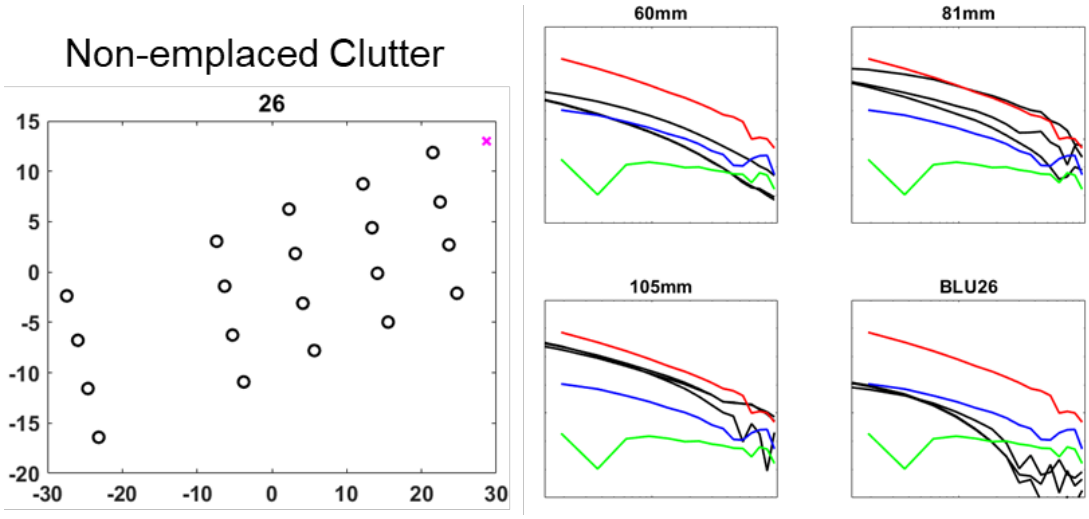

Figure 89. Polarizability Curves for a Native Clutter Object (Presumed but Not Confirmed).

While we didn't excavate and confirm that this item was indeed clutter, it appears to be irregular and does not exhibit features we would expect from a UXO object.

7.7 OPERATIONAL EASE OF USE

We determined the ease of use of the system by overseeing and reviewing operations including system deployment, recovery, and data collection. Deployment and data collection using the integrated crawler-based towed EM array provided information on launch and recovery (LAR) requirements, topside support, and data processing and analysis toward survey mapping and detection and classification lists production.

In general, we experienced relatively smooth operations from the set-up stage through to completing surveys to demobilization at the end of the day. Very little calibration of the system is required. A functional test of power and communications of all systems was conducted without any issues. The crawler platform was mobilized and positioned initially through a small handheld controller that attaches directly to the crawler platform. This is convenient for moving the crawler in dry conditions without the need to set up the OCS and radio link. Once the crawler was nominally in position at the site, we completed checkout of the radio link and OCS remote control. The radio ethernet hub interface and camera visualization was readily attained and confirmed. Next, the battery management and auxiliary sensors that measure motor and controller states was confirmed functional, and a short test drive of the crawler was conducted. These crawler checkout tasks took approximately 1 hour to complete.

Attaching the EM array sled is a straightforward task and involves sliding the boom mount over the encoder interface attachment and bolting it in place. The marinized ethernet interface cable was attached to the SurfROVer junction box. The EM array was then powered by connecting the battery pressure vessel to the interface. The system logged data of adequate quality and passed an initial instrument verification test (using calibration spheres in a so-called "spike" test).

The operator control (Figure 90) of the crawler system was relatively straightforward. It was observed that continuous turning with the tow system took some practice. The challenge is that the crawler essentially executes skid-steer control of turning maneuvers. This involves disproportional effort being supplied to the right and left motors to make the turn. Tracking of the array involves developing some operator intuition on when to straighten out of a turn to optimize tracking of the trailing sled. Because the same crawler helmsman was controlling the system as in previous demonstrations, this did not take much time. The helmsman operator primarily focused on the camera views on the crawler for perception and awareness and the navigation guide user interface for navigating the system. An analyst sat next to the helmsman and monitored EM array data acquisition and navigation tracking to assure quality control of proper waypoint and line following guidance.

Figure 90. Operator Control Station Showing the Helmsman with Joystick Control and Multiple Screens with Camera Views and System Feedback.

The operator can access 3 or 4 camera views, scanning sonar range and bearing display, crawler status interface (displaying real-time battery status, navigation, and radio communications information) crawler and tow sled navigation - waypoint tracking software interface, and the FlexEM data acquisition and configuration control user interface from the top side control station

The displays available are configurable, but generally utilize; (i) two-three camera views on monitors, (ii) dynamic display of the battery management system and radio link state, (iii) system navigation display with map trackline view and left-right tracking and warning indicator, and (iv) the EM array data acquisition and quality control display. These are shown in Figure 91.

For the majority of our surveys the helmsman elected to utilize a mast-mounted forward-looking camera view as the submerged camera views tended to produce very low visibility. He also utilized an OCS-mounted camera looking out at the entire site, which could be zoomed to the position of crawler.

During this demonstration we were also able to verify the modifications and improvements made to the system based on lessons learned from our 2016 demonstrations. These included integration of the wireless link to the crawler, improved battery management system, and improvements to the overall operator control station and navigation guidance systems. Although the wireless radio link worked without any issues or failures, the mechanical implementation of the antennas on the crawler mast should be made more robust for longer term deployments. Specifically, the antenna covers and connectors should be improved and ruggedized for waterproofing and potential impact or shock tolerance. The functionality and range-capability of the units worked well, and these radios are recommended for future production operations.

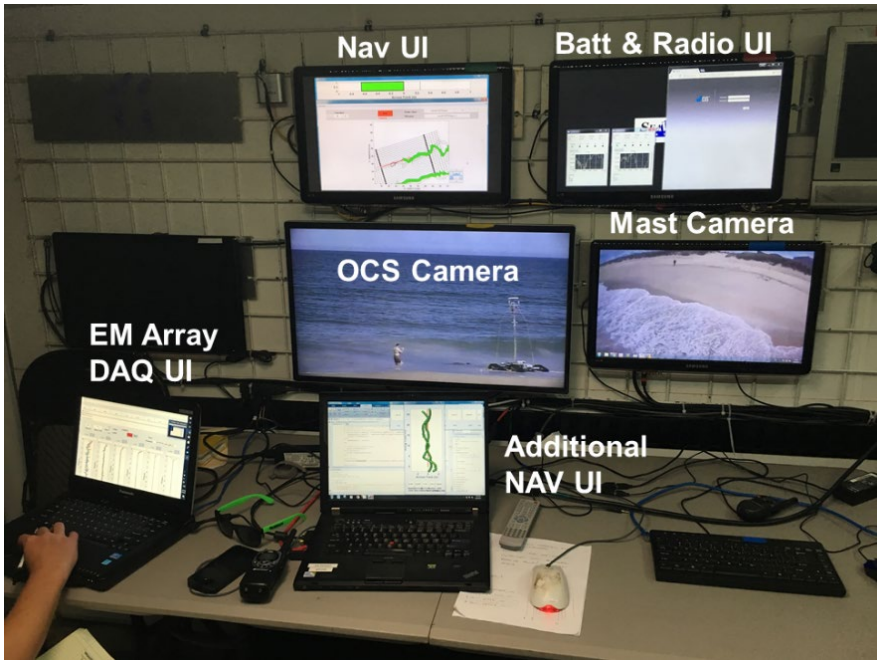

Figure 91. Operator Control User Interface Monitors Annotated to Illustrate the Nominal Set Up.

The OCS is configurable for a particular operator or site-specific preferences.

A few technical implementation issues were observed during our demonstration. As mentioned previously the stability of the mast to resist sway may need to be improved in order to reduce positioning errors from the rover GPS antenna motion. One possible mitigation to this issue could include the addition of rigid sway bars that help to brace the mast. Although qualitatively it appears that the tensioned stay ropes could be tightened adequately, we may desire to integrate a way to keep them from loosening up during operations. In addition, the spreader bars at the top of the mast should be more rigidly attached and epoxied in place.

After completion of our full grid coverage surveys, we performed a couple of additional surveys to test the system in water deeper than that in our grid surveys. During one of these "deep water" surveys, that system halted its forward advance and stopped moving. Multiple attempts were made to maneuver free from the cause of the stoppage but were unsuccessful. Subsequent investigations revealed that one of the crawler track axials had become entangled in a 2.5-inch treated manila docking line rope (the type usually used for deck, docking, and anchoring lines on a vessel). The system was pulled back to shore and it was obvious that the rope entanglement was the unfortunate cause of the survey stoppage. This resulted in a bent axial and some minor damage to the crawler track assembly. Repairs have been made so that the system is fully functional again and ready for follow-on surveys. Photographs of the rope entanglement are shown in Figure 92.

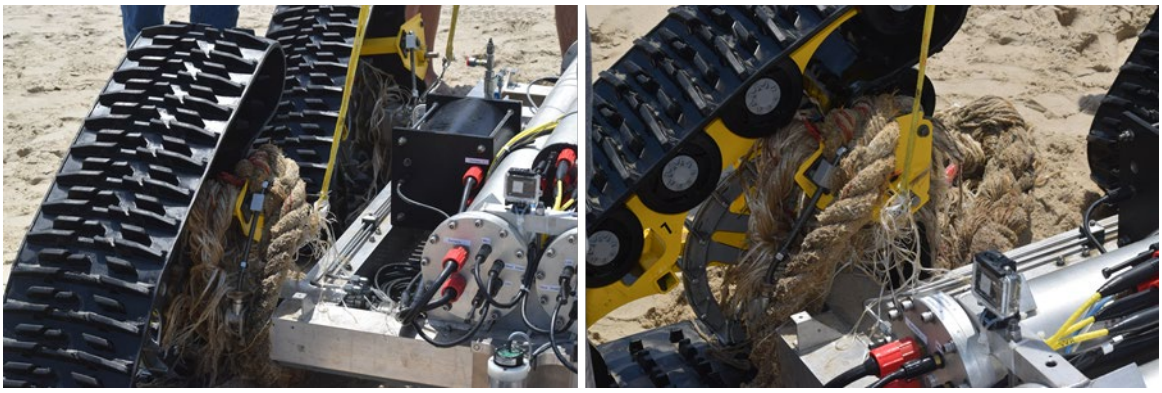

Figure 92. Photographs of the Manila Deck Rope That the Crawler Track Axial Was Entangled in At the Conclusion of Our Surf Zone Grid Surveys.

The line was fully wrapped around the axial and entangled in one of the sprockets, which fully halted motion of that track.

The photographs in Figure 93 show the front-on view of the rope entangled on the starboard forward axle and the damaged track wheel assembly after the rope cut free and track removed. It was determined that this type of entanglement is unlikely to be a common occurrence during operations and was an unfortunate event rather than more likely event that requires mitigation. A possible mitigation strategy for such an entanglement event may be to add flooded cowling covers around the sprocket and axle.

Figure 93. Photographs of the Starboard Forward Axal Showing the Rope Entangled and Wrapped Around the Axal and Track Sprocket.

When the track was removed and rope cut free, the track assembly was revealed and exhibited some permanent damage. The axle and sprocket were fixed and replaced, and the system is again fully functional.

7.8 LAUNCH AND RECOVERY

Mobilization, set up, and checkout of the crawler system was mostly straightforward. The crawler platform was loaded and transported inside the operator control station (OCS) trailer. Once the crawler platform was unloaded from the trailer, we mobilized the trailer onto the FRF pier by towing it from a truck to the control station location. AC power was run to the trailer, but in previous demonstrations we have run the operator control station from a small generator so that all operations are self-sufficient. A GPS base station was established nearby and powered from the OCS trailer. Also, the radio link for communication and data to/from the crawler was established nearby the trailer (we note that the antennas could be mounted directly to the roof of the trailer). The entire set up took approximately 3-4 hours and was completed without incident.

Recovery of the system was very simple given that our shore-based deployment. We simply drove the platform back to the loading area, demobilized subunits as needed, and cleaned (thorough freshwater rinse) and loaded the platform back into the OCS trailer. Demobilization took a few hours and consisted of disassembling the antenna mast, removing and cleaning the EM array batter pressure vessels, and disconnecting and disassembling the EM array. The EM array boom mount and sled were disconnected and packed and loaded separately.

8.0 COST ASSESSMENT

8.1 COST MODEL

The cost elements that were tracked during the demonstration at the Duck FRF site are detailed in Table 6. The provided cost elements are based on a simple and incomplete cost model developed for the integrated crawler-EM system used in our demonstrations. The integrated system does not yet have a price developed for purchase or lease. Therefore, some aspects of the price elements must be estimated for the purposes of cost assessment.

Table 6. Cost Model for a Detection/Discrimination Survey Technology

Cost Element	Data Tracked	Estimated Costs
Instrument cost	N/A (See description below)	All major equipment and instrumentation are on-loan to the project by participating performers; estimated costs of the Flex-EM or similar array are $1000/day or $5,000/wk
Support equipment lease rates	Lease rates for major components Engineering estimates based on current development Lifetime estimate Consumables and repairs	RTK-GPS: $ 1,200/wk
Mobilization and demobilization	Cost to mobilize to site Derived from demonstration costs	Equipment Prep (est.): $ 3,600 Shipping (MI-NC-MI): $ 4,110 *TOTAL Mob/Demob: $ 7,710*
Site preparation	Time and cost to setup test site (relates to beach IVS set up)	Test Target Prep: $ 1,240
System setup costs	Unit: $ cost to set up and calibrate Data requirements: Hours required Personnel required Frequency required	Crawler System Setup: $ 5,250 EM Array Setup/QA: $ 1,275 RTK-GPS Setup: $ 1,750 *TOTAL Setup: $ 8,275*
Survey costs	Unit: $ cost per acre Data requirements: Hours per acre Personnel required	0.5 acres/hour at 100% coverage 100% coverage ($/acre): $ 1,256 50% coverage ($/acre): $ 629 25% coverage ($/acre): $ 314
Detection data processing costs	Unit: $ per hectare as function of anomaly density Data Requirements: Time required Fixed costs and Personnel required	Fixed Costs: $ 1,250 1 person (analyst at $100/hr) 2 mins. / anomaly (average) Per anomaly (100/acre): $ 3.33 Per acre (100/acre): $ 333

Instrument Cost: EM sensors applicable for underwater UXO applications vary in size and complexity. Although we do not have lease prices for the Flex-EM sensor, we estimate costs based on the commercially available similar sensor arrays. The EM-61S has a daily rate of $95 and fixed mobilization charge of $125. Two EM-61S systems would then be $250/day. The Geometrics G-882 TVG array rents for $375/day (plus $750 mobilization cost).

Support Equipment Lease Rates: Support equipment includes the RTK-GPS and, as such, has associated lease rates that were tracked. This equipment is categorized as required. All associated labor costs were tracked and aggregated to form the cost element assessment.

Mobilization and Demobilization: The cost for mobilization and demobilization activities are derived from actual costs including packing and shipping from Dexter, MI to Duck, NC. The number of personnel and labor hours were tracked for specific mobilization /demobilization tasks.

Site Preparation: The cost for site setup and preparation including target seeding were tracked based on actual labor hours and logistical costs associated with this cost element. This included the use of a two people for at least one-half of a day to install and survey IVS targets and associated calibration fiducials.

Instrument Set Up Costs: The cost for preparation and set up of instrumentation including the crawler-based EM system, topside control components, launch and recovery, and supporting equipment. Time associated with non-recurring engineering or additional set-up required for engineering analyses was not included. We estimate 8 hours of labor for initial setup of the operator control station, subsystem mounting and cabling, and GPS mast setup. We estimate four hours labor for EM array setup and QA including EM array mounting and cabling. Configuration, setup, and checkout of the RTK-GPS system will take approximately four hours. Overall, this results in an estimated instrument setup cost of $8,275.

Survey Costs: Costs are estimated from the incurred cost of labor and equipment (based on day-rate lease estimates) during survey mode operations. Area was calculated based on data acquired from the system navigation data.

Detection Data Processing Costs: Detection-level processing costs will be pro-rated based on the prescribed data flow and standard procedures that are being demonstrated. Costs were estimated based on individual labor hours and any required fixed costs (e.g., for software licensing). Our estimate for data processing costs are $333 per acre assuming approximately 100 anomalies per acre.

9.0 SYNTHESIS AND CONCLUSIONS

The overarching goal of this demonstration project was to assess a combination of platform and sensing systems in order to deliver a UXO mapping survey and characterization technology in very challenging nearshore environments. Nearshore environments such as swash zone, surf zone with breaking waves, and shallow tidal areas provide hydrodynamic and bottom conditions are particularly challenging from the standpoint of mobility and stability of sensing platforms in order to acquire high quality geophysical data. To overcome the limitations of current diver/man-portable or ship-towed configurations, we evaluated both platform and sensor performance to demonstrate and characterize a tailored and integrated robotic bottom crawler-towed sensor solution in representative nearshore UXO sites.

This demonstration built off successful engineering tests and demonstrations in Michigan, New Hampshire, Maryland, and North Carolina in 2015 and 2016. In November of 2016, we completed an initial demonstration of the crawler-towed EM technology in both the surf zone and sound areas adjacent to the FRF facility. During those demonstrations, we verified that the system could be deployed to provide high quality data for detection and localization in multiple hydrodynamic conditions (waves and surf to sound) and bottom types (sand to muddy). We also utilized the many observations and lessons learned from those tests as a basis for modifications and improvements toward the demonstrations conducted in July of 2017, as reported here. The primary modifications to the system included replacement of the fiber-optic tether system with a wireless radio link from the crawler to the topside control station in addition to topside user interface improvements and various additions or improvements to optimize the subsea platform and integration with EM sled. On the crawler, we implemented a greatly improved battery management system, a new tow point encoder unit, and completely self-sufficient and isolated power supply for the EM array. These improvements all benefited the overall operations of the system during our demonstrations.

The system we demonstrated included improvements and optimization based on the 2016 version, but was largely the same mobile platform, drivetrain, mast and GPS positioning subsystem, and EM sled system as in previous demonstrations. The SeaView Systems SurfROVer crawler was configured for remote control operations through a set of ethernet radios mounted on the operator control station and crawler antenna mast. The EM array was offset and towed 5 meters behind the crawler by a rigid fiberglass towbar. The EM sensor system consisted of the WRT FlexEM 2-meter wide array. After installing a grid of 20 targets over an area extending from the beach into the surf zone just south of the FRF pier to approximately 2 meters water depth, we performed full coverage surveys. These surveys resulted in approximately 29.5 MB of data covering roughly 3500 m^2 of coverage area at and approximate full coverage rate of 0.5 acres per hour.

Data from our full coverage surf zone surveys were analyzed using post-processing software to measure performance area coverage, target detection and localization, and classification. All targets were detected at SNR > 20 dB for a 100% probability of detection. The target localization accuracy was better than 30cm CEP for all target encounters exceeding our performance metric of 100cm CEP. However, the variance in target positions were approximately 50cm, which was higher than our target metric of 35cm. This was found to be mainly due to wobbler and sway of the GPS mast and motion of the GPS rover antenna atop of the mast. We also observed and analyzed data to assess the overall stability of the system in the relatively dynamic surf zone conditions during our operations.

We found the crawler-towed system to be very stable in the face of crashing waves up to 1.8 meters tall and forceful currents in the swash and surf zones during ebb and flood cycles between wave breaking events. In some cases, the EM sled appeared to lift from the bottom (perhaps related to heavy cavitation) and sway before the motion of the crawler was enough to pull it back in track. This added to the uncertainty of the array position, although we were able to mitigate this through analysis of tow point encoder and relative differences between crawler- and sled-mounted IMU data.

We also showed that the demonstrated configuration of the EM array was capable of some level of target classification when multiple transects were aggregated together and inverted for magnetic polarizability curves. Inverted polarizability curves were matched to library curves for a subset of targets and analyzed. Although we were only able to compile a limited number of target encounters and even fewer clutter encounters, the consistency of the inverted polarizabilities yield promise for reducing the number of clutter items by as much as 50-75%. Classification with the array configuration demonstrated is expected to be limited by the degree of angular illumination of the primary transmitted magnetic field. Additional experiments with methods to switch the two side-by-side transmitter coils on the array indicate potential paths to improved classification that are less dependent (or completely independent) on relatively positioning between adjacent transect overpasses. Moreover, a third transmitter could be added to form a triangular ("arrowhead") arrangement to increase the angular diversity of the primary field excitation. This holds great promise for dynamic classification implementations in the marine environment. There are tradeoffs to consider when adding additional coils to the towed array. Specifically, the added footprint has implications for hydrodynamic stability and potentially turning radius of the overall system.

Overall, the demonstrations reported on here illustrated to what degree the crawler-towed EM system can fill gaps in current nearshore geophysical mapping, detection, and UXO classification. Specifically, we proved that the system could; (i) be mobilized and deployed in a cost-effective manner for shore-based operations, (ii) effectively cover surf zone target areas with 100% coverage transects, (iii) detect and localize UXO targets from 60mm to 105mm in size buried beneath the seafloor to within 50cm radius, and (iv) reduce clutter through analyses of inverted polarizabilities with moderate levels of confidence and effectiveness.

10.0 REFERENCES

Bachman, C.M., Abelev, A., Bounds, M.T., Fusina, R.A., Kremens, R., Difrancesco, G., Vermillion, M., Mattis, G., Edwards, K.B., and Estrada, J., 2016, Ssan Yong 2014 Remote Sensing Experiment, Naval Research Laboratory Memorandum Report NRL/MR7230-16-9667, 282 pp.

Bellis, V., O'Connor, M.P., and Riggs, S.R., 1975, Estuarine shoreline erosion in the Albemarle-Pamlico region of North Carolina: North Carolina Sea Grant Publication UNC-SG-75-29, 67p.

Birkemeier, W.A., Miller, H.C., Wilhelm, S.D., DeWall, A.E., Gorbics, C.S., 1985. A User's Guide to the Coastal Engineering Research Center's (CERC's) Field Research Facility, IR CERC-85-1. U.S. Army Corps of Engineers, Vicksburg, MS (p. 136).

Byrnes, M. R. 1989. SuperDuck Beach Sediment Sampling Experiment, Report 1, Data Summary Report. Miscellaneous Publication CERC-89-18, U.S. Army Engineer Waterways Experiment Station, Coastal Engineering Research Center, Vicksburg, MS.

Coastal Planning & Engineering of North Carolina, Inc., 2014, Environmental Assessment For the Town of Duck Shoreline Protection Project, 167 pp.

Coastal Planning & Engineering of North Carolina, Inc., 2015, Comprehensive Marine Sand Search and Borrow Area Design Report: Towns of Duck, Kitty Hawk, and Kill Devil Hills, North Carolina. 48p. (Prepared for the Towns of Duck, Kitty Hawk, and Kill Devil Hills, North Carolina).

Drake, T.G., 1997, Final Report for Field Studies of Nearshore Sedimentary Structures, Miscellaneous Report CHL-97-3, North Carolina State University, 155 pp.

Dolan, R., Lins, H., 2000, The Outer Banks of North Carolina, USGS Professional Paper 1177-B, Prepared in cooperation with the National Park Service, 43 pp.

Eames, G.B., 1983, The late Quaternary seismic stratigraphy, lithostratigraphy, and geologic history of a shelf-barrier-estuarine system, Dare County, North Carolina: M.S. Thesis, Department of Geology, East Carolina University, Greenville, NC, 196p.

Haines, J.W., and G. Gelfenbaum, 1995, Field measurements of turbulent stresses during the Duck94 nearshore processes experiment, EOS Transactions of American Geophysical Union, [#O22B-10], 76 (46), pp. 298.

Inman, D.L. and Dolan, R., 1989, The Outer Banks of North Carolina: Budget of sediment and inlet Ivantysynova, M. 2000. Displacement Controlled Linear and Rotary Drives for Mobile Machines with Automatic Motion Control. 2000 SAE International OFF-Highway & Powerplant Congress, Milwaukee, Wisconsin, USA. SAE Technical Papers 2000-01-2562. doi:10.4271/2000-01-2562.

Ivantysynova, M. 2000. Displacement Controlled Linear and Rotary Drives for Mobile Machines with Automatic Motion Control. 2000 SAE International OFF-Highway & Powerplant Congress, Milwaukee, Wisconsin, USA. SAE Technical Papers 2000-01-2562. doi:10.4271/2000-01-2562.

Laudato, S.J., Schultz, G., Keranen, J., and Miller, J, 2016, Dynamic EMI sensor platform for digital geophysical mapping and automated clutter rejection for CONUS and OCONUS applications, Proceedings of the SPIE, Defense and Security Symposium 9823, 982305-982305-10.

Leatherman, S.P., K. Zhang, and B.C. Douglas. 2000. Sea level rise shown to drive coastal erosion. EOS, Transactions American Geophysical Union 81(6):55-57.

Leatherman, S.P., T.E. Rice, and V. Goldsmith, 1982. Virginia barrier island configuration: a reappraisal. Science, 215: 285-287.

Mallinson, D., Riggs, S., Thieler, R., Culver, S., Foster, D., Corbett, R., Farrell, K., and Wehmiller, J., 2005, Late Neogene and Quaternary evolution of the northern Albemarle Embayment (mid-Atlantic continental margin, USA), Marine Geology, 217: 97-117.

McNinch, J.E. 2004. Geologic control in the nearshore: shore-oblique sandbars and shoreline erosional hotspots, Mid-Atlantic Bight, USA. Marine Geology 211: 121-141.

Meisburger, E.P., C. Judge, and S.J. Williams, 1989. Physiographic and geologic Setting of the Coastal Engineering Research Center's Field Research Facility. Miscellaneous Paper CERC-89-9, U.S. Army Corps of Engineers, Waterway's Experiment Station, 28p.

O'Connor, M.P., Riggs, S.R., Winston, D., 1972. Recent estuarine sediment history of the Roanoke Island area, North Carolina. In: Nelson, B.W. (Ed.), Environmental framework of coastal plain estuaries. Geological Society of America Memoir, 133,pp. 453–463.

Riggs, S.R., Belknap, D.F., 1988. Upper Cenozoic processes and environments of continental margin sedimentation: eastern United States. In: Sheridan, R.E., Grow, J.A. (Eds.), The Atlantic Continental Margin, U.S. Geological Society of America. The Geology of North America, pp. 131–176.

Riggs, S.R. and O'Connor, M.P., 1974, Relict sediment deposits in a major transgressive coastal system: North Carolina Sea Grant Publication UNC-SG-74-04, 37p.

Riggs, S.R., 1996, Sediment evolution and habitat function of organic-rich muds within the Albemarle estuarine system, North Carolina: Estuaries, v.19, p.169-185.

Riggs, S.R., Cleary, W.J., Synder, S.W., 1995. Influence of inherited geologic framework on barrier shoreface morphology and dynamics. Mar. Geol. 126, 213- 234.

Riggs, S.R., York, L.L., Wehmiller, J.F., Snyder, S.W., 1992. Depositional patterns resulting from high-frequency Quaternary sea-level fluctuations in northeastern North Carolina. In: Quaternary Coasts of the United States: Marine and Lacustrine Systems. SEPM Spec. Publ. No. 48, 141-153.

Rogers, S. and D. Nash. 2003. The Dune Book. North Carolina Sea Grant, Raleigh, North Carolina, 28 pp.

Schlee, J.S., Manspeiser, W., and Riggs, S.R., 1988, Paleoenvironments offshore Atlantic U.S.margin: In

Schultz, G., Keranen, J., Miller, J., and Shubtiidze, F., 2014, Acquisition and processing of advanced sensor data for ERW and UXO detection and classification, Proceedings of the SPIE, Defense and Security Symposium 9072, 90720H-90720H-9.

Schultz, G., Shubititidze, F. J. Miller, and Evans, R., 2011, "Active source electromagnetic methods for marine munitions", Proceedings of the SPIE, Defense and Security Symposium, 8017, 8017OU; doi:10.117/12.884023.

Sheridan, R.E. and Grow, J.A. (eds.), The Atlantic continental margin of the United States: Geology of North America, Geological Survey of America Decade of North American Geology v.I-2, p.365- 385.

Smith, G.M., Thomson, A.G., Wilson, A.K., Hill, R.A., and Purcell, P.W., 2007, Airborne remote sensing for monitoring the impact of coastal zone management, International Jour of Remote Sensing, 28, 1433-1435.

Staube, D.K., Holem, G.W., Byrnes, M.R., Anders, F.J., Mesiburg, E., 2993, SUPERDUCK Beach Sediment Experiment: Beach profile change and foreshore sediment dynamics, Coastal Engineering Research Program Report, CERC-93-4, May 1993, 51 pp.

Thieler, E.R., D.S. Foster, E.A. Himmelstoss, 2014. Geological framework of the northern North Carolina, USA inner continental shelf and its influence on coastal evolution. Marine Geology 348: 112-130.

USACE (United States Army Corps of Engineers). 2010. Final Environmental Impact Statement May 2010. Beach nourishment project, Town of Nags Head, North Carolina. U.S. Army Corps of Engineers, Wilmington District. Washington, NC. 172 pp.

USACE (United States Army Corps of Engineers). 2000. Final feasibility report and environmental impact statement on hurricane protection and beach erosion control: Dare County beaches (Bodie Island portion), Dare County, North Carolina. Vol I and Vol II, US Army Corps of Engineers, Wilmington District, South Atlantic Division.

Relevant websites referenced or accessed:

www.frf.usace.army.mil

navigation.usace.army.mil/CHL_Viewer/FRF

Page Intentionally Left Blank

APPENDIX A POINTS OF CONTACT

POINT OF CONTACT Name	ORGANIZATION Name Address	Phone Fax E-mail	Role in Project
Dr. Gregory Schultz	White River Technologies, 115 Etna, Rd. Lebanon, NH 03776	Phone: 802 356-4788 schultz@whiterivertech.com	Principle Investigator
Joe Keranen	White River Technologies, 115 Etna, Rd. Lebanon, NH 03776	Phone: 802 683-9169 keranen@whiterivertech.com	Senior Systems Engineer
Dr. Jesse McNinch	USACE-CEERD-HF-A, Field Research Facility 1261 Duck Road Kitty Hawk, NC 27949-4472	Phone: 252 261-3511 Jesse.Mcninch@usace.army.mil	Co-Investigator, FRF Site Contact
Dr. Tim Crandal	Seaview Systems Inc 7275 Joy Road Dexter, MI 48130	Phone: 408-887-6008 tcrandle@seaviewsystems.com	Lead Crawler Engineer
Dr. Herb Nelson	SERDP/ESTCP	Phone: 571-372-6400 herb.nelson@nrl.navy.mil	Program Director